DEUTSCHE internationale Zeitschrift

für zeitgenössische Wissenschaft

№53
2023

DIZZW 2020

DEUTSCHE internationale Zeitschrift
für zeitgenössische Wissenschaft

DIZZW 2020

DEUTSCHE internationale Zeitschrift
für zeitgenössische Wissenschaft

ISSN (Print) 2701-8369
ISSN (Online) 2701-8377

Deutsche internationale Zeitschrift für zeitgenössische Wissenschaft

• • •

№53 2023

Deutsche internationale Zeitschrift für zeitgenössische Wissenschaft ist eine internationale Fachzeitschrift in deutscher, englischer und russischer Sprache.

Periodizität: 24 Ausgaben pro Jahr
Format - A4
Alle Artikel werden überprüft.
Freier Zugang zur elektronischen Version des Journals

German International Journal of Modern Science

• • •

№53 2023

German International Journal of Modern Science is an international, German/English/Russian/Ukrainian language, peer-reviewed journal.

Periodicity: 24 issues per year
Format - A4
All articles are reviewed.
Free access to the electronic version of journal.

- Edmund Holst (Salzburg) AT
- Michaela Meissner (Köln) DE
- Klara Amsel (Liège) BE
- Briana French (Cambridge) GB
- Joleen Parsons (Manchester) GB
- Dragomir Koev (Sofia) BG
- Stanislav Štěpánek (Praha) CZ
- Valeriya Kornilova (Kyiv) UA
- Dmitriy Aksenov (Lviv) UA
- Valentin Bragin (Moscow) RU
- Mirosław Bednarski (Warsaw) PL
- Daniela Villa (Florence) IT
- Mattia Molteni (Rome) IT
- Sylwia Krzemińska (Ljubljana) SI
- Käte Kraus (Vienna) AT
- Eleonora Lehmann (Berlin) DE
- Alexander Dressler (Marseille) FR
- Zdzisław Małecki (Warsaw) PL
- Adrián Borbély (Budapest) HU

Artmedia24

Anschrift: Industriestraße 8,74589 Satteldorf Deutschland.

E-mail: info@dizzw.com
WWW: www.dizzw.com

Chefredakeur: Reinhardt Roth

Druck: Einzelfirma Artmedia24, Industriestraße 8,74589 Satteldorf Deutschland

Artmedia24

Address: Industriestrasse 8,74589 Satteldorf Germany.

E-mail: info@dizzw.com
WWW: www.dizzw.com

Editor in chief: Reinhardt Roth

Printing: Artmedia24, Industriestrasse 8,74589 Satteldorf Germany.

Edition: № 53/2023 (March) – 53th

Passed in press in March 2023

Printed in March, 2023

Printing: Artmedia 24, Industriestrasse 8,

74589 Satteldorf, Germany.

CONTENT

EARTH SCIENCES

MATHEMATICAL SCIENCES

MEDICAL SCIENCES

PHYSICAL SCIENCES

EARTH SCIENCES

CAUSES OF EARTH CLIMATE CHANGE, AS A RESULT OF SPACE IMPACT, DISPELLING THE MYTH ABOUT ANTHROPOGENIC GLOBAL WARMING

Arushanov M.L.
doctor of geographical sciences, professor
Research Hydrometeorological Institute
Uzbekistan, 100052, Tashkent, Chingiz Aitmatov street, 72
DOI: 10.5281/zenodo.7795979

ПРИЧИННЫ ИЗМЕНЕНИЯ КЛИМАТА ЗЕМЛИ, КАК РЕЗУЛЬТАТ КОСМИЧЕСКОГО ВОЗДЕЙСТВИЯ, РАЗВЕИВАЮЩЕЕ МИФ ОБ АНТРОПОГЕННМ ГЛОБАЛЬНОМ ПОТЕПЛЕНИИ

Арушанов М.Л.
доктор географических наук, профессор
Научно-исследовательский гидрометеорологический институт
Узбекистан, 100052, Ташкент, улица Чингиза Айтматова, 72

Abstract

Based on the work of scientists from various fields and the author's own research, a chain of cause-and-effect processes is revealed that determines the dynamics of the climate system of the planet Earth over a period of hundreds of thousands of years. It is shown that catastrophic climate changes occur with periods of 12 and 24 thousand years in resonance with the periods of interaction of the solar system with galactic shock waves, which manifest themselves on the planet as a result of cosmic impact. The impact is on the core of the Earth and, as a result, on the parameters that determine the state of the climate system, the changes in which are completely unrelated to the anthropogenic component, which is presented as the main factor in global warming.

Аннотация

На основании работ учёных различных направлений и собственных исследований автора раскрывается цепь причинно-следственных процессов, определяющих динамику климатической системы планеты Земля на периоде сотен тысяч лет. Показано, что катастрофические изменения климата проходят с периодами 12 и 24 тыс. лет в резонансе с периодами взаимодействия солнечной системы с галактическими ударными волнами, проявляющиеся на планете, как результат космического воздействия. Воздействие оказывается на ядро Земли и, как следствие, на параметры, определяющие состояние климатической системы, изменения которой совершенно не связаны с антропогенной составляющей, выдаваемой как главнейший фактор глобального потепления.

Keywords: climate, anthropogenic warming, Earth's core, volcanoes, earthquakes, melting glaciers, galactic interaction, shock waves, ocean currents, magma, mantle, geothermal heat.

Ключевые слова: климат, антропогенное потепление, ядро Земли, вулканы, землетрясения, таяние ледников, галактическое взаимодействие, ударные волны, океанические течения, магма, мантия, геотермальное тепло.

Введение.

Проблема современных изменений климата выдвинула задачу поиска фундаментальных причин этих изменений. Причина изменения климата, как следствие антропогенного загрязнения атмосферы – миф, выдуманный корпорациями с целью обогащения и сдерживания развития экономики других стран, отходит на второй план в силу последних данных о 12-ти и 24-ёх тысячелетних колебаниях климатической системы с катастрофическими последствиями, хотя серьёзные попытки продвижения антропогенной причины продолжаются. Точнее говоря, эти циклы были и ранее известны, но в силу их огромного (в рамках длительности жизни человека) периода не принимались во внимание. Когда же, в связи с участившимися катастрофическими природными явлениями в последние десятилетия, учёные различных научных направлений (физики, астрофизики, гелиогеофизики, сейсмологи, геологи, метеорологи и др.) обратили внимание на факт, что современной эпохе соответствует 12-и тысячный цикл колебаний климатической системы, манипуляторам от науки становится более сложно выполнять заказ магнатов.

В настоящее время в понимании климатических изменений на основе физических и химических исследований атмосферных процессов, численного моделирования достигнут большой прогресс, хотя фундаментальные причины этих изменений остаются под вопросом.

В данной статье на основе анализа работ геофизических и гелиогеофизических, геологических,

сейсмологических, астрофизических научных направлений и собственных работ автора сделана попытка выявить причинно-следственную цепь экстремальных изменений климатической системы, наблюдаемых в данную эпоху.

Используемые данные и методы

В качестве основных данных использованы реконструированные (дендрологические) данные о приземной температуре воздуха и диоксида углерода (CO_2) на 400 тыс. периоде, а также экспериментально наблюдённые данные о них за период 1860-2020 гг.

Методы анализа динамики указанных данных основывались на применении аппаратов корреляционного, спектрального [26] и причинного [1,4-7] анализов, вейвлет-преобразовании [25]. Если первые три из пяти методов широко используются в гидрометеорологических исследованиях, то последние в гидрометеорологических исследованиях используется реже.

Причинный анализ предназначен для выявления наличия (отсутствия) причинной связи, в отличие от статистической, между двумя исследуемыми процессами *A* и *B*. Анализ основан на вычислении функции причинности γ

$$\gamma = \frac{i_{B/A}}{i_{A/B}}, \quad 0 \le \gamma \le \infty, \qquad (1)$$

где $i_{B/A} = \frac{H(B/A)}{H(B)}$, $i_{A/B} = \frac{H(A/B)}{H(A)}$ – функции независимости i; $H(B), H(A), H(B/A), H(A/B)$ – шенноновские безусловные и условные энтропии, соответственно; $0 \le i \le 1$. Смысл функций i поясняется предельными значениями γ:

- γ = 0: *B* является однозначной функцией *A,* но не наоборот – предельно необратимый процесс $A \Longrightarrow B$;
- γ = 1: *A* и *B* в одинаковой степени зависят друг от друга – отсутствие причинности;
- γ = ∞: *A* является однозначной функцией *B,* но не наоборот – предельно необратимый процесс $B \Longrightarrow A$.

Непрерывное вейвлет-преобразование (ВП) функции *f*(t) – это ее свертка с семейством (как правило, комплекснозначных) функций *G*((t – b)/a) [26]

$$W(b,a) = \frac{1}{\sqrt{a}} \int_{-\infty}^{\infty} f(t) G^* \left[\frac{t-b}{a} \right] dt, \qquad (2)$$

где звездочка означает комплексное сопряжение; G(t) – «материнская» вейвлет-функция. Материнская функция должна быть выбрана из интегрируемых с квадратом (следовательно, меняющих знак) функций, локализованных вблизи нулевого значения своего аргумента так, что среднее значение вейвлет-функции равны нулю

$$\int_{-\infty}^{\infty} G(t) t^2 dt = 0, \quad z \le Z. \qquad (3)$$

Выражение (3) – так называемое условием допустимости, выполняющее локализацию ВП одновременно во временной и частотной областях, что позволяет, в отличие от преобразования Фурье, проследить степень устойчивости колебаний во времени на фиксированной частоте. При Z=1 коэффициенты *b, a* нечувствительны ни к какому линейному тренду трансформируемого временного ряда.

В дальнейшем функцию *W(a, b)* будем называть амплитудной вейвлет-функцией и вместо непрерывного преобразования (2) рассматривать его аналог [Арушанов, 2015] – дискретное преобразование:

$$W(a,b) = \frac{1}{n(a.b)} \sum_{k=0}^{N-1} f_k(t) G^* \left(\frac{t_k - b}{a} \right), \qquad (4)$$

где $n(a,b) = \sum_{k=0}^{N-1} e^{-\frac{1}{2}\left(\frac{t_k - b}{a}\right)}$.

Понятие «Климат»

Древнегреческий астроном Гиппарх из Никеи ввёл термин «климат» («наклон»), имея ввиду наклон солнечных лучей. Значительно позже (19 век) А. Гумбольдт добавил к «наклону» влияние подстилающей поверхности океана и суши на атмосферу. В настоящее время имеется ряд географических определений и типизаций климата [12,13].

За последние 30 лет были достигнуты определённые успехи в понимании динамики климатической системы. Эти успехи связаны с развитием теории нелинейных динамических систем (теории хауса), в которой центральным понятием является *странный аттрактор*[*] Лоренца [33]. На основании этой теории А. С. Монин, Д. М. Сонечкин вводят определение климата: «*Климат – это нетривиальная вероятностная мера, сосредоточенная на странном аттракторе климатической системы*» [39]. Несколько позже в работе [1] вводится другое определение климата: «*Климат – это открытая периодически меняющаяся термодинамическая система, сохраняющая состояние стационарности или близкое к нему с постоянным значением производства энтропии на определённых интервалах времени».* Общим для этих двух определений является введенная в определение «мера», т.е. некая количественная характеристика. Хотя эти меры математически различны, но физически достаточно близки. Действительно в этих двух определениях ключевым является «климатическая система», которая в первом случае характеризуется вероятностной мерой, во втором – производством энтропии. Таким образом, и в том и в другом случае климат рассматривается, как открытая термодинамическая

[*] Притягивающее множество целых неустойчивых траекторий в фазовом пространстве динамической системы.

система, элементы которой обмениваются веществом, энергией и импульсом. Термодинамические силы (отклонения термодинамических параметров от их равновесных значений) вызывают в системе потоки энтропии и вещества, что приводит к росту энтропии системы – *производству энтропии*.

Реакция климатической системы на внешние факторы

Поскольку по определению климатическая система – это открытая термодинамическая система, то согласно И. Пригожину [46] её динамика определяется воздействием внешних факторов, схематично показанных на рис. 1.

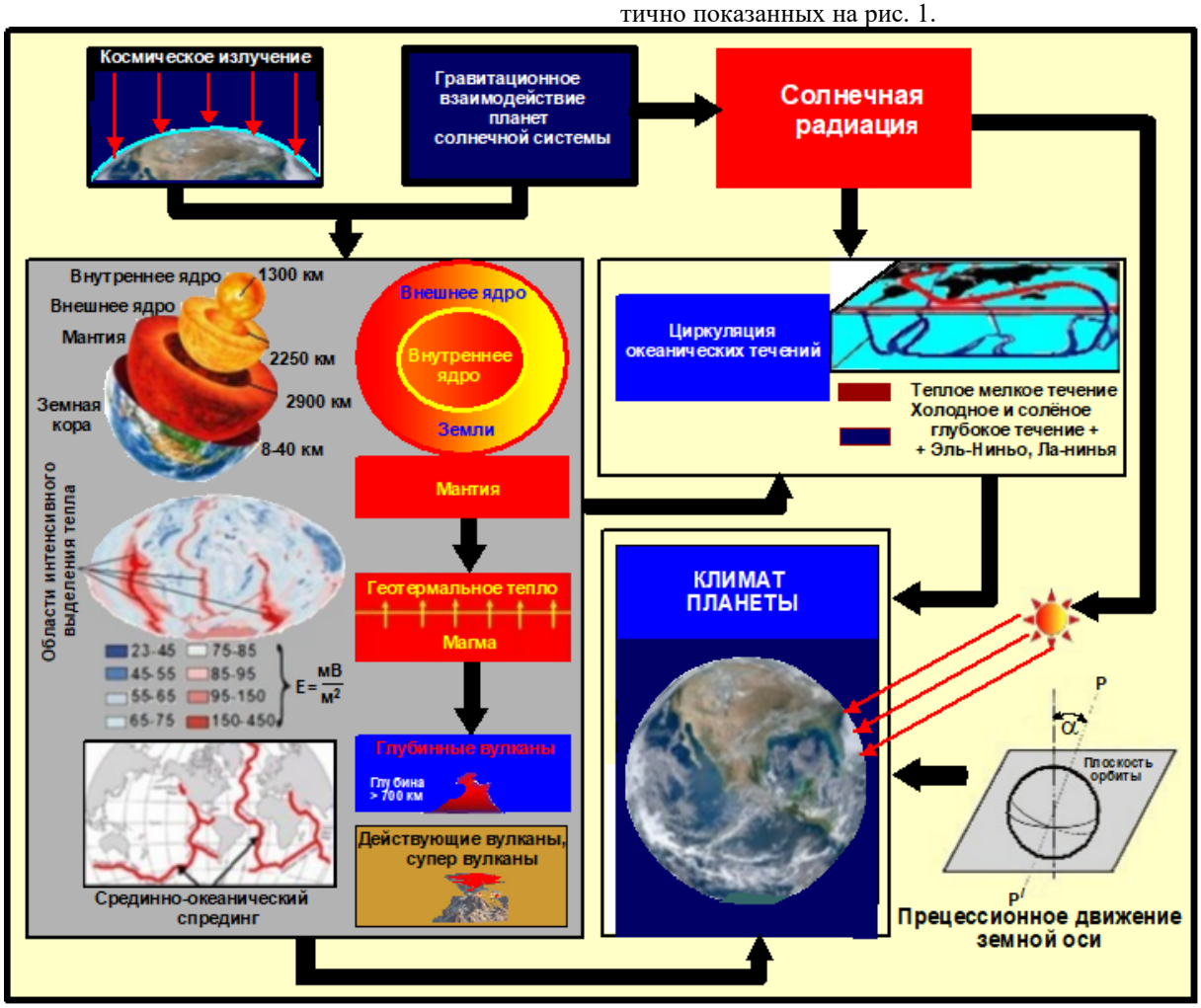

Рис.1. Внешние факторы, определяющие динамику климатической системы.

Далее, следуя схеме на рис. 1 рассмотрим вкратце каждый из внешних (относительно атмосферы) факторов, начиная с ядра Земли.

Ядро Земли. Самая глубокая геосфера Земли с повышенной плотностью, состоящая из внешнего (жидкого) и внутреннего (твердого) ядра, имеющего радиус около 3500 км, т.е. составляющий почти половину радиуса Земли, и состоящее из железо-никелевого сплава [40]. Поскольку внутренне ядро не соединено жёстко с твёрдой земной мантией, то оно вращается с отличной от остальной части Земли скоростью [9, 54]. Посредством наблюдения изменений в характеристиках сейсмических волн, проходящих через внутреннее ядро, сейсмологи на основе анизотропии скорости передачи волны рассчитали скорость вращения внутреннего ядра, которая составила около одного градуса добавочного вращения в год [14,56].

Главенствующая роль жидкого ядра Земли – создание и поддержание магнитного поля планеты с преобладанием дипольной компоненты, величина которой изменяется около некоторого среднего значения. Соотношение минимума и максимума этой величины 1:2. Период смены полярности ~$2\cdot10^5$ лет. Геомагнитное поле весьма изменчиво, так что даже его среднее (осевой диполь) не является стационарным, а колеблется с периодом ~$2\cdot10^3$ лет [56]. Для нас в дальнейшем важным является тот факт, что колебания геомагнитного поля обнаруживают высокую корреляцию с вариациями скорости вращения Земли [52], которые имеют общую причину – магнитогидродинамические колебания крутильного типа в земном ядре.

Мантия – часть геосферы, расположенной под корой и выше ядра. В ней находится большая часть вещества Земли, занимающая 80 % её объёма [19]. Границей между корой и мантией служит граница Мохоровичича на глубине от 7 (под океанами) до 70 километров (под складчатыми поясами), начиная с которой происходит скачкообразное увеличение скоростей продольных сейсмических волн. Мантия подразделяется на верхнюю и нижнюю, разделённые слоем Голицына (около 673 км).

Геотермальное тепло – энергия тепла Земли с источником из раскаленных недр, направленный к поверхности Земли. Земля представляет собой тепловую машину. Это означает, что энергия, вызывающая геодинамические явления, генерацию геомагнитного поля, сейсмичность и вулканизм – является результатом тепловых процессов, показателем которых можно считать величину теплового потока. Распределение теплового потока по земному шару неоднородно (рис. 1, 2). Такая неоднородность прямо указывает на очаги повышенной интенсивности восходящих движений магмы в областях срединно-океанического спрединга (раздвигание океанического дна), а также повышенной активностью океанических (глубинных) извержений вулканов.

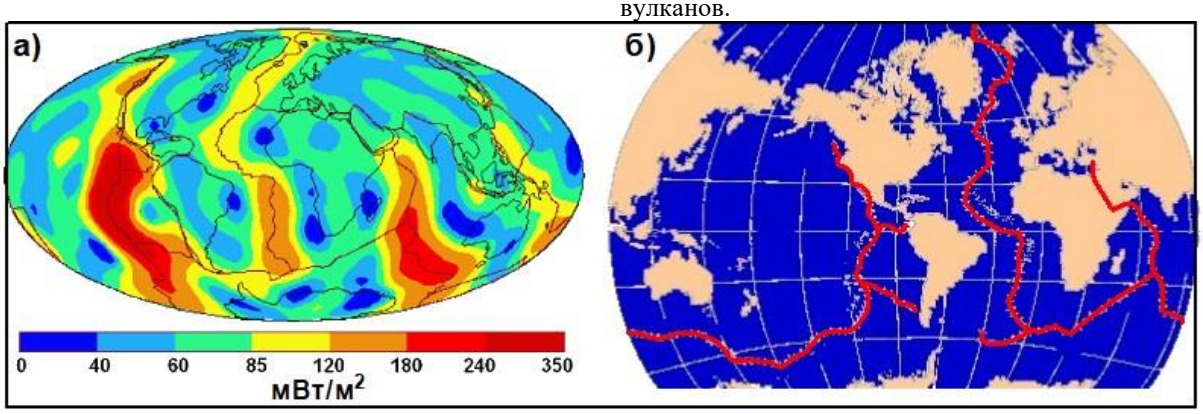

Рис. 2. Карта теплового потока Земли (а) и областей срединно-океанического спрединга (б).

Взаимодействие «океан-атмосфера», океанические течения. Вопросы крупномасштабной океанической циркуляции важны для понимания механизмов изменчивости климатической системы. Здесь большой вклад внесли работы школы П. С. Линейкина [30-32], направленные на исследования особенностей океанического термоклина и крупномасштабной циркуляции Мирового океана, теории деятельного слоя и методов расчета характеристик верхнего перемешанного слоя в океане. Все эти научные направления, связанные с теорией климата, привели к качественно новому пониманию функционирования климатической системы и позволили объяснить многие (ранее непонятные) механизмы ее эволюции на временных масштабах от нескольких лет до тысячелетий, обусловленные внутренней океанической динамикой и взаимодействием атмосферы с океаном.

Из-за бо́льше́й теплоемкости относительно теплоёмкости воздуха, инерционность температуры океана значительно больше последнего. Это различие в середине 70-х годов прошлого столетия, по предложению Г. И. Марчука, было использовано Ш. А. Мусаеляном в долгосрочном прогнозе температуры воздуха, где в качестве предиктора взята температура океана с 3-х месячным запаздыванием [41,42]. Кроме того, океан является регулятором облачности и радиационного баланса поверхности Земли, обеспечивая более половины общего меридионального переноса тепла в системе океан-атмосфера [11,28,35,36,38,45]. Таким образом, океан-атмосфера – взаимосвязанная система, в которой океан отвечает за формирование низкочастотной части спектра изменчивости [1].

Мировые океанические течения (рис. 1, 3) играют важную роль в формировании климата на Земле и существовании жизни в морях и океанах, формируются под действием ветра, космических влияний и различий в свойствах воды на разных участках Мирового океана. Все течения делятся на множество классификаций (рис. 3) в зависимости от их природы, периодичности, глубины и температуры. Течения называются тёплыми и холодными или нейтральными в зависимости от температуры окружающей воды.

В Северном полушарии течения циркулируют по часовой стрелке, а в Южном □□против. Течения в северной части Индийского океана меняют направление в зависимости от сезона.

Климатической системе свойственны крупномасштабные автоколебательные процессы, такие как Южное колебание (перераспределение масс воздуха в низких широтах Южного полушария между Индийским и Тихим океанами) и колебания океана – Эль-Ниньо (теплая фаза) и Ла-Нинья (холодная фаза). При Эль-Ниньо происходит значительное потепление воды в центральной и восточной частях экваториальной зоны Тихого океана и, как следствие, возмущение всей планетарной атмосферной циркуляции, учащение опасных явлений погоды и стихийных бедствий далеко от места своего возникновения.

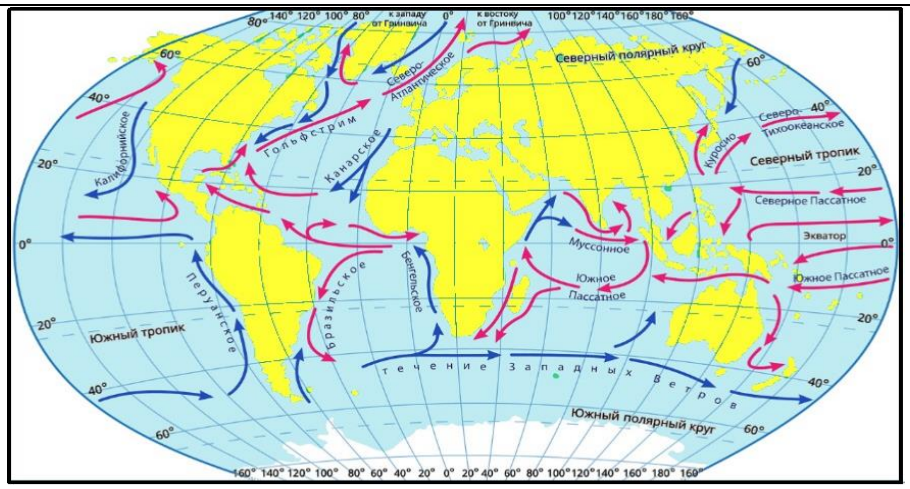

Рис. 3. Океанические течения на планете Земля.

В среднем цикличность этого автоколебания составляет 4–4,5 года, но отмечается усиление его интенсивности в последние десятилетия [44].

Извержения вулканов. Вулканы Земли – одни из модуляторов колебаний климата, приводящие, с одной стороны, к повышению температуры поверхности Земли, а с другой стороны, к ее понижению за счёт загрязнения атмосферы частицами пепла и аэрозолями, отражающие солнечную радиацию. Например, извержение 70 тыс. лет назад супервулкана Тоба [17], привело к наступлению «вулканической зимы» на несколько лет и почти полному исчезновению людей. Другие извержения, меньшие по степени взрыва, такие как на острове Сумбава в 1815 году и извержение вулканов в Южной Америке в 530 годах нашей эры [53], вызвали массовый голод и вспышки чумы. Однако, необходимо иметь ввиду, что вулканы не всегда однозначно влияют на климат, одновременно вызывая и таяние льдов, и «вулканическую зиму». Так, в работе [43], изучая отложения ила, формировавшиеся на дне пересохшего Балтийского ледникового озера, авторы пришли к выводу, что оно представляло собой крупный временный водоем, покрывавший существенную часть современной Скандинавии в ледниковую эпоху летом, когда талая вода с ледников начинала стекать в котловину будущего Балтийского моря. По оценкам геологов оно возникло около 12000 лет назад (конец ледникового периода), просуществовав несколько тысячелетий.

Толщина донных отложений ила* (аналог годичных колец деревьев) позволила авторам работы [43] показать какую роль в формировании Балтийского озера сыграли вулканы. Вопреки ожиданиям, оказалось, что в течении времени извержений, т.е. при выбросе большого количества аэрозолей в атмосферу, скорость таяния ледников не падала, а росла или оставалась прежней, в то время как температура понижалась на 3,5 ºС на территории Скандинавии. Таким образом, в этом процессе определяющую роль играет пепел, понижающий альбедо льда на 15-20%, что и ускорило темпы накопление воды в Балтийском озере, впоследствии ставшим Балтийским морем. В результате вулканы сыграли важную роль в завершении ледникового периода.

Особое место в изменении климатической системы занимают глубинные (океанические) вулканы, о которых будет сказано ниже при рассмотрении причин таяния ледниковых щитов западной Антарктиды, Гренландии и льдов Арктики.

12000-ые циклы гелиогеофизической системы

Под гелиогеофизической системой будем подразумевать физическое состояние объектов солнечной системы, а именно, Солнца (солнечная активность), планет солнечной системы, в частности, геофизические процессы, включающие, климатическую систему в трактовке данной в разделе «Климат», гляциологические процессы таяния ледников, сейсмические и вулканические процессы, скачки ядра Земли, вариации магнитного поля и скорости вращения Земли.

Наша планета вошла в период глобальных климатических изменений. Наблюдённые данные говорят о росте количества и силе землетрясений, частоте и мощности ураганов и торнадо, наводнений и пожаров, появлению многочисленных трещин и провалов в новых континентальных разломах и пр., но преподносить, что все эти катастрофические процессы происходят из-за деятельности человека – это не просто ошибка, а преступление.

Климат имеет циклический характер, менялся всегда по естественным причинам, но на определенных периодах эти изменения носят катастрофический характер. Такими периодами являются 12 и 24-х тыс. летние периоды. В настоящее время планеты солнечной системы вступили в активную фазу 24000-го периода. Встаёт вопрос: «какими причинами вызвана эта цикличность?». Не имея возможности в рамках статьи изложить подробно причины этой цикличности, отметим, что Земля, вращаясь вместе с Солнечной системой в пределах Галактики, периодически встречается с ее спиральными

* Чем шире каждый слой ила, тем больше воды должно было поступать в озеро со склонов отступающих ледников.

рукавами [27] (рис. 4). При этом система испытывает взаимодействие с галактическими ударными волнами*, проявляющиеся воздействием на планету в виде космического излучения. В результате галактические ударные волны ответственны за существование критических периодов в эволюции планеты. Хронологическая летопись ключевых эпизодов геодинамики практически повторяет временную шкалу галактического масштаба [27]. Высокочастотные составляющие колебаний взаимодействия с периодами 12000 и 24000 лет, соответствуют резким изменениям климата и катастрофическим явлениям на Земле во время пересечения солнечной системой близких и дальних областей галактических ударных волн (галактического взаимодействия) в рукавах Ориона [23].

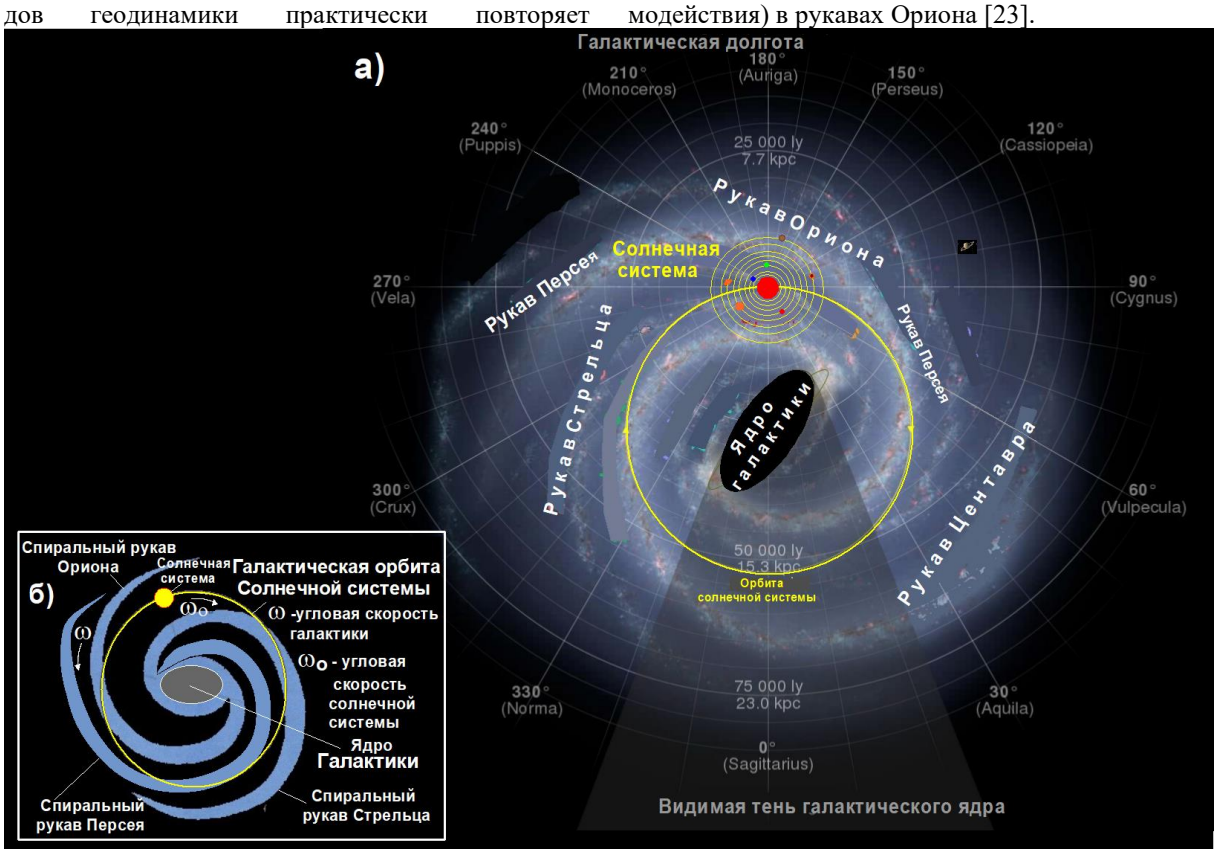

Рис. 4. Модель внешнего вида Млечного Пути с деталями структуры и галактическими долготами (а); б) – схематичное представление современного расположения солнечной системы относительно галактических рукавов.

Проявление указанных выше циклов в динамике климатической системы Земли показано на рис. 5 на примере реконструированных данных о температуре и диоксиде углерода (CO_2) на основе спектрального анализа, выполненного различными методами (Фурье и вейвлет-преобразование). Как следует из рис. 5 полученные спектры колебаний обнаруживают пики на периодах от 10 до 30 тысяч лет. При этом отчетливо проявляется устойчивость периодов около 12 и 24 тыс. лет в амплитудной вейвлет-функции (белая штриховка на рис. 5) как температуры, так и CO_2.

В контексте названия данной статьи весьма важно распределение функции причинности, которое однозначно показывает отсутствие причинной связи на нулевом лаге между температурой и диоксидом углерода. При этом корреляционная функция обнаруживает на этом же лаге высокую корреляцию.

Высокая корреляция между температурой и CO_2 и является причиной глубокого заблуждения, касаемо антропогенного глобального потепления.

Таким образом, космическое излучение, являясь генератором процессов на Земле причинно-следственных превращений, начиная с воздействия на ядро Земли, вызывает высокую корреляцию между составляющими климатической системы, хотя между некоторыми из них, как температура и CO_2, причинная связь отсутствует. Более того, причинная связь между ними обнаруживается на отрицательных временных лагах, т.е. не CO_2 является причиной изменения температуры, а наоборот, что подтверждается и на положительных лагах, где функция причинности находится в области обратной причинности (рис. 5е).

* Область взаимодействия между магнитосферой звезды или планеты и окружающей средой, в которой наблюдается повышенная плотность вещества.

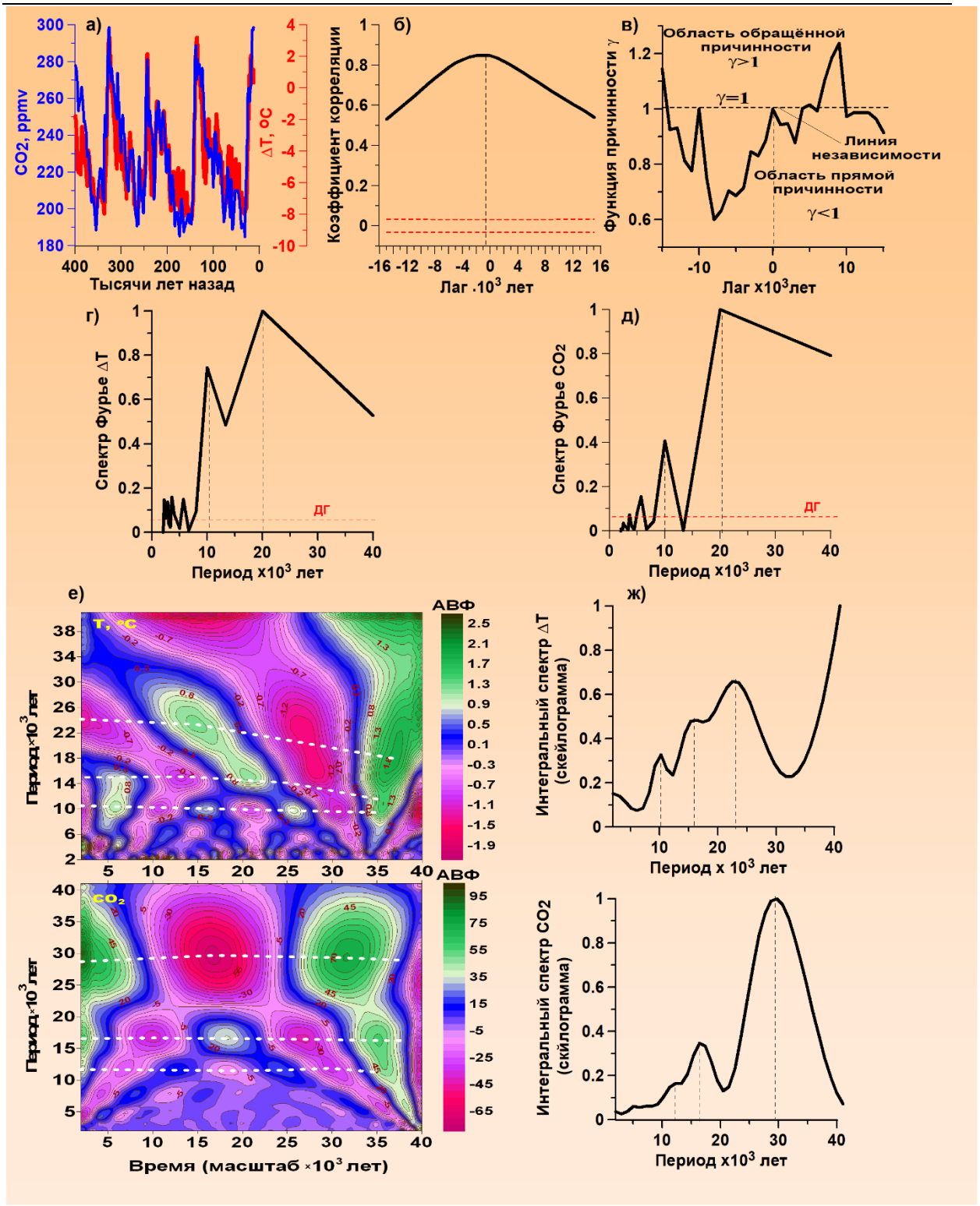

.

Рис. 5. Проявление 12, 24-х тысячелетней цикличности в динамике температуры воздуха и CO2 на планете Земля.

Примечание: а) – временной ход отклонений ΔT от средней температуры воздуха и CO2 на 400 тысячном периоде; б) – временная корреляционная функция между ΔT и CO2; в) – функция причинности между ΔT и CO2. г), д) – спектры Фурье; ж) – амплитудные вейвлет функции (АВФ) ΔT и CO2; е) – скейлограммы ΔT и CO2.

Этот же вывод на основании совершенно других подходов делается рядом исследователей в работах [16,18,34,48,49,50,51]. Правильность этого вывода следует из физической сущности парникового эффекта в атмосфере. Действительно, в плотной атмосфере Земли, а именно, в тропосфере (наиболее плотном слое), преобладает конвективный перенос тепла, а механизм излучения (радиационный перенос) – в верхних разряжённых слоях (стратосфера, мезосфера, термосфера). Таким образом среднее, например, за месяц, распределение температуры в толще тропосферы близко к адиабатическому – расширение и охлаждение воздуха при подъёме и сжатие и разогрев при опускании. Тогда, с учётом средней поверхностной температуры Земли, равной 288К, на любом уровне земной тропосферы (p > 0,2 атм) [50]

$$T = 288\left(\frac{p}{p_o}\right)^{\alpha}, \qquad (4)$$

где $\alpha = \dfrac{R}{\mu\left(c_p + c_w + c_r\right)}$ – показатель адиабаты, зависящий от состава и влажности атмосферы, c_p – удельная теплоёмкость при постоянном давлении, c_w – удельная теплоёмкость, характеризующая суммарный тепловой эффект процессов конденсации влаги во влажной атмосфере, c_r – удельная теплоёмкость, характеризующая поглощения теплового излучения Земли и Солнца, μ – молярная масса воздуха; В (4) p_o – давление на уровне моря.

Физика явления состоит в том, что поглощение парниковыми газами ИК-излучения разогревает воздушные массы, что усиливает передачу тепла путём конвекции, т.е. в выражении показателя адиабаты знаменатель увеличивается и согласно (4) происходит уменьшение температуры.

Таким образом, вынос тепла из тропосферы происходит, главным образом, за счёт конвекции, обеспечивающей более эффективный перенос тепла по сравнению с радиацией. В результате с увеличением концентрации углекислого газа и поглощения им теплового излучения возрастает конвективный массообмен воздуха, выносящий это тепло за пределы тропосферы. Этот вывод, в корне опровергающий антропогенную причину глобального потепления, подтверждается экспериментальными данными [37,22] ледяных кернов Антарктиды (рис. 6).

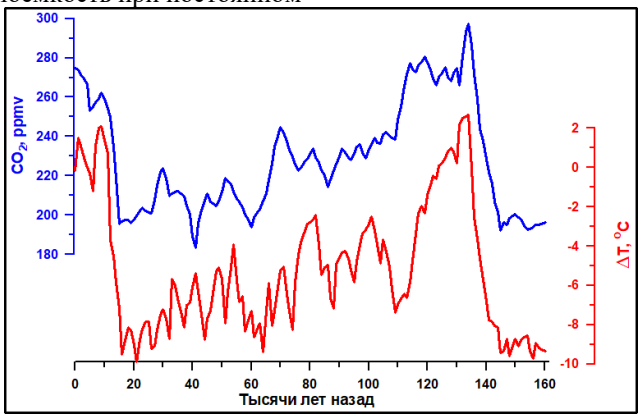

Рис. 6. Реконструированные CO_2 и температура воздуха.

Кривые на рис. 6 температуры и диоксида углерода, реконструированные на основе изотопного анализа данных бурения ледникового покрова Антарктиды однозначно показывают, что изменения температуры на протяжении последних более 160 тыс. лет опережают соответствующие им изменения концентраций CO_2 в среднем на 550 лет – время полного перемешивания верхнего (активного) слоя воды в Мировом океане [50], в котором заключена основная масса углекислого газа (содержание CO_2 в 90 раз превосходит его содержание в атмосфере). Этот результат практически совпадает с распределением CO_2 и температуры, приведенные на рис. 5а для 400 тысячелетнего периода.

Глобальный энергетический скачок

Прохождение Солнечной системы через галактические рукава (дальнюю и ближнюю точки взаимодействия), сопровождается вариациями интенсивности галактических космических лучей. Это взаимодействие оказывает импульсное воздействие на объекты солнечной системы, в частности, на Землю, проявившееся в 1998 году в скачке центра масс ядра Земли относительно центра масс мантии в результате чего произошло смещение железного ядра на север, появление биения и диссонанса [54,55] и, как следствие, уменьшение электромагнитного поля внутри ядра и ослабление магнитного поля Земли, аномальный дрейф северного магнитного полюса. С момента скачка центра масс ядра относительно центра масс мантии началось экспоненциальное увеличение катастрофических природных явлений и катастрофическое изменение климата. На рис. 7 приведен график динамики катастрофических явлений, на которых виден экспоненциальный их рост, начиная с 1998 г.

Циклическое смещение ядра с его огромной массой (17 масс Луны) оказывает гравитационное воздействие на все оболочки Земли [3]. Под воздействием галактических ударных волн синхронно произошёл глобальный энергетический скачок на всех планетах солнечной системы [10,54,55] при прохождении последней ближней точки взаимодействия в рукаве Ориона. Аналогичная цикличе-

ская макроперестройка планетарной системы произошла около 12000 лет назад, в которой синхронизация климатических катастроф является следствием галактических процессов.

Таяние льдов Арктики и Гренландии, Антарктиды (западная часть) происходит вследствие геотермального теплового потока, увеличившегося за последнее тридцатилетие в два раза, особенно с момента скачка ядра, как результат подъёма магмы. Данный факт основан на впервые выполненной фиксации выброса потока нейтрино* из недр на Антарктической станции ANITA [20], что прямо указывает на движение магмы внутри планеты и, по-видимому, на активизацию ещё каких-то процессов. Кроме того, увеличению скорости и высоты подъёма магмы соответствует увеличение частоты извержения глубинных вулканов в нижней мантии Земли**.

Таким образом, миф о причине таяния льдов в Арктике, Гренландии и Антарктиде, связанной с антропогенным воздействием диоксида углерода, ещё раз развеивается строгими научными фактами, ибо это таяние происходит из-за действия геотермального тепла недр Земли, т.е. под действием не внешнего (атмосфера) фактора, а внутреннего (ядро Земли).

Выводы

Главенствующим генератором катастрофических климатических изменений на протяжении эволюции Земли было, есть и будет галактическое воздействие на солнечную систему при её прохождении галактических рукавов, с максимумом колебаний в высокочастотной области с периодом 12 тыс. лет. На планетах солнечной системы, в частности планете Земля, это воздействие в первую очередь проявляется в изменении физического состояния внутреннего ядра планеты, проявляющегося в скачке, и как следствие, в изменении его электромагнитного поля, магнитного поля Земли, скорости вращения Земли (прецессия, длительность суток). Смещение ядра Земли вызывает активизацию магмы, которая, в свою очередь, повышает выделения геотермального тепла, что является причиной таяния ледников в областях с наименьшей толщиной земной коры. В совокупности все эти факторы проявляются в глобальном изменении климатической системы. На фоне таких грандиозных процессов объяснение глобального потепления из-за антропогенного загрязнения атмосферы диоксидом углерода не просто неправильно, а является, в связи с вероятными ещё более катастрофическими процессами, научным преступлением.

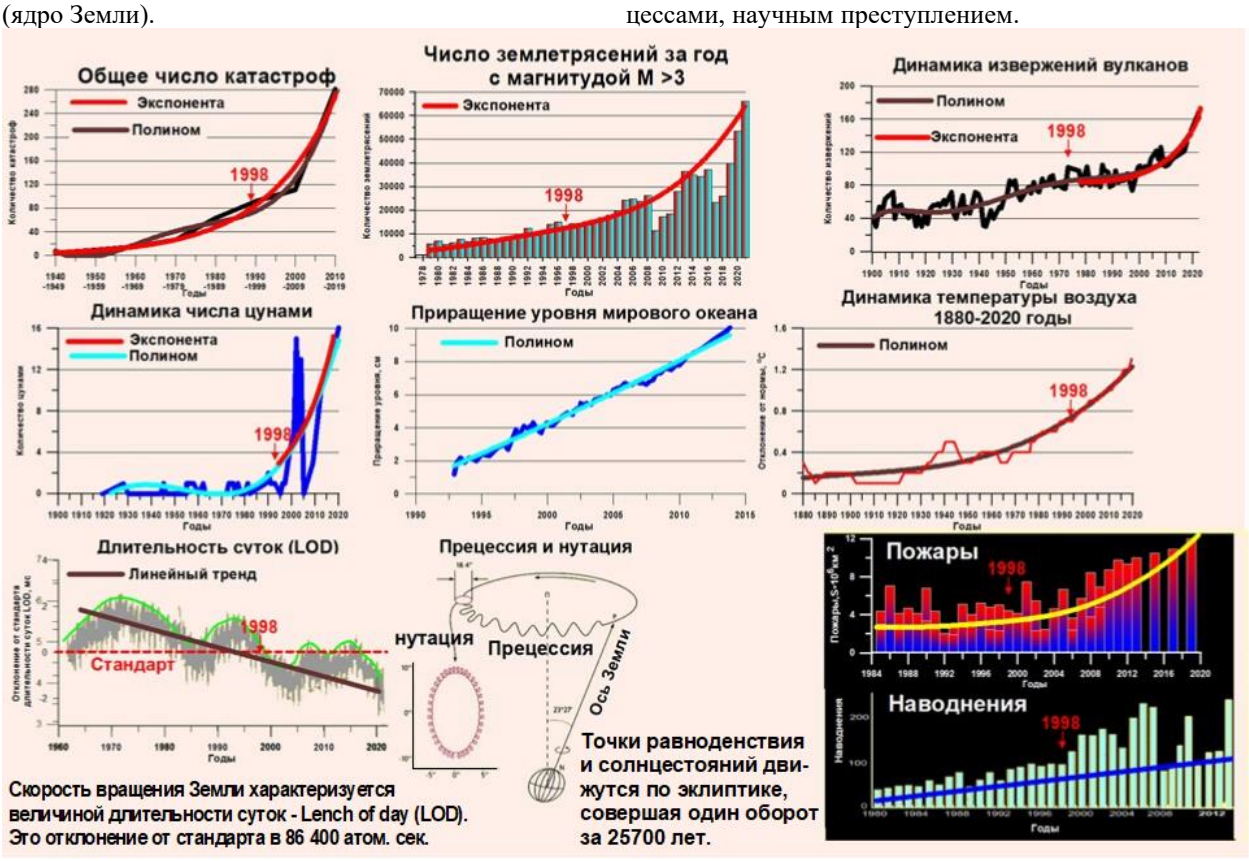

Рис. 7. Динамика катастрофических явлений.

* Ранее фиксировалось только космическое нейтрино.

** Ученым удалось зафиксировать землетрясение на рекордно большой глубине - 751 км.

References

1. Arushanov M. L. Climatic spectrum of planet Earth. – Tashkent: NIGMI, 2010. 160 p.

2. Arushanov M. L. Practical issues of using wavelet transform in meteorology. – Tashkent: NIGMI, 2015. – 50 p. (in Russian)

3. Arushanov M. L. Gravity, solar activity, rotation of the Earth – weather indicators for long periods. – Tashkent: NIGMI, 2014. – 147 p. (in Russian)

4. Arushanov M. L., Goryachev A. M. Effects of causal mechanics in meteorology. – Tashkent: SANIGMI. – 2003. – 160 p. (in Russian)

5. Arushanov M. L., Goryachev A. M. To a problem on the necessity of the registration of effects of causal mechanics on an example of simple barotropic model of an atmosphere // Meteorol. &Atmos. Phys. 92/1–2. – 2006. – P. 10–18.

6. Arushanov M. L, Korotaev S. M Causal analysis and its application for studying physical processes in the atmosphere // Meteorology and Hydrology, N6. – 1994. – S. 15–22.

7. Arushanov M. L On the need to take into account the effects of causal mechanics in hydrodynamic forecast and climate models //Reports of the Academy of Sciences of Uzbekistan, №6, 2002. – P. 12–14. (in Russian)

8. Atmospheric CO_2 Rise and Tropical Warming // Science, №318. – 2007. – P. 435–447.

9. Aurnou J. M., Brito D. P., Olson L. Mechanics of inner core super–rotation // Geophysical Research Letters, vol. 23, №23. –1996. – P. 3401–3404.

10. Barkin Yu. V. Explanation of some planetary natural phenomena // Proceedings of the XVIII International Scientific Conference on Marine Geology. – M.: №5. – 2009 – P. 215–218. (in Russian)

11. Bjerknes J. Atlantic air–sea interaction // Adv. Geophys. V. 10. No. 1. –1964. – P. 1–82.

12. Blutgen I. Geography of climates. T1 – M.: Progress, 1972. – 354 p. (in Russian)

13. Blutgen I. Geography of climates. T2 – M.: Progress, 1973. – 426 p. (in Russian)

14. Bullen K. E. An Earth model based on a comprcssibilitv–pressure hypothesis // Monthly Noti – Roy. Astron. Soc., Geophys. Suppl., v. 6, № 1. – 1950. – P. 12–22.

15. Bullien K.E. An introduction to the theory of seismology. – London: Cambridge Univ. Press, 1963. – 210 p.

16. Caillon N., Severinghaus J. P., Jouzel J., Barnola J. M., Kang J., Lipenkov V. Y. Timing of atmospheric CO_2 and Antarctic temperature changes across termination III // Science №299. – 2003. – P. 1728–1731.

17. Chesner C. A., Rose W. I., Deino A., Drake R., Westgate J. A. Eruptive history of Earth's largest Quaternary caldera (Toba, Indonesia) clarified //GEOLOGY, v. 19. – 1991. – P. 200–203.

18. Cuffey K. M., Clow G. D. Temperature, clusters, and ice sheet elevation in central Green–land through the last deglacial transition //J. of Geophysical Research Atmospheres, №102. – 1997. – P. 383–396.

19. Earth //Physical encyclopedia under. ed. A. M. Prokhorova. – M.: Soviet Encyclopedia, 1990. – P. 78–80. (in Russian)

20. Electronic resource: Laboratory in Antarctica discovered neutrinos that cast doubt on current physical theories, 2020. – https://www.atomic–energy. en/ news /2020/ 01/29/100990

21. Engdahl E. R, Flynn E. A. and Massé R. P. Differential PkiKP travel times and the radius of the core // Geophys. J. R. Astr. Soc, vol. 40, № 3. – 1974. – P. 457–463.

22. Fischer H., Wahlen M., Smith J., Mastroianni D., Deck B. Ice core records of atmospheric CO2 around the last three glacial terminations // Science283. – 1999. – P. 1712 – 1714.

23. Gingerich O. Discovery of the spiral arms of the Milky Way // Tr. Symp. MAC. N106 «The Milky Way Galaxy». – 1985. P. 59–70.

24. Goncharov M. A., Raznitsin Yu. N., Barkin Yu. V. Peculiarities of deformation of the continental and oceanic lithosphere as a consequence of the northern drift of the Earth's core // Geodynamics and tectonophysics, no. 3(1). – 2012. – P. 27–54.

25. Grossmann A, Kronland-Martinet R, Morlet J. Reading and understanding continuous wavelet transform // Springer-Verlag, Berlin. – 1989. – P. 3-20.

26. Jenkins G., Watts D. Spectral analysis and its applications. – M.: Mir, 1971. – 314 p.

27. Khristoforova N. N. On the influence of the spectral structure of the galaxy on the evolution of the planet // Georesources, No. 1(2). – 2000. – S. 15–27. (in Russian)

28. Kondratiev K.Ya. Global climate change: reality, assumptions and fiction // Issled. Earth from space, No. 1. – 2002. – P. 3–31. (in Russian)

29. Lineikin P.S. On nonlinear wave disturbances in the main oceanic thermo–cline // Dokl. 1978. Issue. 241. No. 6. S. 1436−1439. (in Russian)

30. Lineikin P.S., Frolov A.V. Non–stationary two–parameter model of the main oceanic thermocline // Meteorology and Hydrology. 1979. No. 1. S. 72−85. (in Russian)

31. Lineikin P.S., Maderich V.S. Theory of the oceanic thermocline. L.: Gidrometeoizdat, 1982. – 272 p. (in Russian)

32. Lineikin PS Basic questions of the dynamical theory of the baroclinic layer of the sea. L.: Gidrometeoizdat, 1957. – 139 p. (in Russian)

33. Lorenz E. N. Dimension of weather and climate attractors // Nature. V. 353. – 1991P. 241-244.

34. Lorius C., Jouzel J., Raynaud D., Hansen J. & Treut H. Le. The ice–core record: climate sensitivity and future greenhouse warming // Nature, vol. 347. – 1990. – P. 139–145.

35. Marchuk G. I., Skiba Yu. N. Numerical calculation of the adjoint problem for the model of thermal interaction of the atmosphere with oceans and continents // Izv. USSR Academy of Sciences, vol. 12, no. 5. – 1976. – pp. 459–469. (in Russian)

36. Marchuk G. I., Dymnikov, V. B., Zalesny, V. N., Lykosov V. Ya., Galin. S. P. Mathematical modeling of the general circulation of the atmosphere and ocean – M.: Nauka, 1984. – 320 p. (in Russian)

37. Mokhov I.I., Bezverkhniy V.A., Karpenko A.A. Milankovich cycles and the evolution of the characteristics of the climatic regime and atmospheric composition according to ice core data from the Antarctic station "Vostok" // Materials of glaciological research, v. 95 – 2003. – P. 3–8.

38. Monin A.S. Hydrodynamics of the atmosphere, ocean and earth interiors. St. Petersburg: Gidrometeoizdat, 1999. – 524 p. (in Russian)

39. Monin A.S., Sonechkin D.M. Climate fluctuations according to observations: triple solar and other cycles. – M. Nauka, 2005. – 191 p. (in Russian)

40. Monnereau M., Calvet M., Margerin L.; Souriau A. Lopsided Growth of Earth's Inner Core // Science, vol. 328, no. 21. – 2010. – P. 1014–1017.

41. Musaelyan Sh. A. On the nature of some superlong atmospheric processes. – L.: Gidrometeoizdat, 1978. – 141 p. (in Russian)

42. Musaelyan Sh. A. Problems of predictability of the state of the atmosphere and hydrodynamic long–term weather forecast. – L.: Gidrometeoizdat, 1984. – 183 p. (in Russian)

43. Muschitiello1 F., Pausata S.R., Lea J. M., Mair6 W.F., Wohlfarth B. Enhanced ice sheet melting driven by volcanic eruptions during the last deglaciation //Nature Communications, №. 8. – 2020. – P. 1–9.

44. Perevedentsev Yu. P. Theory of climate. – Kazan: KGU, 2009. – 503 p. (in Russian)

45. Polonsky A. B. The role of the ocean in climate change. – Kyiv: Naukova Dumka, 2008. – 184p.

46. Prigogine I. From existing to emerging. Time and complexity in the physical sciences. – M.: Nauka, 1985. – 217 p. (in Russian)

47. Samurović K. Coastal Ice Loss is Outpacing Mainland Ice Gains on Both Antarctica and Green–land // Glaciology, July N2. – 2020. – P. 12–24. (in Russian)

48. Shakun J. D., Clark P. U., He F., Marcott S., Mix A. C., Liu Z., Otto–Bliesner B., Schmittner A., Bard E. Global warming preceded by increasing carbon dioxide concentrations during the last deglaciation //Nature vol. 484. – 2012. – P. 49–54.

49. Sorokhtin O. G. Adiabatic theory of the greenhouse effect // Physics, N11(787). – 2005. – S. 3–25. (in Russian)

50. Sorokhtin O. G. Greenhouse effect: myth and reality // Bulletin of the Russian Academy of Natural Sciences, vol. 1, no. 1. – 2001. – C. 6–21. (in Russian)

51. Stott L., Timmermann A., Thunell R. Southern Hemisphere and Deep-Sea Warming Led Deglacial Atmospheric CO2 Rise and Tropical Warming //Science 318(5849). 2007. – P 12-21.

52. Tsygankov S.S. On a possible mechanism of generation and inversion of the geomagnetic field // Physical mezamekhanika, №123. – 2009. – S. 101–112. (in Russian)

53. Volcanoes. Electronic resource: https://ru.wikipedia.org/wiki/Volcanoes of South America

54. Xu X, Song X. Evidence for inner core super–rotation from time–dependent differential PKP trav–eltimes observed at Beijing Seismic Network // Geophysical Journal International, vol. 152, N3. – 2003. – P. 509–514.

55. Yang Yi, Song Xi. Multidecadal variation of the Earth's inner–core rotation // Nature Geoscience v. 16. – 2023. – P. 189–197.

56. Zharkov VN Internal structure of the Earth and planets. – M.: Nauka, 1971. – 413 p. (in Russian)

MATHEMATICAL SCIENCES

ROBUST PARAMETRIC MODIFICATIONS OF THE Z-TEST STATISTIC

Cvetkov Vasil
Chief Assist. Prof. PhD Eng.
University of Architecture, Civil Engineering and Geodesy.
1164, 1 Hristo Smirnenski Blvd.
Sofia, Bulgaria
ORCİD: 0000-0001-9628-6768
DOI: 10.5281/zenodo.7795991

Abstract

The conventional z-test statistic, which is one of the most popular statistics, is based on the mean of a sample and the standard error of the mean. Consequently, in case of a violation of the normality of the data, the traditional z-test may lead to incorrect test conclusions. The main aim of this article is to present two robust parametric modifications of the traditional z-test statistic.

In order to minimize the effect of non-normality due to the presence of the outliers and some potential contaminated observations in a sample we use either the center or the C_2 statistic and their standard errors, respectively, instead of the mean and the standard error of the mean. The statistical power of one-sample z-tests based on the mean, center and C_2 statistics were compared by generating of random number samples with different sizes and known expectations. These samples were derived from some popular distributions. The comparison shows that the z-tests based on the center and the C_2 statistics are more powerful and efficient than the traditional one.

In addition, real-data illustrations by implementing both one-sample z-test and two-sample z-test are also provided.

Keywords: one sample z-test; two sample z-test; type II error; statistical power; systematic error in precise levelling

Introduction

The traditional z-test statistic (1) is one of the most widely used statistical methods.

$$Z = \frac{\bar{X}-\mu}{\sigma/\sqrt{n}} \qquad (1)$$

Statistic (1) is a quite accurate, effective and reliable when there is no lack of normality of the data. However, if the distribution of the analysed data is not normal, statistic (1) is likely to lead to incorrect conclusions. The main reason for this is the expanded value of the standard deviation σ in the denominator of (1). In addition, the mean $\bar{X}$ is strongly affected by the observations in the tails of the distribution, which probability of appearance is overweighted contrary to these observations which are close to the median. Due to this drawback of the traditional z-test statistic the statistical power of a hypothesis test decreases, i.e. the obtained type II error of the test is greater. That is to say, it is more likely to incorrectly accept the null hypothesis H_0 when an alternative hypothesis H_1 is true.

In order to strongly minimize or even fix this disadvantage of the conventional z-test statistic we can redefine (1) in (2) under $H_0 : \mu=\mu_0$.

$$Z_c = \frac{\check{X}-\mu_0}{\sigma_{\check{X}}} \qquad (2)$$

In equation (2) by the $\check{X}$ are denoted either the center or C_2 statistic. The notation $\sigma_{\check{X}}$ means the standard error of the used statistic in the nominator. How both the center and C_2 statistics can be calculated, one can find in the study [1]. The proves, that the above statistics are unbased and more effective than the means are given in [2], where is also shown that (2) is a pivotal quantity and converges to a normal distribution. What is more, as the sample size $n \to \infty$ then the center statistic converges to C_2 statistic.

The main objective of the current article is to demonstrate the higher statistical power of (2) over (1).

Simulations and Results

In order to compare the statistical power of both (1) and (2) four different distributions are used, e.g. binomial, normal, gamma and uniform. Random samples with different sizes based on these distributions are generated 1000 times and the type II error for each iteration is calculated separately for the mean, the center and C_2 statistic. Based on these results the statistical power of (1) and (2) is obtained. All tests are performed with the same significance level $\alpha=0.05$ under the null hypothesis $H_0 : \mu=\mu_0$. The alternative hypothesis is $H_1 : \mu\neq\mu_0$. The parameres of each distribution, the results concerning the distibutions and specific conditions as μ_0 are given in the titles of Table 1, Table 2, Table 3 and Table 4 below.

Table 1

The power of a One Sample Z-Test with use of a B (n, p = 0.9), μ_0 = np-npq/20, α = 0.05

n	Mean	Center	C_2
30	0.205	0.340	0.353
40	0.222	0.384	0.394
50	0.228	0.398	0.407
60	0.257	0.445	0.452
70	0.284	0.482	0.488
80	0.313	0.528	0.533
90	0.340	0.550	0.555
100	0.385	0.612	0.617
200	0.746	0.916	0.917
300	0.937	0.996	0.997
400	0.974	1.000	1.000
500	0.991	1.000	1.000

Table 2

The power of a One Sample Z-Test with use of a Gamma(r = 2, θ = 1), μ_0 = 1.91, α = 0.05

n	Mean	Center	C_2
30	0.185	0.312	0.327
40	0.179	0.311	0.324
50	0.179	0.299	0.310
60	0.181	0.316	0.326
70	0.188	0.319	0.328
80	0.186	0.324	0.333
90	0.202	0.333	0.338
100	0.188	0.341	0.349
200	0.249	0.387	0.392
300	0.280	0.457	0.461
400	0.308	0.502	0.506
500	0.323	0.585	0.588

Table 3

The power of a One Sample Z-Test with use of a N (μ = 0, σ = 1), μ_0 = 0.2, α = 0.05

n	Mean	Center	C_2
30	0.300	0.437	0.449
40	0.341	0.478	0.486
50	0.366	0.517	0.524
60	0.394	0.543	0.548
70	0.440	0.596	0.601
80	0.440	0.616	0.620
90	0.496	0.661	0.664
100	0.525	0.691	0.694
200	0.718	0.855	0.856
300	0.856	0.941	0.942
400	0.927	0.977	0.978
500	0.964	0.993	0.993

Table 4

The power of a One Sample Z-Test with use of a U (a = 0, b = 3.464), μ_0 = 1.93, α = 0.05

n	Mean	Center	C_2
30	0.285	0.413	0.422
40	0.324	0.444	0.450
50	0.361	0.487	0.492
60	0.385	0.503	0.505
70	0.441	0.562	0.565
80	0.459	0.573	0.575
90	0.476	0.581	0.583
100	0.497	0.602	0.604
200	0.726	0.795	0.795
300	0.841	0.880	0.880
400	0.901	0.928	0.930
500	0.959	0.971	0.971

Graphical representations of the results given in Table 1, Table 2, Table 3 and Table 4 are shown in Figure 1 below.

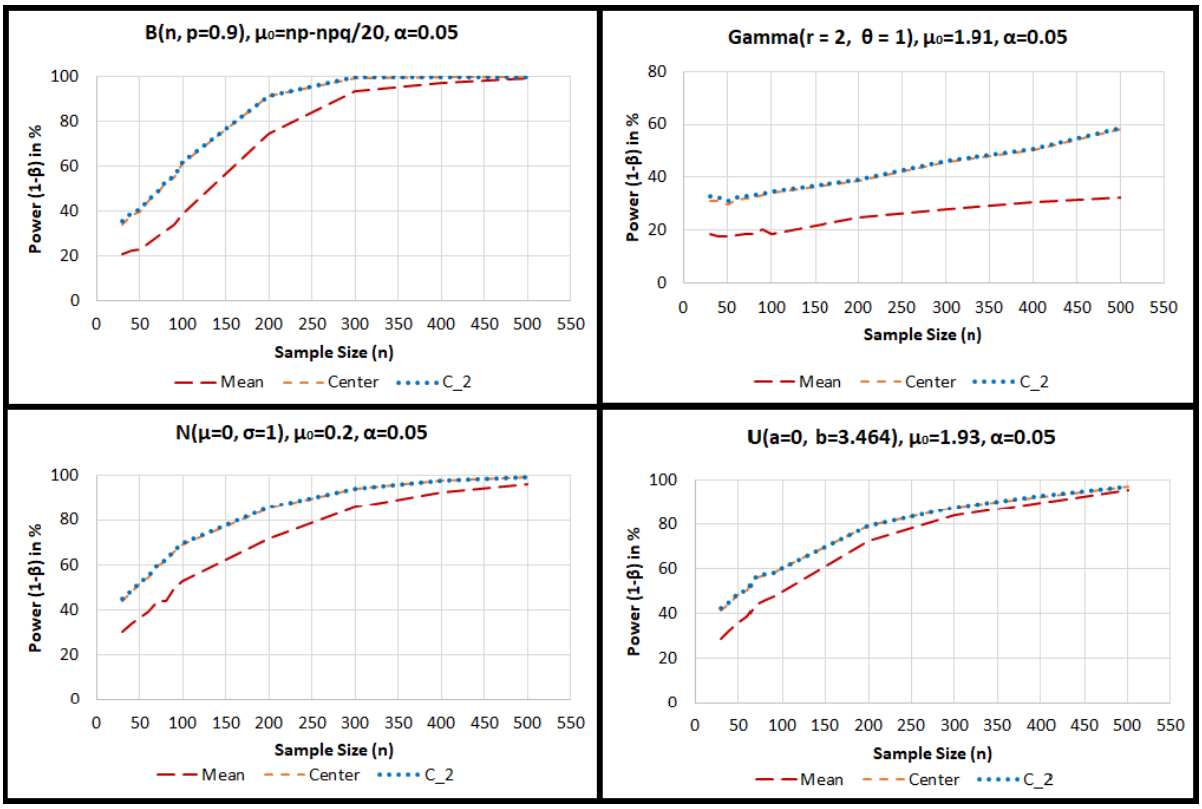

Figure 1: Graphs of the data given in Tables 1-4.

According to the results, which are illustrated above, the following conclusions can be made:

- Even for symmetric distributions as the normal, binomial and uniform the power efficiency of (2) over (1) is almost 0.50%. In case of strongly skewed distribution as the Gamma (2, 1) the power of (2) is approximately 10 times greater than that of (1).
- Apart from the kind of distribution, the statistical power of z-test statistic based on the center approximates these of C_2 statistic, especially when the size of a sample is greater than 100.

A real-data One-Sample Z-Test Example

In order to illustrate the use of (2) with real data let us conider the data given in Sample 1 below.

Sample 1

-0.376	0.046	-0.265	-0.956	0.959	-0.741	0.391	-0.604	-0.364	0.298
-1.068	-1.096	0.498	-0.478	-0.866	0.314	0.836	0.695	0.087	1.093
1.624	0.088	0.125	0.548	0.421	0.468	-1.003	-0.660	1.265	-0.831
0.464	-0.830	0.710	0.386	1.572	0.614	0.392	1.082	0.535	0.813
0.267	0.247	-0.180							

The real numbers in Sample 1 are discrepancies in the sections of the line 2 in the Third Levelling of Bulgaria divided by the length of the corresponding sections. The expectation of these discrepancies is zero, due to the fact that the levelling of each section starts and finishes in the same point and the orthometric height of the point is supposed to be unchangeable during the levelling. Consequently, our test $\mu_0 = 0$. We want to know whether there is any systematic effect in our measurements. We are also interested in if the systematic error is significant on a predefined confidence level $\alpha = 0.05$.

So, we form our null hypothesis $H_0 : \breve{X} = \mu_0$ against the alternative hypothesis $H_1 : \breve{X} \neq \mu_0$. Some impression about the distribution of the standardized discrepancies one can get from the bihistogram given in Figure 2. The results obtained by one-sample z-test by use of the (1) and (2) are given in Table 5.

Table 5

One-Sample Z-Test Results concerning Sample 1, μ_0=0

Description	Notation	Mean	Center	C_2
Expected Value	$\check{X}$	0.1516	0.1968	0.1986
Standard Deviation	σ	0.7291	0.5522	0.5442
Standard Error	$\sigma_{\check{X}}$	0.1112	0.0842	0.0830
Sample Size	n		43	
Z(two-tail, α=0.05)	$Z_{crit.}$		1.96	
Observed Z	$Z_{obs.}$	1.3633	2.3373	2.3928
p-Value($Z_{obs.}$, two-tail)	p-Value	0.1728	0.0194	0.0167
Type II Error	β	0.7241	0.3529	0.3327
Power	1-β	0.2759	0.6471	0.6673

According to the results shown in Table 5, the one-sample z-test based on (1) produced a mean $\bar{X}$ = 0.1516 and $Z_{obs.}$ = 1.3633. The critical z-test statistic Z (two-tail, α=0.05) = 1.96, which is greater than $Z_{obs.}$ = 1.3633. Consequently, the traditional one-sample z-test did not reject the null hypothesis at confidence level α=0.05. In other words, we can claim at 95 % confidence that the mean $\bar{X}$ = 0.1516 is not significantly different from 0 or there is not any significant systematic error in the analyzed discrepancies in line 2.

On the other hand, the results based on (2) by the use of either the center or C_2 statistic show a different picture. Based on their results, the null hypothesis must be rejected due to the fact that $Z_{obs.}$ = 2.3373 > Z (two-tail, α=0.05) = 1.96 and $Z_{obs.}$ = 2.3928 > Z (two-tail, α=0.05) = 1.96 for the center and C_2 statistic, respectively. According to these results, we can conclude that there is a significant systematic error in the discrepancies in the sections in line 2. The systematic error can be assessed to be equal to 0.20 mm/km and its standard error is 0.08 mm/km.

According to the produced type II errors, we should put trust in the results based on (2), the center and C_2 statistics. One can see that the power of (2) is approximately 2.3 times greater than that of (1). More information on how type II error is calculated, one can find in [5].

A real-data Two-Sample Z-Test Example

The previous section presented a hypothesis test for a single population parameter. This section extends the use of the modified z-test statistic, based on either the center or C_2 statistic, to the case of two independent populations. The real numbers in Sample 2 are discrepancies in the sections of line 8 in the Third Levelling of Bulgaria divided by the length of the corresponding sections. The expectation of these discrepancies is zero, due to the same reason given above for the discrepancies in line 2.

Sample 2

0.845	0.727	-0.746	-0.019	1.060	0.604	0.563	0.596	-0.042	0.766
-0.543	-0.678	0.378	-0.352	-1.394	-2.484	-0.623	0.328	-0.175	-0.296
0.246	-0.516	-0.771	-0.961	-0.079	-1.558	0.268	-0.285	0.018	0.073
-0.477	-0.531	-0.231	0.422	-0.612	2.460	-0.542	0.122	0.237	0.354
-0.556	0.772	-0.863	0.247	0.895	-0.021	-0.864	-0.342	-0.697	-0.432

Our task is to test whether the discrepancies in both lines 2 and 8 come from the same population with the location parameter μ=0. Therefore, our null hypothesis H_0 will be given as $H_0 : \mu_1 - \mu_2 = 0$, and the alternative hypothesis H_1 will be defined as $H_1 : \mu_1 - \mu_2 \neq 0$. Consequently, the two-sample z-test statistic can be written as (3).

$$Z_c = \frac{\check{X}_1 - \check{X}_2}{\sqrt{\sigma^2_{\check{X}_1} + \sigma^2_{\check{X}_2}}} \qquad (3)$$

In equation (3), the centers or C_2 statistics of both analyzed samples are denoted by $\check{X}_1$, $\check{X}_2$, and their standard errors are $\sigma_{\check{X}_1}$ and $\sigma_{\check{X}_2}$, respectively. A graphical comparison between Sample 1 and Sample 2 is done by the bihistogram pictured in Figure 2. The two-sample z-test results concerning the means, centers and C_2 statistics are given in Table 6.

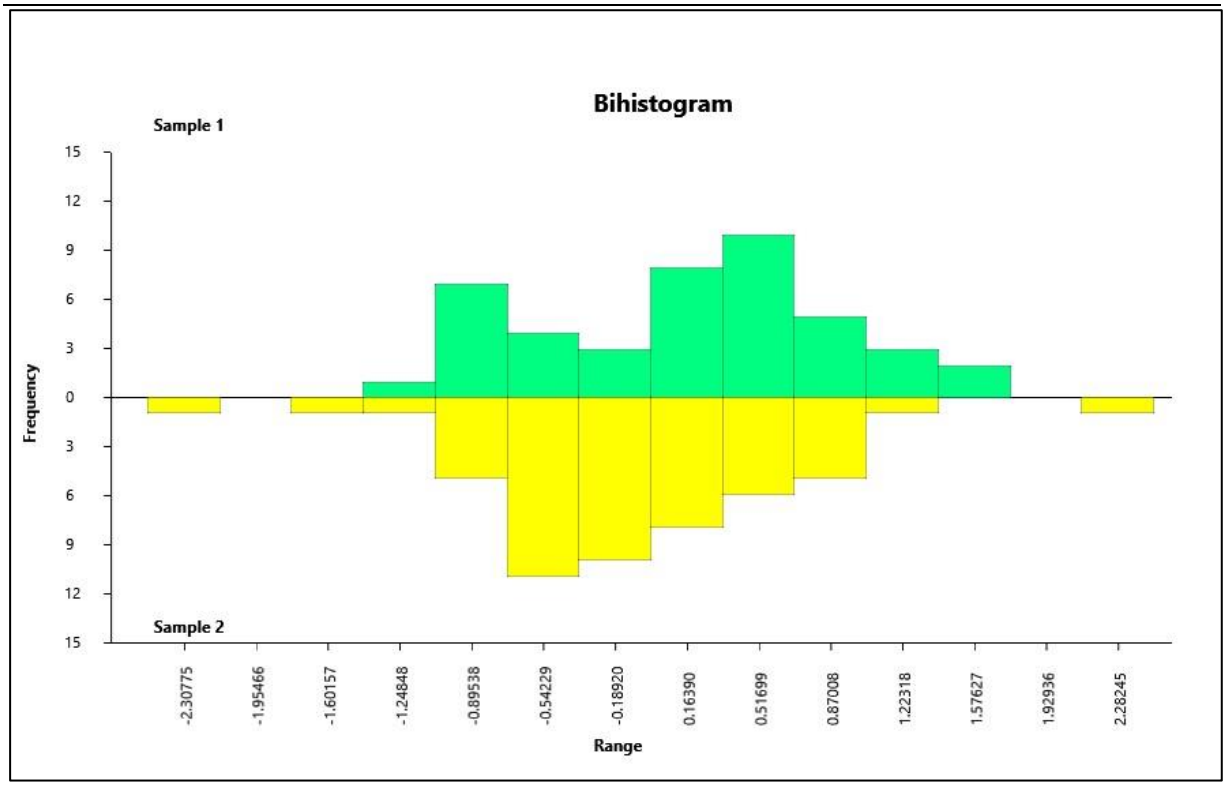

Figure 2: Bihistogram of Sample 1 and Sample 2.

Table 6

Two-Sample Z-Test Results concerning Sample 1 and Sample 2, $\Delta_0=0$

Description	Notation	Mean	Center	C_2
Location 1	$\check{X}_1$	0.1516	0.1968	0.1985
Location 2	$\check{X}_2$	-0.1141	-0.1250	-0.1253
Difference in Locations	$\check{X}_1$-$\check{X}_2$	0.2657	0.3218	0.3239
Standard Error of $\check{X}_1$	$\sigma_{\check{X}_1}$	0.1112	0.0842	0.0830
Standard Error of $\check{X}_2$	$\sigma_{\check{X}_2}$	0.1103	0.0749	0.0736
Z(two-tail, α=0.05)	Zcrit.		1.96	
Observed Z	Zobs.	1.6964	2.8556	2.9196
p-Value($Z_{obs.}$, two-tail)	p-Value	0.0898	0.0043	0.0035
Type II Error	β	0.6038	0.1852	0.1686
Power	1-β	0.3962	0.8148	0.8314

According to the results given in Table 6, the traditional two-sample z-test based on the means did not reject the null hypothesis at confidence level α=0.05, owing to the result of $Z_{obs.}$ = 1.3633 < Z (two-tail, α=0.05) = 1.96. In other words, we can claim at 95 % confidence that the means of both samples 1 and 2 are equal. Moreover, there are no significant systematic errors in the discrepancies of the sections in both lines at used confidence level.

In contrast, the results based on either the center or C_2 statistic shows a different picture. According to these results, the null hypothesis must be rejected, due to the fact that $Z_{obs.}$ = 2.8556 > Z (two-tail, α=0.05) = 1.96 and $Z_{obs.}$ = 2.9196 > Z (two-tail, α=0.05) = 1.96 for the center and C_2 statistic, respectively. According to the results, there is a significant difference in the systematic errors of the section discrepancies in both lines 2 and 8, which even reflect on the different sign of the assessment of the expectations of both samples.

Analyzing Table 6, one can see that the power of the tests based on both the center and C_2 statistics is more than twice greater than that of the traditional variant concerning samples 1 and 2. More information how type II error is calculated, can be found in the book [5]. Additional comparison between traditional two-sample z-test and the proposed here robust variant based on a center statistic are given in [3]. In order to facilitate their calculations concerning z-tests, anyone is invited to test CBSTAT software [4].

Conclusions

In this paper, two more robust modifican of the conventional z-test were proposed. Both statistics the center and C_2 were used in these modifications, instead of the mean. The standard errors of the center and C_2 staristics, respectively were used, instead of the standard error of the sample mean. Through Monte Carlo simulations the statistical power of the traditional z-test and the proposed modifications were compared. It has been shown that the proposed methods overperform the classical one. The simulation results were fully supported by the real data, which were obtained in the Third Levelling of Bulgaria.

In order to use z-test, however, the sample size should be greater than 30 [2] or even greated than 40 [5] . When this requirement does not meet, one should use the robust modifications of t-test based on the center and C_2 statistics. The robust modifications of the one-sample t-test, the paired two-sample t-test and the independent two-sample t-test are going to be presented in future publications.

References

1. Cvetkov V. (2022). ALTERNATIVE MEASURES OF CENTRAL TENDENCY. Deutsche Internationale Zeitschrift Für Zeitgeössische Wissenschaft, 38, 4-8. https://doi.org/10.5281/zenodo.7002877 .

2. Cvetkov V. (2023). THE CENTRAL LIMIT THEOREM AND THE MEASURES OF CENTRAL TENDENCY. Deutsche Internationale Zeitschrift Für Zeitgenössische Wissenschaft, 49, 14-21. https://doi.org/10.5281/zenodo.7594733.

3. https://center-based-statistics.com/html/zTest.html , (visited on 14.03.2023)

4. https://center-based-statistics.com/html/download.php, (visited on 14.03.2023)

5. Montgomery, Douglas C.; Runger, George C. (2014). Applied Statistics and Probability for Engineers (6th ed.). Wiley. ISBN-13 9781118539712.

MEDICAL SCIENCES

CLINICAL AND HEMATOLOGICAL ASPECTS OF PRIMARY MYELOFIBROSIS

Andrianova A.,
student, Faculty of General Medicine, SUMPh "Nicolae Testemitanu"
Chisinau, Republic of Moldova
Musteata L.
Associate Professor of the Department of Hematology
SUMPh "Nicolae Testemitanu"
Chisinau, Republic of Moldova
DOI: 10.5281/zenodo.7857980

КЛИНИКО-ГЕМАТОЛОГИЧЕСКИЕ АСПЕКТЫ ПЕРВИЧНОГО МИЕЛОФИБРОЗА

Андрианова А.,
студентка, Факультет общей медицины, USMF „Nicolae Testemițanu"
Кишинёв, Республика Молдова
Мустяцэ Л.
Доктор медицинских наук,
доцент Дисциплины Гематологии,
ГУМФ им. Николае Тестемицану
г. Кишинёв, Республика Молдова

Abstract

Primary myelofibrosis (PMF) is a chronic clonal stem cell disease that causes an accumulation of marrow fibrosis and dysfunction, hypermetabolic states, and extramedullary myeloid metaplasia. The onset of the disease is often asymptomatic, which causes a late referral to a specialist, the disease being already confirmed in the fibrotic stage with a massive splenomegaly, which lowers the survival rate of patients with an established diagnosis. The insufficiency of data on clinical aspects, manifestations, risk factors, treatment and prognosis of PMF in the Republic of Moldova, served as the purpose for studying the given pathology in order to avoid the increase in morbidity, frequent relapses of the disease, the appearance of immune complications of the disease that can lead to death patients [1].

Аннотация

Первичный миелофиброз (ПМФ) представляет собой хроническое клональное заболевание стволовых клеток, которое вызывает накопление фиброза и дисфункции костного мозга, гиперметаболические состояния и экстрамедуллярную миелоидную метаплазию. Начало заболевания часто бессимптомное, что обусловливает позднее обращение к специалисту и соответственно установление диагноза уже в фиброзной стадии с массивной спленомегалией. Это снижает выживаемость больных с установленным диагнозом. Недостаточность данных о клинических аспектах, проявлениях, факторах риска, лечении и прогнозе ПМФ в Республике Молдова послужили целью изучения данной патологии, во избежание роста заболеваемости, частых рецидивов заболевания, возникновения иммунных и других осложнений заболевания, которые могут привести к летальному исходу пациента [1].

Keywords: primary myelofibrosis, myeloproliferative disease, Janus kinase 2, splenomegaly, extramedullary hematopoiesis.

Ключевые слова: первичный миелофиброз, миелопролиферативная болезнь, Янус киназа 2, спленомегалия, экстрамедулярный гемопоэз.

Вступление

ПМФ представляет собой хроническое злокачественное гематологическое заболевание, характеризующееся спленомегалией, лейкоэритробластозом, пойкилоцитозом (дакриоцитами), некоторой степенью фиброза костного мозга, увеличением плотности микрососудов костного мозга и экстрамедуллярным гемопоэзом [1; 2; 3]. Заболевание имеет полиэтиологический характер возникновения заболевания, при котором предрасположенность создается под влиянием внешних факторов, воздействующих на геном здоровой клетки и приводящих к ее злокачественному перерождению [4; 5]. У небольшого числа пациентов заболевание связано с радиацией и воздействием нефтехимических веществ, таких как бензол и толуол. Мутации в гене янус-киназы 2 (JAK2) присутствуют в высокой доле случаев первичного миелофиброза. Мутации в гене рецептора тромбопоэтина или гене кальретикулина также могут вызывать заболевание [6]. Согласно классификации миелопролиферативных новообразований, основанной на диагностических критериях ВОЗ 2008 г., ПМФ относится к группе филадельфийских хромосом-

негативных миелопролиферативных новообразований вместе с истинной полицитемией и эссенциальной тромбоцитемией. Описываются 2 стадии заболевания: префибротическая и фиброзная. Префибротическая стадия может клинически имитировать эссенциальную тромбоцитемию. Эта стадия прогрессирует от гиперпролиферации мегакариоцитов с тромбоцитозом от умеренного до выраженного (88% ≥ 500 × 10^9/Л), иногда с тромбозом или кровотечением, легкой анемией, лейкоцитозом от легкого до умеренного и отсутствием или умеренной спленомегалией, до классического первичного миелофиброза. Фиброзная стадия проявляется прогрессирующей анемии и гепато-, спленомегалии, связанными с гиперкатаболическими чертами усталости, похудания, ночной потливости и субфебрильности. Пациенты также обращаются с такими симптомами как тяжесть в левом подреберье, раннее насыщение и/или диспепсия из-за эффектов давления при увеличении селезенки [6; 7; 8].

Симптомы болезни разнообразны и зависят от степени прогрессирования заболевания. Первичными симптомами являются утомляемость, головная боль, бледность, головокружение, ночная потливость, похудание. Доминирующим и наиболее часто встречаемым, является спленомегалия и гепатомегалии, которые медленно и постепенно прогрессируют. Селезенка может достигать гигантских размеров, занимая всю левую и правую половину живота. Она толстая, бугристая. Сопровождается болевым синдромом в правом подреберье. Массивная спленомегалия вызывает нарушение регуляции экскурсии легких, что играет важную роль при инфекционной пневмонии. При гепатомегалии печень трудно пальпируется и редко вызывает болевой синдром. Портальная гипертензия может возникать из-за заметного увеличения печеночного кровотока и внутрипеченочной обструкции. В основе геморрагического синдрома чаще всего лежит тромбоцитопения, обусловленная снижением продукции тромбоцитов: число тромбоцитов ниже 100×10^9/Л, повышенное отложение тромбоцитов, разрушение в увеличенной селезенке. Картина периферической крови при эритремической или форме Воган: гемоглобин повышен более 160 г/л, эритроциты более 6×10^9/Л. Анемическая форма проявляется снижением гемоглобина ниже 100 г/л, ретикулоцитозом с выраженным гемолизом. По мере прогрессирования заболевания нарастает анемия, отмечают полихроматию, анизоцитоз, пойкилоцитоз, появляются каплевидные клетки, ядросодержащие эритроциты. Для тромбоцитемической формы более характерен тромбоцитоз с показателями тромбоцитов более 400 х 10^9/Л. Классическая форма характеризуется умеренной гиперплазией гранулоцитарных и мегакариоцитарных почек, с легкой степенью мегакариоцитоза. Для больных характерна лейкоэритробластическая картина периферической крови [9; 10].

Для диагностики заболевания имеют значение данные объективного клинического обследования, общего анализа крови, биохимического анализа крови, которые свидетельствуют о возможном повышении уровня молочной кислоты, билирубина, мочевой кислоты, щелочной фосфатазы, лактатдегидрогеназы. Наиболее информативным методом является трепанобиопсия, позволяющая выявить характерную фибробластическую картину. Количество фиброзной ткани сильно варьирует в зависимости от стадии заболевания. В начале заболевания костный мозг выглядит гиперклеточным с повышенным количеством эритробластов, гранулоцитов, мегакариоцитов и фибробластов. По мере прогрессирования заболевания костный мозг становится гиперклеточным или гипопластическим [11]. Также имеет клиническое значение анализ мутаций JAK2. Отклонения такого рода, положительны примерно в 50% случаев, но отрицательные результаты анализов не исключают наличия заболевания [12]. Радиологические исследования, такие как рентгенография, КТ, ПЭТ-КТ, являются базовыми методами выявления спленомегалии, гепатомегалии, экстрамедуллярного кроветворения, остеосклероза [13; 14; 15].

Заболевание может осложняться анемией, причиной которой может быть недостаточность костного мозга или секвестрация эритроцитов в селезенке, экстрамедуллярное кроветворение, портальная гипертензия, подагра или мочекаменная болезнь почек. На фоне угнетения имунной системы, возможны осложнения инфекционного типа [16].

При постановке диагноза и оценке прогноза заболевания используется Международная прогностическая система оценки (IPSS) для миелодиспластических синдромов, используемая для впервые диагностированного первичного миелофиброза, а для прогнозирования может использоваться Международная динамическая прогностическая система оценки (DIPSS) для миелодиспластических синдромовб которая моет выявить прогрессирование или определить выживаемость по мере прогрессирования заболевания. IPSS для ПМФ использует 5 факторов риска при оценке прогноза: возраст > 65 лет (1 балл); гемоглобин <100 г/л (1 балл); лейкоциты >25,0 × 10^9/Л (2 балла); наличие бластных клеток ≥1% (1 балл); конституциональные симптомы (1 балл). Больные имеющие 0 баллов, относятся к группе низкого риска, имеющие 1 фактор относятся к группе промежуточного риска 1, имеющие 2 балла относятся к группе промежуточного риска 2, а те у кого ≥3 относятся к группе высокого риска. В систему DIPSS к вышеперечисленным добавляются следующие факторы: неблагоприятный кариотип, потребность в гемотрансфузии, уровень тромбоцитов <100,0 х 10^9/Л или ≥100,0 х 10^9/Л. [17; 18; 19].

Лечение проводят в зависимости от выраженности проявления симптомов заболевания. В случае больных с селезенкой умеренных размеров, отсутствием тромбоцитоза, лейкоцитоза в общем анализе крови, назначают симптоматическое лечение заключающееся в назначении препаратов железа, витаминотерапии, эротропоэтина, дезагрегантов, кровопусканий. Лечение цитостатиками назначают

для купирования гипертромбоцитоза и уменьшения размеров селезенки при наличии спленомегалии. Среди цитостатиков используются Гидроксикарбамид, Милеран, Циклофосфамид, 6-меркаптопурин, Цитарабин. Учитывая патогенез ПМФ, не малое значение имеют ингибиторы гена JAK2. Таким предтавителем является Руксолитиниб, который уменьшает размер селезенки, утомляемость, ночную потливость, зуд, а также потребность в переливании эритроцитов и может привести к увеличению массы тела. Спленэктомия применяется у пациентов с гемолизом, тромбоцитопенией, болезненной спленомегалией, рецидивирующим инфарктом селезенки и портальной гипертензией. Пациенты с подтвержденным дефицитом питательных веществ должны получать фолиевую кислоту, препараты железа или и то, и другое. Пациенты с гемолитической анемией должны получать фолиевую кислоту и трансфузионную терапию эритроцитарной массы. Кортикостероиды назначают при аутоиммунной тромбоцитопении и аутоиммунном гемолизе эритроцитов. Единственным радикальным методом лечения ПМФ является аллогенная трансплантация стволовых клеток (TACS), но она имеет определенные факторы риска для показаний к этой процедуре, такие как возраст старше 60 лет, гепатомегалия, потеря веса, белый количество клеток крови < 4,0 х 109/л и > 30,0 х 109/л, низкое количество тромбоцитов и хромосомные аномалии и зачастую ведет к ранней смертности пациентов [20; 21; 22]

Материалы и методы

Клинико-гематологические аспекты первичного миелофиброза изучались у 60 больных, состоявших на учете у врачей-гематологов Гематологического центра Института онкологии Республики Молдова, в возрасте от 30 до 85 лет (средний возраст 57,5 лет). Для исследования были отобраны 28 мужчин и 32 женщины. Диагноз устанавливали по морфологическим изменениям, соответствующим миелопролиферативному заболеванию и выявленным при трепанобиопсии подвздошной кости. Наиболее частым симптомом была сплено-/гепатомегалия, которая выявлялась при пальпации больных и подтверждалась при ультразвуковом исследовании. В общем анализе крови часто выявляли анемию, тромбоцитемию/тромбоцитоз, умеренный лейкоцитоз с отклонением влево с появлением небольшого процента миелоцитов, метамиелоцитов. Клиническое стадирование ПМФ проводилось в соответствии с классификацией миелоидных новообразований ВОЗ 2018 г., в которой выделены префибротическая и фиброзная стадии заболевания. Для стадирования патологического процесса больным проводили следующие исследования: мазок периферической крови, трепанобиопсию подвздошной кости с морфологическим и иммуногистохимическим исследованием биоптата. Обработанный материал табулировался с помощью простых, групповых и комбинированных таблиц. Статистическую обработку результатов исследования проводили компьютеризированными методами вариационного анализа с использованием специальных программ (Microsoft Office Excell 2013 для MAC IOS). При анализе первичных данных рассчитывались проценты и средние значения. Для оценки общей выживаемости больных изучали период времени между датой подтверждения диагноза и летальным исходом. Для этого был использован табличный метод формирования кривых выживания, предложенный Капланом Э. и Мейером П..

Результаты

Отсутствие специфических клинико-гематологических признаков в начале заболевания повлияло на то, что у 57 (95%) больных диагноз был установлен уже в фиброзной стадии заболевания. Только у 27 (45%) больных заболевание было установлено в первые 3 месяца от появления клинических симптомов и первого обращения к врачу. При этом у 11 (18,3%) больных на установление диагноза ушло 12 месяцев. Наиболее важными и значимыми клиническими признаками были спленомегалия у 54 (90%) пациентов и гепатомегалия у 42 (70%) пациентов. В общих анализах крови уровень гемоглобина колебался от 75 г/л до 211 г/л. Форма Вогана была выявлена у 9 (15%) больных. Уровень лейкоцитов от 4,0 до 13,0 х 10^9/Л. Уровень тромбоцитов варьировал от 312 до 690 х 10^9/Л. В лейкоцитарной формуле выявлен сдвиг влево, с появлением метамиелоцитов и миелоцитов в периферической крови. Первичный миелофиброз во всех случаях подтверждался клинико-морфологическим исследованием и трепанобиопсией подвздошной кости. Для уточнения диагноза, помимо физикального обследования больных, ультразвуковое исследование органов брюшной полости, рентгенологическое исследование, генетический тест JAK2. Аутоиммунная гемолитическая анемия диагностирована в 10 (16,6%) случаях, аутоиммунная тромбоцитопения в 4 (6,6%) случаях. Лечение проводилось Гидроксикарбамидом, Милераном и Интерфероном-α. При форме Воган выполнялась флеботомия. По данным проведенного исследования выявлены факторы риска, такие как: возраст пациента > 65 лет, уровень гемоглобина > 100 х 10^9/Л, уровень лейкоцитов > 25 х 10^9/Л, выявление бластных клеток >1%, наличие конституциональной клинических признаков. Они играют важную роль в общей выживаемости пациентов. После первого года общая выживаемость составила 96,1%, через 3 и 5 лет — 90,5%.

Выводы

Все собранные данные и полученные результаты доказывают нам, что первичный миелофиброз является заболеванием, которое поддается контролю. За счет тщательного наблюдения врачей-специалистов, своевременно установленного диагноза и предпринятых мер лечения, а так же строгости в соблюдении предписанного лечения, качество жизни пациентов может быть улучшенно, течение заболевания продленно, а выживаемость увеличенна.

References

1. Arber D. A., Orazi A., Hasserjian R., et al. The 2016 revision to the World Health Organization classification of myeloid neoplasms and acute leukemia. In: Blood, The Journal of the American Society of Hematology. 2016, nr. 127(20), pp. 2391-2405;
2. Butina M., Richards N., Singh I., et al. Primary Myelofibrosis. In: International Journal of Biomedical Laboratory Science. 2021, nr.10, pp 102-111;
3. Guglielmelli P., Pancrazzi A., Bergamaschi G., et al. Anaemia characterises patients with myelofibrosis harbouring MplW515L/K mutation. In: British journal of haematology. 2007, nr. 137(3), pp. 244-247;
4. Abdulkadyrov K. M., Shuvaev V. A., and Martynkevich I. S. Primary mielofibrosis: own experience and news from diagnostic and treatment. In: Oncohematology. 2015, nr. 2, pp. 26-36;
5. Ghukasyan D. Extramedullary Stress Erythropoiesis as an Adaptive Response to High-Altitude Hypoxemia. University of California, Riverside, 2022, 33p;
6. Guglielmelli P., Pancrazzi A., Bergamaschi G., et al. Anaemia characterises patients with myelofibrosis harbouring MplW515L/K mutation. In: British journal of haematology. 2007, nr. 137(3), pp. 244-247;
7. Tefferi A., Thiele J., & Vardiman J. W. The 2008 World Health Organization classification system for myeloproliferative neoplasms: order out of chaos. In: Cancer: Interdisciplinary International Journal of the American Cancer Society. 2009, nr. 115(17), pp. 3842-3847;
8. Thiele J., Kvasnicka H. M., Facchetti F., et al. European consensus on grading bone marrow fibrosis and assessment of cellularity. In: haematologica. 2005, nr. 90(8), pp. 1128-1132;
9. Provan D., Singer C. R., Baglin T., Oxford handbook of clinical haematology. Volumul 4. Oxford university press., 2009, 870 p;
10. Мещарикова Л.М., Пороткова О.В., Ковалева Л.Г., et al. Первичный миелофиброз. Онкогематология. 2011, (4), с 50-58;
11. Agarwal A., Morrone K., Bartenstein M. Bone marrow fibrosis in primary mielofibrosis: pathogenic mechanisms and the role of TGF-b. In: Stem Cell investigation, 2016; nr. 3: 5;
12. Ассесорова Ю. Ю. Аномалии кариотипа при хронических миелопролиферативных новообразованиях. Вестник гематологии, 2022, том 8, (3), 32-39.
13. Oon S. F., Singh D., Tan T. H., et al. Primary myelofibrosis: spectrum of imaging features and disease-related complications. In: Insights into Imaging. 2019, nr. 10(1), pp. 1-14;
14. Roberts A. S., Shetty A. S., Mellnick V. M., et al. Extramedullary haematopoiesis: radiological imaging features. In: Clinical radiology. 2016, nr. 71(9), pp. 807-814;
15. Vancauwenberghe T., Snoeckx A., Vanbeckevoort D., et al. Imaging of the spleen: what the clinician needs to know. In: Singapore medical journal. 2015, nr. 56(3), pp. 133;
16. Corcimaru I. F. Hematologie. Chișinău , Centrul editorial-poligrafic Medicina, 2007, 387p;
17. Cervantes F., Dupriez B., Pereira A., et al. New prognostic scoring system for primary myelofibrosis based on a study of the International Working Group for Myelofibrosis Research and Treatment. In: Blood, The Journal of the American Society of Hematology. 2009, nr. 113(13), pp. 2895-2901;
18. Gangat N., Caramazza D., Vaidya R., et la. DIPSS plus: a refined Dynamic International Prognostic Scoring System for primary myelofibrosis that incorporates prognostic information from karyotype, platelet count, and transfusion status. In: Journal of Clinical Oncology. 2011, nr. 29(4), pp. 392-397;
19. Passamonti F., Cervantes F., Vannucchi A. M., et al. A dynamic prognostic model to predict survival in primary myelofibrosis: a study by the IWG-MRT (International Working Group for Myeloproliferative Neoplasms Research and Treatment). In: Blood, The Journal of the American Society of Hematology. 2010, nr. 115(9), pp. 1703-1708;
20. Cervantes F. How I treat splenomegaly in myelofibrosis. In: Blood cancer journal. 2011, nr. 1(10), pp. 37;
21. Cervantes F. Modern management of myelofibrosis. In: British journal of haematology. 2005, nr. 128(5), pp. 583-592;
22. Hoffman R., Benz Jr E. J., Silberstein L. E., et al. Hematology: basic principles and practice. Volumum 6, Elsevier Health Sciences, 2013, 2679 p;

CARDIAC REHABILITATION OF PATIENTS FOLLOWING MYOCARDIAL INFARCTION

Badan Maxim
medical student, Republic of Moldova
DOI: 10.5281/zenodo.7796010

Abstract

In 2017, mortality from cardiovascular diseases made up 58.4% of all deaths, of which ischemic heart disease (IHD) constituted 52.5% and 8.5% were due to acute myocardial infarction.

Cardiovascular rehabilitation is used to optimize the physical, psychological and social functioning of the patient who suffered a myocardial infarction. The session includes 3 phases: the warm-up, the actual training and the recovery (relaxation) phase. The program is individualized, so it is necessary to correctly select the type, intensity, duration and frequency for maximum therapeutic effect.

Exercise-based medical rehabilitation is a supplement to drug therapy and post-infarction interventional surgery, as it improves cardiopulmonary function, optimizes drug therapy, decreases risk factors, increases exercise tolerance, improves mental status, reduces the risk of repeated heart attack and cardiac mortality, and contributes to a successful return to work.

Keywords: Myocardial infarction, cardiovascular rehabilitation, physical exercises

Introduction

The incidence of myocardial infarction is continuously increasing. In 2015, mortality from cardiovascular diseases reached 17 million (31%) of the total of 54 million deaths worldwide, of which the share of coronary diseases constituted 48%.

Annually cardiovascular diseases cause 3.9 million (45%) deaths in Europe and over 1.8 million (37%) deaths in the European Union (EU). The global cost of CVD for the EU economy was estimated at 210 billion euro per year. [2]

The mortality of patients with STEMI is influenced by multiple factors, among them advanced age, Killip class, delay in treatment, the existence of STEMI networks based on the emergency medical system, therapeutic strategy, the presence of antecedents of myocardial infarction, diabetes, renal insufficiency, the number of coronary arteries the ejection fraction of the left ventricle is also affected.[3] Although the incidence of myocardial infarction is low in industrialized countries, partly due to improved health systems and the implementation of effective public health strategies, it is increasing in developing countries such as South Asia, parts of Latin America, and Eastern Europe. [4]

The term "cardiac rehabilitation" refers to coordinated interventions aimed at optimizing the physical, psychological and social functioning of the cardiac patient, in addition to stabilizing, slowing or even reversing the progression of the underlying atherosclerotic processes, thereby reducing morbidity and mortality.

The program involves education, exercise, risk factor modification, and counseling. It is targeted by specialized medical personnel and adapted to each individual.

The recovery of patients with cardiovascular diseases has positive results because it improves exercise tolerance, thus leading to a decrease in mortality.

A meta-analysis based on a review of 48 randomized trials comparing the outcomes of exercise-based rehabilitation with usual care showed a 20% reduction in total mortality and a 26% reduction in the cardiac death rate with exercise-based rehabilitation physical. [5]

As a consequence, healthcare professionals have designed cardiac rehabilitation (CR) programs for patients with MI. RC generally consists of three phases:

I - acute phase of CR after an acute event (1-14 days)

II - Second phase of cardiac rehabilitation (1-6 months)

III - The third (maintenance) phase of cardiac rehabilitation (6-12 months) [6]

RC aims at physical recovery, improvement of quality of life, psycho-social health and a decrease in the recurrence of hospitalization and death.

Aim of the study:

Studying the influence of therapeutic physical exercise complexes used in the rehabilitation of patients with myocardial infarction to assess the beneficial effects on health.

Results:

Literature data suggest the importance of medical rehabilitation treatment for post-infarction patients in combination with pharmacological treatment. The session includes 3 phases: the warm-up, the actual training and the recovery (relaxation) phase. The program is individualized, so it is necessary to correctly select the type, intensity, duration and frequency for maximum therapeutic effect, periodically 3 to 5 sessions per week, with the recommended duration from 20 to 60 minutes. The criterion to dose physical effort is frequency of cardiac contractions. [7]

The warm-up period, which aims to increase myocardial blood supply, increase the flexibility of soft tissues, joint mobilization.

The actual, supervised training is considered optimal with a duration of 20-30 minutes; it has been shown by numerous studies that the best results are obtained through anaerobic exercises that include repetitive movements and engage large muscle groups. [8]

The recovery period consists of performing low-intensity exercises and stretching; gradual recovery prevents the appearance of rhythm disturbances.

The beneficial effects are:

1) Anti-atherosclerotic, due to improving the lipid profile, increasing insulin sensitivity.

2) Anti-ischemic -decreasing myocardial O2 demand, increasing coronary flow.

3) Antithrombotic - decrease in platelet aggregation, increase in fibrinolysis, decrease in fibrinogen, decrease in blood viscosity.

4) Antiarrhythmic-increasing vagal tone, decreasing adrenergic activity. [9][10]

Conclusions:

Exercise-based medical rehabilitation is a supplement to drug therapy and post-infarction interventional surgery, as it improves cardiopulmonary function, optimizes drug therapy, decreases risk factors, increases exercise tolerance, improves mental status, hemodynamic and metabolic function, reduces the risk of reinfarction and cardiac mortality. As part of a cardiac rehabilitation program, physical activity helps reduce psychological maladjustment and contributes to a successful return to work.

References

1 Fourth universal definition of myocardial infarction (2018) European Heart Journal, Volume 40, Issue 3, 14 January 2019, Pages 237–269, https://doi.org/10.1093/eurheartj/ehy462

2 WILKINS, E., et al. European Cardiovascular Disease Statistics 2017. In: European Heart Network. Brussels. 2017. 192 pagini. www.ehnheart.org

3 2015 ESC Guidelines for the management of acute coronary syndromes in patients presenting without persistent ST-segment elevation: Task Force for the Management of Acute Coronary Syndromes in Patients Presenting without Persistent ST-Segment Elevation of the European Society of Cardiology (ESC). European Heart Journal, Volume 37, Issue 3, 14 January 2016, Pages 267–315, https://doi.org/10.1093/eurheartj/ehv320

4 Chadwick Jayaraj, J., Davatyan, K., Subramanian, S. S., & Priya, J. (2019). Epidemiology of Myocardial Infarction. Myocardial Infarction. doi:10.5772/intechopen.74768

5 Leon, A. S. (2005). Cardiac Rehabilitation and Secondary Prevention of Coronary Heart Disease: An American Heart Association Scientific Statement From the Council on Clinical Cardiology (Subcommittee on Exercise, Cardiac Rehabilitation, and Prevention) and the Council on Nutrition, Physical Activity, and Metabolism (Subcommittee on Physical Activity), in Collaboration With the American Association of Cardiovascular and Pulmonary Rehabilitation. Circulation, 111(3), 369–376. doi:10.1161/01.cir.0000151788.08740.5c

6 Piepoli, M. F., Corrà, U., Benzer, W., Bjarnason-Wehrens, B., Dendale, P., Gaita, D., … Schmid, J.-P. (2010). Secondary prevention through cardiac rehabilitation: from knowledge to implementation. A position paper from the Cardiac Rehabilitation Section of the European Association of Cardiovascular Prevention and Rehabilitation. European Journal of Cardiovascular Prevention & Rehabilitation, 17(1), 1–17. doi:10.1097/hjr.0b013e3283313592

7 Dr Arthur S. Leon (2000). Exercise Following Myocardial Infarction. , 29(5), 301–311. doi:10.2165/00007256-200029050-00002

8 Pollock, M. L., Gaesser, G. A., Butcher, J. D., Desprs, J.-P., Dishman, R. K., Franklin, B. A., & Garber, C. E. (1998). ACSM Position Stand: The Recommended Quantity and Quality of Exercise for Developing and Maintaining Cardiorespiratory and Muscular Fitness, and Flexibility in Healthy Adults. Medicine & Science in Sports & Exercise, 30(6), 975–991. doi:10.1097/00005768-199806000-00032

9 Ekblom, Orjan; Ek, Amanda; Cider, Åsa; Hambraeus, Kristina; Börjesson, Mats (2018). Increased Physical Activity Post–Myocardial Infarction Is Related to Reduced Mortality: Results From the SWEDEHEART Registry. Journal of the American Heart Association, 7(24), –. doi:10.1161/JAHA.118.010108

10 Xing, Ying; Yang, Si-Dong; Wang, Man-Man; Feng, Ya-Shuo; Dong, Fang; Zhang, Feng (2020). The Beneficial Role of Exercise Training for Myocardial Infarction Treatment in Elderly. Frontiers in Physiology, 11(), 270–. doi:10.3389/fphys.2020.00270

CELLULAR AND INTRACELLULAR REGENERATION. CURRENT ASPECTS

Buzuc I.V.
Undergraduate Student
Nicolae Testemițanu State University of Medicine and Pharmacy
bd. Ştefan cel Mare şi Sfânt 165, Chişinău, Republic of Moldova
DOI: 10.5281/zenodo.7796020

Abstract

Regeneration refers to the process by which organisms repair and replace damaged or lost cells, tissues or organs. This process is essential for maintaining health. Regeneration can occur in several ways, depending on the type of tissue or organ and the severity of the injury. Some cells, can replace quickly, while other cells, can be much more difficult to replace or regenerate. Cellular regeneration refers to the process by which cells replace damaged or lost ones. This process can be different depending on cell type and tissue, as some cells may have a greater ability to multiply and replace than others. Intracellular regeneration refers to the process by which cells can repair their individual cellular components, such as proteins, organelles, or damaged DNA.

The article represents a narrative synthesis of specialized literature, with the aim of explaining the mechanisms of cellular and intracellular regeneration that take place in the human body.

Keywords: differentiation, epithelia, hypertrophy, myocardium, proliferation, regeneration, stem cells.

Mechanisms of cellular and intracellular regeneration

Regeneration consists of two distinct stages – proliferation and differentiation. These stages are more obviously expressed in the case of cellular regeneration. At the proliferation stage, young and undifferentiated cells multiply. These cells are called cambial cells (lat. cambium – "change") or stem cells. In the differentiation stage, young cells mature and improve structurally and functionally. This modification, of increasing ultrastructure by differentiation (or maturation), is the main mechanism of regeneration at the intracellular level. As regeneration occurs at the intracellular level, the restoration of tissue structure and function can occur at different levels (repair of DNA, formation of new enzymes, increase in the number of mitochondrial cristae, enlargement of ER cisternae, synthesis of new mitochondria, ribosomes, etc.). [2,14]

Classification of tissues according to the form of regeneration

In phylogeny and ontogeny, the structural and functional specialization of tissues has led to selection favoring a predominantly cellular form in some tissues, a predominantly or exclusively intracellular form in others (Table 1). [12]

Table 1

Forms of regeneration in various tissues

Cellular regeneration	Intracellular regeneration	
Bone tissue Epithelial tissues Loose connective tissue Hematopoietic tissue Lymphoid tissue	Predominantly cardiac tissue	Exclusively the central nervous system (pyramidal, ganglion cells, etc.)

In some tissues such as epithelial or hematopoietic ones, the cellular form of regeneration is predominant over the intracellular one. In simple terms, the process by which these tissues are regenerated involves cell division, followed by the differentiation and specialization of some of the resulting daughter cells. After cell division, undifferentiated daughter cells remain in an undifferentiated state and act as reserve stem cells. As old cells age and die, stem cells begin to divide to produce new daughter cells. Following this division, one of the daughter cells differentiates and specializes to take over the role of the dead cell, while the other remains as a stem cell. Thus, the number of stem cells is kept constant, ensuring constant tissue regeneration and repair. [2,8]

In the case of the central nervous system (including ganglion cells and pyramidal cells) and myocardium, intracellular regeneration is the sole or predominant form of regeneration, and these tissues lack stem cells. In these cases, the cells that are in the process of differentiation lose their ability to proliferate irreversibly, which leads to a stability of the total number of cells. Over time, part of the cells die irreversibly through apoptosis, and this process intensifies with the aging of the body. [2,8,12,14]

Cellular regeneration of epithelia

Epithelial tissues are normally in a state of continuous renewal, and their regenerative capacities are very high and are achieved through the mitotic proliferation of stem cells, that is, at the cellular level. The skin epithelium has the highest capacity for regeneration at the cellular level. [8,12]

Through cell division, epithelial stem cells produce new cells that differentiate into mature epithelial cells similar to those lost. Stem cells in stratified epithelium are found in the basal layer, whereas in monolayer epithelium, such as that of the small intestine, they are located in the crypts. In the case of mesothelium,

stem cells are among the mesotheliocytes. The ability of most epithelia to regenerate serves as the basis for their rapid recovery process under pathological conditions, known as reparative regeneration. [12,15,16]

A constant physiological regeneration takes place in the glands as they carry out their secretory activity. Merocrine and apocrine glands contain long-lived cells, and their regeneration after secretion occurs by intracellular regeneration processes and sometimes by proliferation. In contrast, in holocrine glands, regeneration occurs through the division of stem cells from the excretory ducts, and the new cells, through differentiation, become glandular cells. [8,12]

Epidermal stem cells (EpiSCs) are primarily responsible for the regeneration of this tissue, as they have the ability to differentiate into several cell types. EpiSCs have the ability to multiply indefinitely and are mainly located in three separate areas: in the basal layer of the epidermis, in the bulb area of the hair follicle, and at the base of the sebaceous glands. The stem cells in the basal layer are responsible for the development of keratinizing epithelial cell lines under physiological conditions and ensure regeneration in case of superficial damage to the epidermal covering. The other group of stem cells is responsible for the development of superficial epitheliocytes, hair and glands, and is involved in the regeneration of deep and extensive skin lesions (pic.1). [9,12,13,16,19]

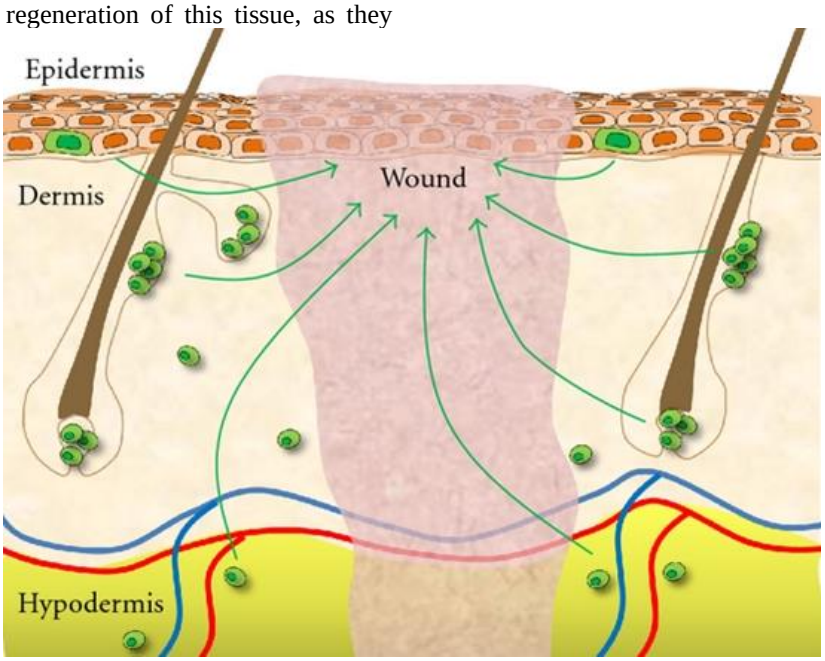

Pic.1. Location of epidermal stem cells

Stem cells have the ability to differentiate into a variety of specialized cells, but they also divide to maintain a constant number of similar stem cells through symmetric or asymmetric division (pic.2). In the asymmetric division model, a stem cell generates a differentiated cell and another stem cell. On the other hand, under the symmetric division model, one stem cell produces either two differentiated cells or two stem cells. [11,18,19]

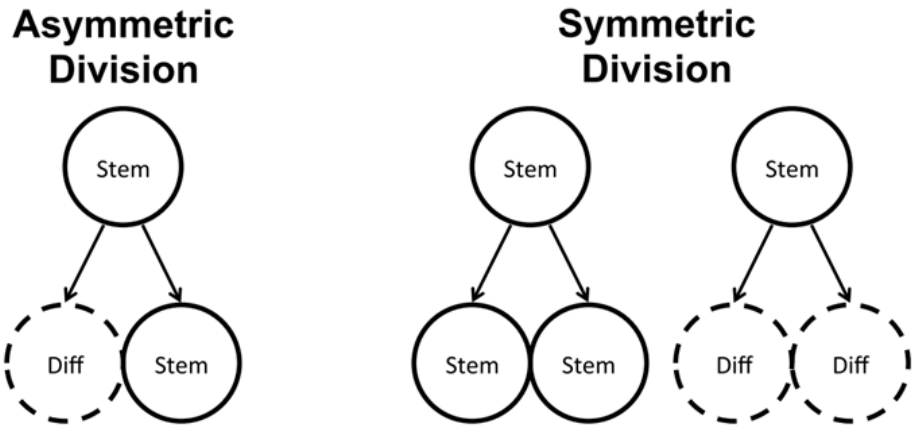

Pic.2. Asymmetric and symmetric division of stem cells

Growth factors and cytokines play an important role in the regeneration process of epithelial lesions. In the inflammation stage of wound regeneration, neutrophils release cytokines such as interleukin (IL)-1α, IL-1β and tumor necrosis factor (TNF)-α, which have the role of attracting and activating other cells, as well as intensifying the inflammatory process. Macrophages subsequently move to the affected area, eliminate pathogens, promote the migration of EpiSCs and keratinocytes, and induce extracellular matrix (ECM) synthesis by secreting cytokines and growth factors such as transforming growth factor (TGF)-α-β, fibroblast growth factor (FGF) and platelet-derived growth factor (PDGF). After the lesion is completely covered by a layer of keratinocytes, the molecular signals responsible for proliferation stop. After that, the keratinocytes stratify to gradually restore the damaged epidermal layer. [13,19]

Intracellular regeneration of the myocardium

Even though significant progress has been made in the early diagnosis and prevention of cardiovascular diseases, their prevalence is increasing globally. Heart failure in particular is a major problem, being the leading cause of death, disability and financial costs. About 38 million people worldwide are affected by this condition. Typically, the heart does not work properly after an injury that affects blood flow. This problem occurs because heart cells cannot be replaced once they have been destroyed, due to the fact that they cannot multiply in adulthood. According to estimates, only a small fraction – less than 1% of the heart cells in an adult's heart regenerate each year. [1,7,10]

During embryonic and fetal development, heart growth is primarily determined by the mitotic division of cardiac cells. These cells are generated either by differentiation of cardiac progenitors or by proliferation of already existing cardiac cells. The process of cardiac cell proliferation during fetal development is essential for the proper formation of cardiac structures, including maturation of the ventricular wall. After birth, the myocardium begins to expand in volume, but soon there is a transition to cardiac hypertrophy, which involves an increase in the size of the cardiomyocytes instead of an increase in their number. This leads to the exit of myocardial cells from the cell cycle. During this transition, cardiomyocytes undergo cell cycle changes, including acytokinetic mitosis (nuclear division without cell division), and endoreduplication (increasing the number of DNA copies without nuclear division and cellular) (pic.3). [3,4,5,6,19]

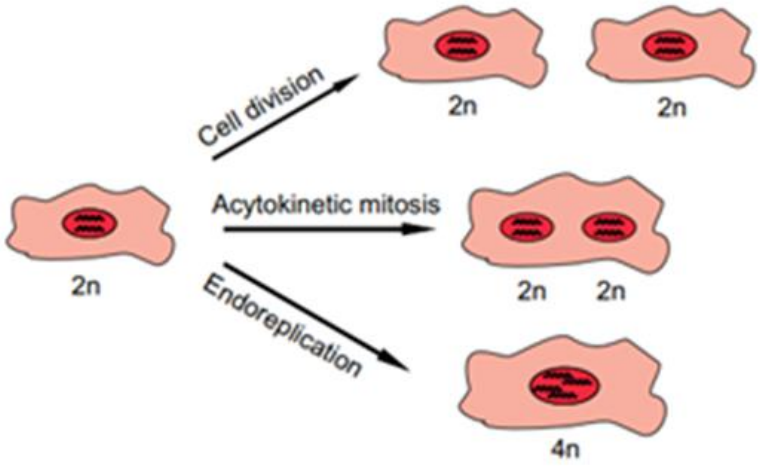

Pic.3. Cell cycle variations in CM after birth

Physiological regeneration of myocardial cells occurs at the intracellular level and is characterized by high intensity and speed, due to the high pressure exerted on the myocardium. This regeneration is further intensified during intense physical exertion and in conditions of pathological conditions such as heart defects or hypertension. In such cases, the components of the sarcoplasm of myocardial cells constantly degrade, being replaced by newly formed ones. With the increase in the load exerted on the heart, both hypertrophy (increase in size) and hyperplasia (increase in number) of the organelles, including myofibrils, sarcomeres, mitochondria, etc. appear. This process leads to cardiomyocyte hypertrophy (pic.4). [4,8,10,17]

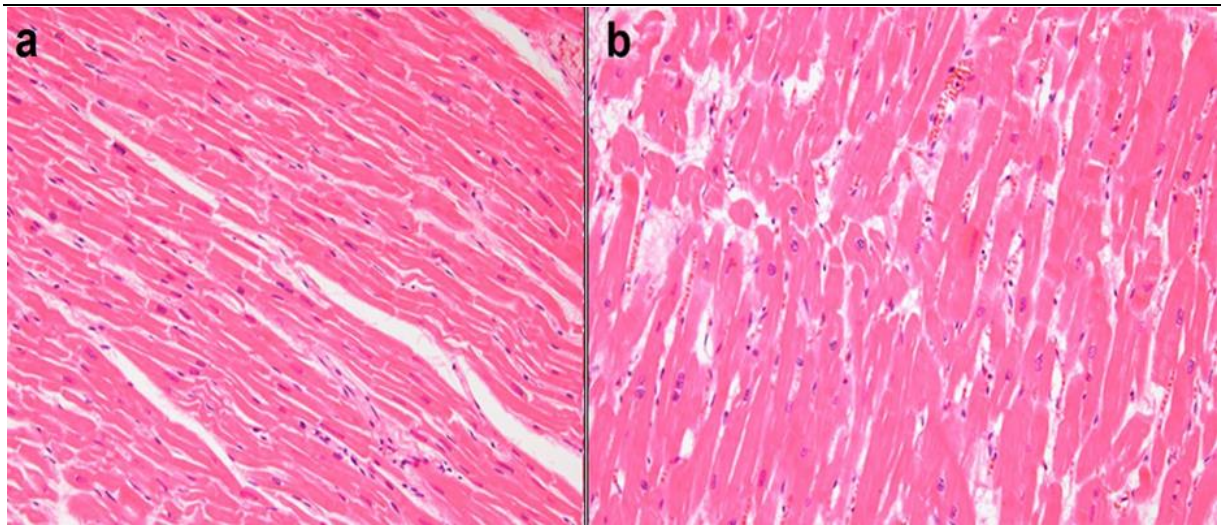

Pic.4. Hypertrophy of the myocardium: a – normal myocardium; b – hypertrophied myocardium

At an early age, cardiomyocyte polyploidization occurs and binuclear cells appear. Myocardial hypertrophy is characterized by adaptive growth corresponding to its vascular bed. In pathological conditions, such as heart defects that cause hypertrophy, this adaptation does not occur, and after a certain time, due to malnutrition, some of the affected cardiomyocytes die and are replaced by scar tissue (pic.5). [4,8,10]

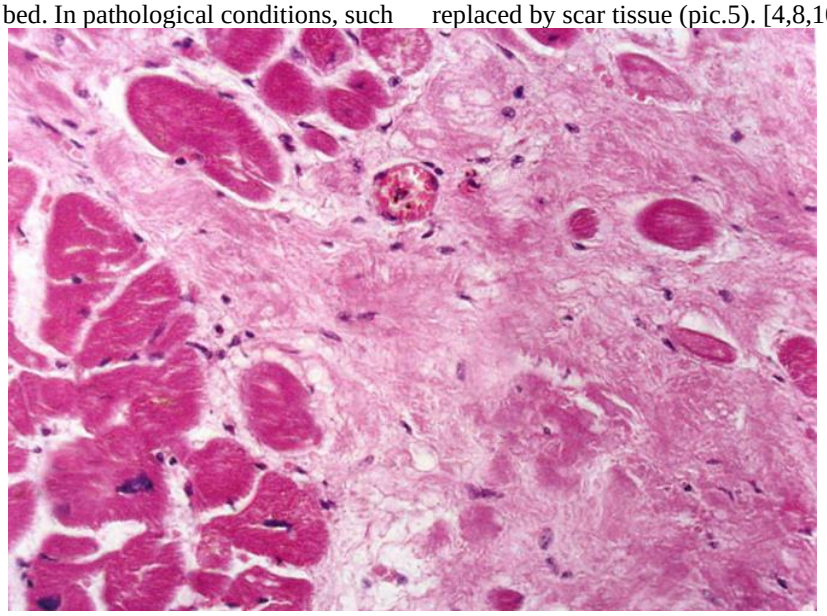

Pic.5. Post-infarction cardiosclerosis

When heart muscle tissue is damaged, for example in the case of injury or myocardial infarction, there are no stem cells that can replace the lost heart cells. Instead, the processes of regeneration and adaptation occur intracellularly in the neighboring cardiomyocytes, which hypertrophy and take over the function of the dead cells. This is called reparative regeneration of cardiac muscle tissue which also occurs in focal or diffuse dystrophy. Instead of dead cardiomyocyte cells, a scar of connective tissue (also called post-infarction cardiosclerosis) is formed (pic.5). [8,10]

Conclusions

Regeneration is classified as cellular, when active mitotic division of stem or adult cells occurs to restore the structure and function of damaged tissue; the intracellular one, is characterized by the proliferation or hypertrophy of intracellular components to increase the compensation capacity in stress situations. Cellular regeneration is characteristic of tissues that are in a continuous state of renewal, for example the epidermis of the skin and the mucosa of the digestive tract. These tissues are constantly exposed to the aggressive action of external and internal factors, therefore, they rapidly regenerate due to stem cells, which proliferate to replace old cells. Intracellular regeneration is specific to tissues where cells have lost the capacity for mitotic division and stem cells are absent. For example, the myocardium cannot restore the number of cells lost in case of injury, partial recovery occurs due to hypertrophy of the remaining cells, and the defect is replaced by a scar.

References

1. Ali H., Braga L., Giacca M. Cardiac regeneration and remodelling of the cardiomyocyte cytoarchitecture. FEBS Journal. 2019 Jan 1. https://doi.org/10.1111/febs.15146.

2. Basic regularities of physiological and reparative regeneration. (n.d.). Basic Patterns of Physiological and Reparative Regeneration. https://healthybones.com.ua/articles/Fiziologicheskaya%20i%20reparativnaya%20regeneratsiya#: [Published in Russian]

3. Becker, Cora & Hesse, Michael. (2020). Role of Mononuclear Cardiomyocytes in Cardiac Turnover and Regeneration. Current Cardiology Reports. 22. 10.1007/s11886-020-01289-y.

4. Derks D., Bergmann O. Polyploidy in Cardiomyocytes. American Heart Association, Inc, 2020. Volume 126, Issue 4, pp. 552 – 565. doi.org/10.1161/CIRCRESAHA.119.315408.

5. Eschenhagen, Thomas & Bolli, Roberto & Braun, Thomas & Field, Loren & Fleischmann, Bernd & FrisÃ©n, Jonas & Giacca, Mauro & Hare, Joshua & Houser, Steven & Lee, Richard & MarbÃˇn, Eduardo & Martin, James & Molkentin, Jeffery & Murry, Charles & Riley, Paul & Ruiz-Lozano, Pilar & Sadek, Hesham & Sussman, Mark & Hill, Joseph. (2017). Cardiomyocyte Regeneration: A Consensus Statement. Circulation. 136. 10.1161/CIRCULATIONAHA.117.029343.

6. Giacca, Mauro. (2020). Cardiac Regeneration After Myocardial Infarction: an Approachable Goal. Current Cardiology Reports. 22. 10.1007/s11886-020-01361-7.

7. Leone, Marina & Magadum, Ajit & Engel, Felix. (2015). Cardiomyocyte proliferation in cardiac development and regeneration: A guide to methodologies and interpretations. American journal of physiology. Heart and circulatory physiology. 309. ajpheart.00559.2015. 10.1152/ajpheart.00559.2015.

8. Myadelets O.D. Histology, cytology and human embryology. Part I. Cytology, embryology and general histology. Vitebsk: VSMU, 2014 - 439 p.

9. Ronghua Y., Jingru W., Xiaodong C., Yan S., Julin X. "Epidermal Stem Cells in Wound Healing and Regeneration", Stem Cells International, vol. 2020, Article ID 9148310, 11 pages, 2020. https://doi.org/10.1155/2020/9148310.

10. Senyo S., Lee R., Kühn B. Cardiac regeneration based on mechanisms of cardiomyocyte proliferation and differentiation. Elsevier, 2014. nr. 13(3 Pt B), pp. 532-541.doi: 10.1016/j.scr.2014.09.003.

11. Shahriyari L., Komarova N. Symmetric vs. Asymmetric Stem Cell Divisions: An Adaptation against Cancer? PLoS ONE, 2013. Nr.8(10): e76195. doi:10.1371/ journal.pone.0076195.

12. Strukov A.I., Serov V.V. Pathological anatomy. 5th ed. - Moscow: GEOTAR-Media, 2015, - 880 p. [Published in Russian]

13. Sukmawati T.T., Dosan R. Lessons From Epithelialization: The Reason Behind Moist Wound Environment. The Open Dermatology Journal, 2019, nr. 13(1), pp. 34-40. doi: 10.2174/1874372201913010034.

14. Tseluiko S.S., Krasavina N.P., Semenov D.A. Tissue regeneration. Blagoveshchensk, 2016. - 136 p. [Published in Russian]

15. Uy Gonzales A., Fuchs E. Skin and Its Regenerative Powers: An Alliance between Stem Cells and Their Niche. 2017 Nov 20;43(4):387-401. doi: 10.1016/j.devcel.2017.10.001.

16. Vlasova T.I., Arsent'eva E.V., Marzug B.A. Intracellular mechanisms regulating the behavior of epidermal stem cells during skin regeneration (a review of literature). Izvestiya vysshikh uchebnykh zavedeniy. Povolzhskiy region. Meditsinskie nauki = University proceedings. Volga region. Medical sciences. 2021;(3):142–157. (In Russ.). doi:10.21685/2072-3032-2021-3-14 [Published in Russian].

17. Wikipedia. File: Histopathology of myocardial hypertrophy.jpg. https://en.m.wikipedia.org/wiki/File:Histopathology_of_myocardial_hypertrophy.jpg

18. Wong, Victor & Levi, Benjamin & Rajadas, Jayakumar & Longaker, Michael & Gurtner, Geoffrey. (2012). Stem Cell Niches for Skin Regeneration. International journal of biomaterials. 2012. 926059. 10.1155/2012/926059.

19. Yang, R., Liu, F., Wang, J. et al. Epidermal stem cells in wound healing and their clinical applications. Stem Cell Res Ther 10, 229 (2019). https://doi.org/10.1186/s13287-019-1312-z.

PRIMARY LESION OF GASTROINTESTINAL TRACT IN NON-HODGKIN'S LYMPHOMA

Capanji A.,
student, Faculty of General Medicine,
SUMPh "Nicolae Testemitanu"
Chisinau, Republic of Moldova
Musteata L.
Associate Professor of the
Department of Hematology
SUMPh "Nicolae Testemitanu"
Chisinau, Republic of Moldova
DOI: 10.5281/zenodo.7796035

Abstract

Non-Hodgkin's lymphomas are a group of malignant neoplasms arising from lymphoid tissue, mainly lymph nodes, and are the most common malignant neoplasms of the circulatory system in many countries, including the Republic of Moldova. In most cases, non-Hodgkin's lymphomas begin with lesions of the peripheral lymph nodes (nodal lymphomas), however, in recent years, the number of patients with primary extranodular non-Hodgkin's lymphomas has increased [1]. Features of clinical manifestations, methods of diagnosis and treatment were studied on the basis of data from 50 patients with non-Hodgkin's lymphomas with a primary lesion of the gastrointestinal tract, treated at the Oncological Institute, Chisinau, Republic of Moldova. The overall survival of patients in different stages of the disease was also studied.

Keywords: non-Hodgkin's lymphoma, extranodal lesion, gastrointestinal tract.

Introduction

The gastrointestinal tract is the most common primary localization for extranodal non-Hodgkin's lymphoma, accounting for 20 to 40% of all extranodal lymphomas. Approximately in 60-75% of cases, the primary focus occurs in the stomach, less often in the small intestine, caecum, colon and rectum [2]. Clinical and morphological studies have established that the most common type is gastric histiocytic lymphoma. This tumor occurs in 60% of cases and is currently classified as B-cell lymphoma, which is most common in the Middle East and the Mediterranean and in this sense has also been called "Mediterranean lymphoma" [3]. Most primary gastric lymphomas develop against the background of chronic gastritis. Moreover, other variants of extranodal lymphomas are also associated with chronic inflammatory processes. In 1993, evidence was presented that H. pylori plays an important role in the occurrence of a subgroup of gastric MALT lymphomas [4, 5]. Based on the study of all manifestations of NHL by oncohematologists, it was found that the most important factors for an unfavorable prognosis are: age over 60 years, general condition of the patient, stage III-IV of the disease, the presence of more than one extranodal lesion, bone marrow damage [6]. This formed the basis of the international prognostic index - IPI. According to the number of unfavorable prognostic factors, there are 4 risk groups for early progression of the disease:

- low - absence or presence of one unfavorable factor;
- low/medium - the presence of 2 factors;
- medium / high - the presence of 3 factors;
- high - the presence of 4 factors.

The presence of two or more factors negatively affects the prognosis of the disease, regardless of the morphological variant of the tumor, for example, in diffuse NHL with large B cells, the 5-year survival rate at low risk is 72%, at high risk - 22% [6, 7].

Materials and methods

The study included 50 patients with non-Hodgkin's lymphomas with a primary lesion of the gastrointestinal tract, who were treated in the Oncological Institute, Republic of Moldova, in the period from 1998 to 2021, aged 20 to 78 years (average age - 49 years). In all patients from the study group, the following were studied: age at diagnosis, gender, clinical dates, date and reason for visiting a doctor, date of confirmation of the diagnosis and the time interval from the start of disease to confirmation (duration of the disease before diagnosis), paraclinical dates, methods of treatment, efficacy and complications of treatment, overall survival. The definition of morphological variants of non-Hodgkin's lymphomas was carried out in accordance with the Classification of lymphoid neoplasms proposed by the World Health Organization in 2016. The clinical stage of the disease was established according to the International Clinical Classification adopted in Ann Arbor in 1971. The study results were processed computerized using the Microsoft Excel program. To assess the clinical evolution, was used the tabular method of forming survival curves according to Kaplan E and Meyer P.

Results

In this study, the clinical manifestations, complications and results of treatment of non-Hodgkin's lymphoma with a predominant lesion of the gastrointestinal tract were studied in 50 patients aged 20 to 78 years. By distributing patients by sex and age, it was noted that women are more often affected by this disease. For both sexes, the age of 50 to 69 years prevails, which is 64%. According to the International Clinical Classification adopted in Ann Arbor in 1971, the majority of patients - 22 people (44%) were diagnosed with stage IV of the disease. Stage II E was established in 14 (28%) patients, stage I E in 12 (24%) and stage III E in 2 (4%). note the predominance of lymphoblastic lymphomas (36 cases, or 72%). Very rare are prolymphocytic variants (2 cases, or 4%) and lymphoplasmacytic variants (1 case, or 2%). In 11 (22%) patients, the NHL variant was not detected.

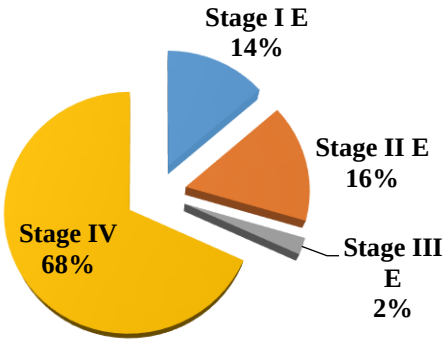

The study of the morphological features of NHL with a predominant lesion of gastrointestinal tract showed that the predominant morphological variants in this group of tumors were tumors with a high degree of malignancy.

Clinical manifestations depend on the organ in which the tumor first formed. For example, with a primary lesion of the stomach, pain in the epigastric region, nausea, vomiting, belching are observed, in rare cases, vomiting of the color of "coffee grounds" is also found. In lesion of the small and large intestine - paraombilical, constipation. Patients also presented symptoms of general intoxication. Most patients (76%) suffered from increased sweating, 62% had weight loss, 36% - 10% temperature.

To confirm the diagnosis, all patients underwent EGD and morphological analysis. In 20 operated patients, the material was removed during the operation. Everything else is in the process of conducting FGDS.

The effectiveness of treatment mainly depends on the stage of the disease. Thus, in stage I E, complete remission was achieved in all patients. In stage II E, the efficiency is already much lower: 43% of patients reached complete remission, 43% - partial remission, treatment was without results in 14% of cases. In the later stages (III E and IV), the treatment turned out to be ineffective already in 29% of cases. Complete remission reached 25% of patients, partial - 46%. In general, the overall effectiveness of treatment was 82.0% (remissions were achieved in 41 out of 50 patients). Of these, complete remissions were obtained in 24 (48.0%), partial - in 17 (34.0%), the effect was absent in 9 (18.0%) patients. Adverse reactions have been studied in patients receiving combined treatment (chemotherapy and radiotherapy) and drug treatment alone. The most common side effect in 34 (68.0%) patients was leukopenia. 28 (41.8%) patients had peripheral neuropathy. The appointment of antiemetic drugs did not worsen the general condition of the patients, the treatment was carried out in a standard volume and according to the scheme.

The survival time of patients with non-Hodgkin's lymphomas with a predominant lesion of the gastrointestinal tract varied from 6 to 98 months. The overall survival of patients after 1 year was 78.1%, after 3 years - 59.4% and after 5 years - 61.9%. The overall survival of patients with stage I E for 1 year was 93.4%, for 3 years - 71.4% and for 5 years - 69.9%. After the treatment, patients in stage I E were good for 1 year 93.4%, in stage II E - 63.9%, for 3 years - 76.5% and 5 years or more - 69.9%. In stage II E, the convincing rates were 91.2%, 71.4% and 63.8%. The overall survival of patients with III E and IV stages after chemotherapy treatment was more than 1 year 75.1%, more than 3 years - 59.4% and more than 5 years - 28.5%.

Conclusion

Non-Hodgkin's lymphomas with a primary lesion of the gastrointestinal tract are a frequent extranodal manifestation of this disease, diagnosed mainly in the late stages and having aggressive forms. They occur more often at the age of 50-69 years and the female sex prevails. Treatment depends on the clinical stage of the disease; in general, remissions reach 82% of patients.

References

1. Smith A., Howell D., Patmore R., et.al.. Incidence of haematological malignancy by sub-type: a report from the Haematological Malignancy Research Network. Br. J. Cancer. 2011;105(11):1684-92.

2. Gebauer A., Merger M., Kilbinger H. Modulation by 5,HT3 and 5,HT4 receptors of the release of 5,hydroxytryptamine from the guinea,pig small intestine. Arch. Pharmacol. 1993; 347:137 - 140.

3. Choi S.Y., Kim S.J., Kim W.S., et al.Aggressive B cell lymphomas of the gastrointestinal tract: clinicopathologic and genetic analysis. Virchows Arch. 2011;459:495-502.

4. Armitage J.O., Weisenburger D.D. New approach to classifying non-Hodgkin's lymphomas: clinical features of the major histologic subtypes. Non-Hodgkin's Lymphoma Classification Project. J. Clin. Oncol. 1998;16(8):2780-95.

5. Arnold I.C., Hitzler I., Engler D., et al.The C-terminally encoded, MHC class II-restricted T cell antigenicity of the Helicobacter pylori virulence factor CagA promotes gastric preneoplasia. J. Immunol. 2011;186:6165-72 .

6. Psyrri A., Papageorgiou S., Economopoulos T.Primary extranodal lymphomas of stomach: clinical presentation, diagnostic pitfalls and management. An. Oncol.2008;19:1992-9

7. Alvarez-Lesmes J., Cassidy D., Garcia-Buitrago M., Montgomery E.A, Lossos I.S, Sussman D. Gastrointestinal Tract Lymphomas: A Review of the Most Commonly Encountered Lymphomas. Arch Pathol Lab Med (2021) 145 (12): 1585–1596.

REGULATION OF CELL PROLIFERATION BY TYROSINE PROTEINKINASES RECEPTORS AND THEIR ROLE IN TRIGGERING DIFFERENT TYPES OF CANCERS

Ceban T.,
student, Faculty of General Medicine, SUMPh "Nicolae Testemitanu"
Chisinau, Republic of Moldova
Simionică E.
PhD, university lector, State University of Medicine and Pharmacy "Nicolae Testemitanu"
Chisinau, Republic of Moldova
DOI: 10.5281/zenodo.7796040

Abstract

Receptor tyrosine proteinkinases (RTKs) are transmembrane proteins that possess kinase activity catalyzing the transfer of phosphate groups from ATP to tyrosine residues in protein substrates. RTKs play an important role in the control of most fundamental cellular processes such as proliferation, differentiation, cell metabolism and survival, cell migration and cell cycle control. Tyrosine proteinkinase receptors comprise 58 different types in humans that are classified into 20 families according to structure and ligand. Mutations in RTKs and aberrant activation of their intracellular signalling pathways lead to the triggering of different types of cancers. In human cancers, four fundamental mechanisms have been found to lead to constitutive activation of RTKs: genomic amplification, gain-of-function mutations, chromosomal rearrangements and autocrine activation. Thus, aberrant activation of receptor tyrosine protein kinase is a potential therapeutic target. In recent decades, several drugs, such as tyrosine kinase inhibitors, have been developed and clinically evaluated to improve the survival of cancer patients.

Keywords: receptor tyrosine proteinkinases, mutations, cancer, tyrosine kinase inhibitors.

Cancer is one of the world's biggest problems, both nationally and globally, with around 10 million people dying every year. In 2020, the International Agency for Research on Cancer reported an estimated 19.3 million new cancer cases and 10 million deaths globally, with data from 185 countries. The most commonly diagnosed cancers worldwide were female breast cancer (2.26 million cases), lung cancer (2.21) and prostate cancer (1.41). The most common causes of death among cancers were lung (1.79 million), liver (830,000) and stomach (769,000) cancers. Cancer is a malignant process involving the aberrant development of cells in a tissue with increased potential to invade other parts of the body. In recent decades, tyrosine-proteinases receptors have been widely studied by researchers, as aberrations in their activation or signalling lead to many pathologies, in particular cancers, leading to the development of a variety of drugs that block RTKs signalling and are successfully applied for the treatment of many types of cancers. [3]

Ninety tyrosine kinase genes and five pseudogenes have been identified in the human genome. Of the 90 tyrosine kinases, 58 are receptor tyrosine kinases distributed in 20 subfamilies and 32 are non-receptor tyrosine kinases distributed in 10 subfamilies. The RTK subfamilies are EGFR, InsR, PDGFR, VEGFR, FGFR, PTK7/CCK4, Trk, Ror, MuSK, Met, Axl, Tie, EphA/B, Ret, Ryk, DDR1/2, Ros, LMR, ALK and SuRTK106/STYK1 (Figure1). [8][7][6]

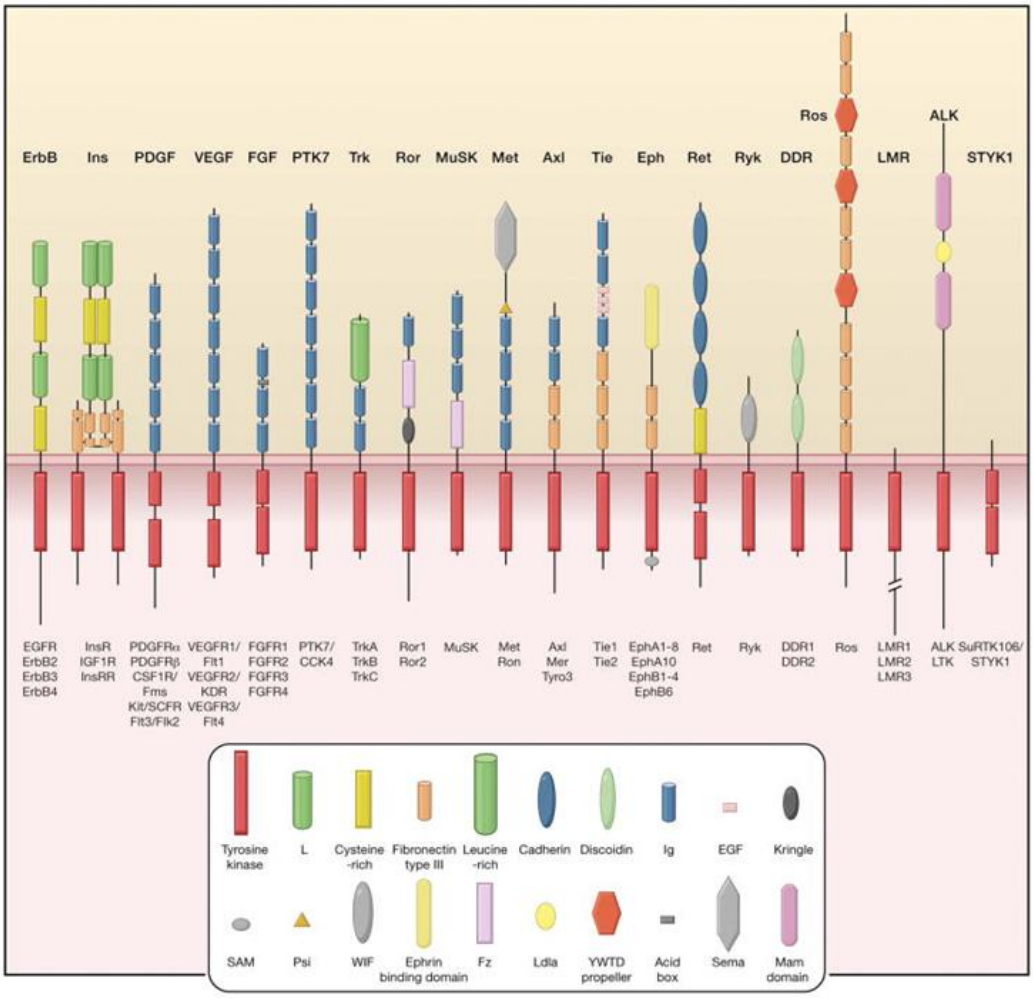

Figure 1. Families of tyrosine proteinkinase receptors.[6]

RTKs consist of an extracellular ligand-binding region, a single transmembrane domain and a cytoplasmic tyrosine kinase domain. Notably, the extracellular domain in each receptor class has a different structure and sequence that confers specificity to its ligand and its recognition. The extracellular domain is involved in the dimerization process of the receptor. The transmembrane domain represented by the α-helix consisting of 20 amino acids allows RTK insertion into the cell membrane. This domain plays a key role in dimer formation and stabilization. In the lipid environment of the cell membrane the α-helix is non-covalently oligomerized. Thus, this process perimitates RTK pre-dimerization in the cell membrane that is able to interact with the corresponding ligand. The cytoplasmic domain includes the tyrosine kinase domain with a small N-terminal lobe that binds ATP and Mg 2+ and a large C-terminal lobe formed by a carboxyl group (catalytic domain) that contains the activation loop. ATP binds in the cleavage between the two lobes and the tyrosine-containing sequence of the protein substrate, interacts with the residues of the C-terminal lobe and subsequently catalyses the transfer of phosphate groups from ATP to the receptor chains. The N- and C-terminal domains vary between RTK families, reflecting the specificity and diversity of intracellular downstream signals. Binding of a ligand to a receptor causes a change in receptor conformation, known as receptor activation. After phosphorylation tyrosines or phosphotyrosines then become binding sites for several cytoplasmic proteins. These proteins further activate several downstream signalling pathways, some of the main ones being the MAPK, PI3K, JAK/STAT and PKC pathways. [9][1][4][12]

Abnormal activation of RTK is a complex process involving not only RTK itself, but also adjacent molecules and surrounding environments. Their association with various cellular components further complicates the mechanism of oncogenic RTK activation. Four main mechanisms leading to aberrant activation in human cancers have been proposed, these are: 1) RTK overexpression; 2) gain-of-function mutations; 3) chromosomal translocations and 4) autocrine activation (Figure 2). Overexpression and genomic amplification has been identified in a variety of cancers: EGFR in glioblastoma, esophageal, lung, thyroid cancer; HER2/ErbB2 in breast, bladder, gastric cancer; MET in gastric and lung cancer. Activation by gain-of-function mutations can occur in the extracellular domain, transmembrane domain and juxtamembrane domain of RTK. Point mutations of FGFR3 in the extracellular domain have been reported in cervical carcinomas. HER2 G660D and V659E mutations in the transmembrane domain have been identified in non-small cell lung cancer. KIT V560G and PDGFRA V561D muta-

tions in the juxtamembrane domain are found in gastrointestinal stromal tumours. Chromosomal rearrangements occur in patients with chronic myeloid leukemia-fusion of the gene encoding tyrosine kinase ABL1 on chromosome 9 with the BCR gene on chromosome 22 (BCR-ABL). Autocrine activation uses messengers such as growth factors and cytokines. Autocrine activation of different RTKs has been well characterized in various cancers, including HGF-MET, TGFα-EGFR and SCF-KIT autocrine loops. [1][10]

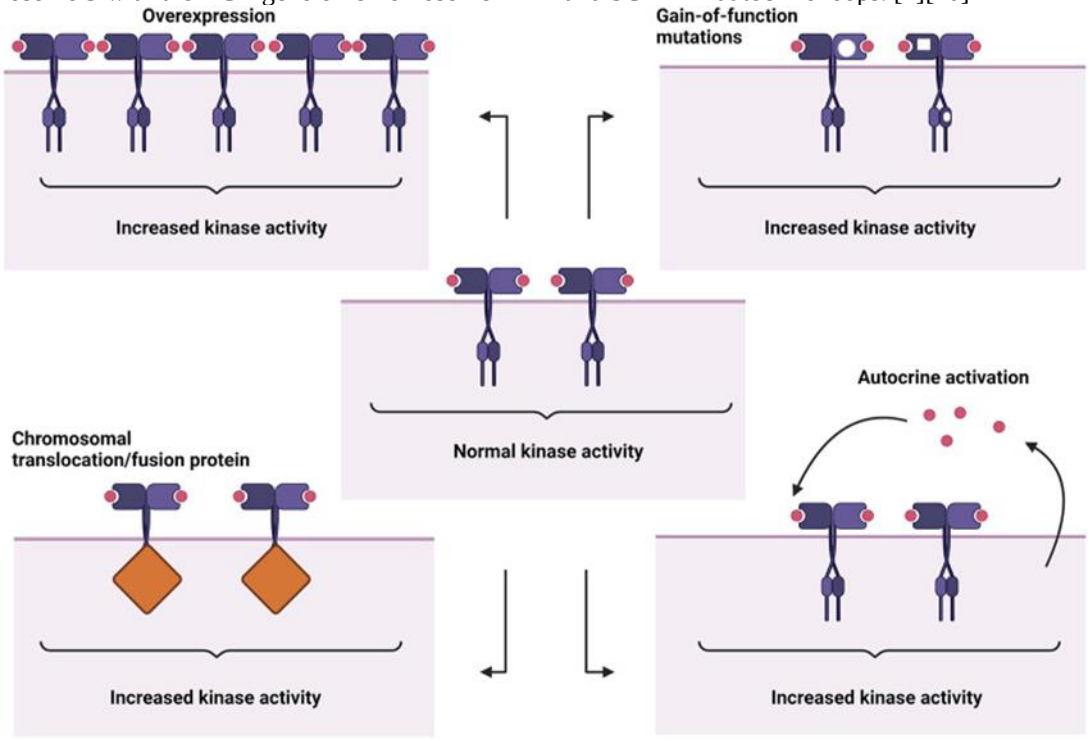

Figure 2. Abnormal mechanisms of RTKs activation.[10]

Recently, there has been an increasing focus on developing new and effective drugs that target tumour cells with minimal side effects. For targeted therapies in cancer as ideal representatives are monoclonal antibodies, which compete for the extracellular domain of the receptor, and small molecule inhibitors of tyrosine kinase, which bind to intracellular molecules preventing conformational changes and RTK activation. Currently there are 74 small molecule protein kinase inhibitors approved by the FDA (Food and Drug Administration) as of 12 February 2023. Small molecule tyrosine kinase inhibitors are classified into reversible inhibitors and irreversible inhibitors. Reversible kinase inhibitors are subdivided into four major subtypes based on binding pocket compliance as well as the DFG (ASP-Phe-Gly) motif. Irreversible kinase inhibitors tend to bind covalently and block the ATP site, resulting in irreversible inhibition. Type I inhibitors: bind competitively to the ATP-binding site of active tyrosine kinases. The DFG motif arrangement in type I inhibitors has the aspartate residue facing the catalytic site of the kinase. For example: crizotinib, erlotinib, bosutinib, dasatinib, geftinib, lapatinib, pazopanib, sunitinib and vemurafenib. Type II inhibitors: bind to inactive kinases, usually at the ATP-binding site. The DFG motif in type II inhibitors is oriented outward, away from the ATP binding site. Due to the outward rotation of the DFG motif, many type II inhibitors can also exploit regions adjacent to ATP binding sites. For example: imatinib, sorafenib, axitinib, nilotinib, ponatinib. Type III inhibitors: do not interact with the ATP-binding pocket. Type III inhibitors bind exclusively to allosteric pockets adjacent to the ATP-binding region. For example: trametinib, cobimetinib, binitinib. Type IV inhibitors: bind to allosteric sites away from the ATP binding pocket. For example: ON012380, preparation under development. Type V inhibitors: are bivalent inhibitors that bind irreversibly, forming covalent bonds with non-catalytic cysteine residues in the ATP binding pocket. For example: afatinib, ibrutinib, osimertinib. [2][5][13][11]

References

1. Du Z, Lovly CM (2018) Mechanisms of receptor tyrosine kinase activation in cancer. Mol Cancer 17:1–13. doi: 10.1186/s12943-018-0782-4

2. Hojjat-Farsangi M (2014) Small-molecule inhibitors of the receptor tyrosine kinases: Promising tools for targeted cancer therapies. Int J Mol Sci 15:13768–13801. doi: 10.3390/ijms150813768

3. Jemal A, Ward EM, Johnson CJ, Cronin KA, Ma J, Ryerson AB, Mariotto A, Lake AJ, Wilson R, Sherman RL, Anderson RN, Henley SJ, Kohler BA, Penberthy L, Feuer EJ, Weir HK (2017) Annual Report to the Nation on the Status of Cancer, 1975-2014, Featuring Survival. J Natl Cancer Inst 109. doi: 10.1093/JNCI/DJX030

4. Karpov OA, Fearnley GW, Smith GA, Kankanala J, McPherson MJ, Tomlinson DC, Harrison MA, Ponnambalam S, Karpov OA, Fearnley GW, Smith GA, Kankanala J, McPherson MJ, Tomlinson DC, Harrison MA, Ponnambalam S (2015) Receptor tyrosine kinase structure and function in health and

disease. AIMS Biophys 2015 4476 2:476–502. doi: 10.3934/BIOPHY.2015.4.476

5. Lee PY, Yeoh Y, Low TY (2022) A recent update on small-molecule kinase inhibitors for targeted cancer therapy and their therapeutic insights from mass spectrometry-based proteomic analysis. FEBS J 1–20. doi: 10.1111/febs.16442

6. Lemmon MA, Schlessinger J (2010) Cell signaling by receptor tyrosine kinases. Cell 141:1117–1134. doi: 10.1016/J.CELL.2010.06.011

7. Mendrola JM, Shi F, Park JH, Lemmon MA (2013) Receptor Tyrosine Kinases with Intracellular Pseudokinase Domains. Biochem Soc Trans 41:1029. doi: 10.1042/BST20130104

8. Robinson DR, Wu YM, Lin SF (2000) The protein tyrosine kinase family of the human genome. Oncogene 19:5548–5557. doi: 10.1038/sj.onc.1203957

9. Ségaliny AI, Tellez-Gabriel M, Heymann MF, Heymann D (2015) Receptor tyrosine kinases: Characterisation, mechanism of action and therapeutic interests for bone cancers. J Bone Oncol 4:1–12. doi: 10.1016/J.JBO.2015.01.001

10. Sudhesh Dev S, Zainal Abidin SA, Farghadani R, Othman I, Naidu R (2021) Receptor Tyrosine Kinases and Their Signaling Pathways as Therapeutic Targets of Curcumin in Cancer. Front Pharmacol 12. doi: 10.3389/FPHAR.2021.772510

11. Thomson RJ, Moshirfar M, Ronquillo Y (2022) Tyrosine Kinase Inhibitors. StatPearls

12. Trenker1 R, Jura1 N (2015) Available online la www.sciencedirect.com ScienceDirect Tyrosine kinase receptor activation: From a ligand perspective. doi: 10.1016/j.ceb.2020.01.0160955-0674

13. PKI | Blue Ridge Institute for Medical Research. https://brimr.org/protein-kinase-inhibitors/. Accessed 5 Mar 2023

AKI ASSOCIATED WITH COVID-19, MOST AFFECTED AGE GROUP, COMORBIDITIES, AND MORTALITY

Cernei Cristina,
Student, Faculty of General Medicine,
The State University of Medicine and Pharmacy "Nicolae Testimițanu"
Republic of Moldova, Chișinău
Tănase Adrian
Associate professor, Department of Surgical Urology and Nephrology
The State Univerisity of Medicine and Pharmacy "Nicolae Testimițanu"
Republic of Moldova, Chișinău
DOI: 10.5281/zenodo.7796050

Abstract

COVID-19 is an infectious disease caused by the SARS-CoV-2 virus that emerged in late 2019. The disease rapidly spread from its origin in Wuhan, China, and has since become an unprecedented global pandemic. Its impact on the world's population has been catastrophic, resulting in over six million deaths worldwide, making it the most significant global health crisis since the 1918 flu pandemic. [1,2,3]

Keywords: AKI, COVID-19, pandemic, comorbidities

Introduction

While COVID-19 primarily affects the respiratory system, it can also have deleterious effects on the kidneys. Severe cases of COVID-19 have been associated with elevated serum creatinine and serum urea levels, hematuria, proteinuria, and AKI, all of which are linked to a higher mortality rate. Among critically ill patients with SARS-CoV2 infection, up to 25% may develop AKI, particularly those with pre-existing comorbidities such as diabetes or hypertension. The mortality rate is significantly higher in patients who require renal replacement therapy for AKI. [4,5]

Aim of the study

Considering the substantial number of patients who developed AKI during hospitalization for COVID-19, our objective is to investigate the most prevalent comorbidities associated with a heightened risk of AKI development. Additionally, we seek to compare mortality rates between two patient groups: those who developed AKI unrelated to COVID-19 and those who developed AKI while infected with COVID-19.

Materials and methods

The study included a group of 66 patients with AKI diagnosis who were hospitalized in "Timofei Moșneaga" Republican Clinical Hospital during the first semester of 2021. The study included 22 (33.3%) patients who had had AKI associated with COVID-19. The age of the patients varies from 37 to 84 years, and the average age is 64.1 years. AKI was diagnosed more often in men – 45 (68,2%) than in women – 21 (31,8%).

Results and discussion

From the data collected from the patient's medical records, the highest rate of AKI not associated with COVID-19 was found in the age group 61-70 years. The increased prevalence of pathology in this age group is probably due to the multiple comorbidities and weakening of the immune system in elderly people (Figure 1).

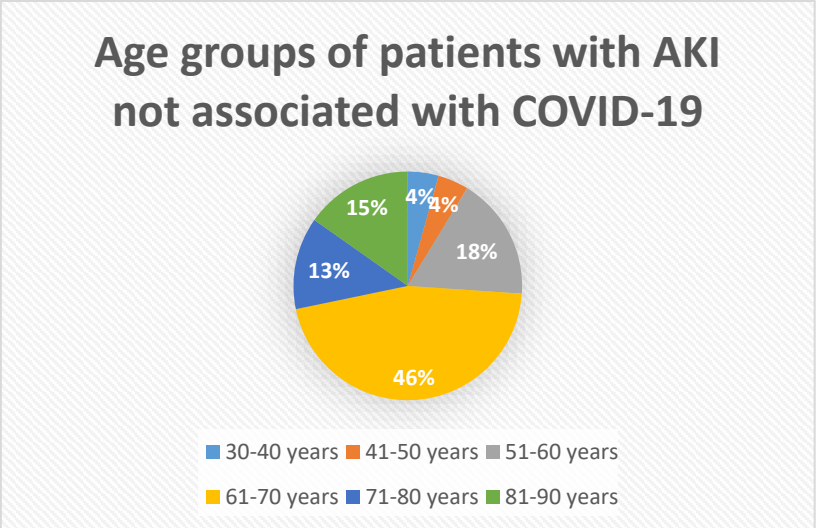

Figure 1. Age groups of patients with AKI not associated with COVID-19.

Upon examining the age distribution of patients with AKI linked to COVID-19, it was observed that the prevalence of the disease was highest in patients aged 71-80 years, with 10 patients (48%) falling within this age group. However, there was also an increase in the prevalence of AKI in the age group of 51-60 years, with 6 patients (29%) affected. This trend suggests a rejuvenation of the pathology in association with SARS-CoV2 infection (Figure 2).

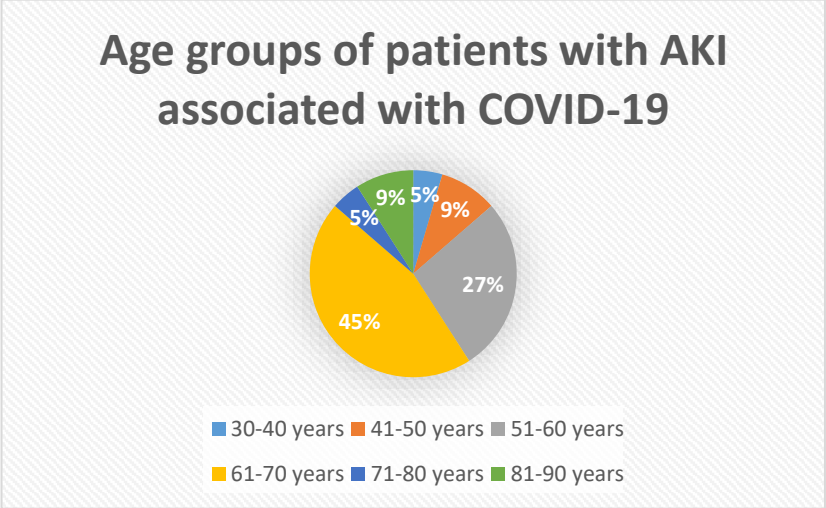

Figure 2. Age groups of patients with AKI associated with COVID-19.

The patient's comorbidities confer an increased risk for AKI development, the most common are diabetes mellitus, hypertension, and heart failure. For this reason, we analyzed the data regarding the patient's associated pathologies to detect the most common one. Diabetes mellitus was detected in 10 (45.5%) of the patients with AKI associated with COVID-19, arterial hypertension was present in 18 (81.8%) patients and heart failure of various etiology was attested in 15 (68.1 %) of the patients. Only two patients did not present any associated chronic pathology at the time of admission (Figure 3).

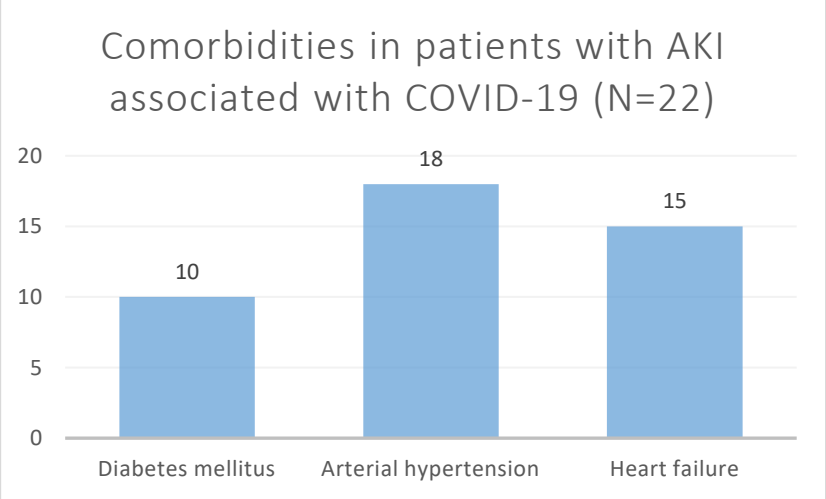

Figure 3. Comorbidities in patients with AKI associated with COVID-19.

Among patients who developed AKI not linked to COVID-19, it was observed that the most prevalent comorbidity was arterial hypertension, present in 28 patients (63.6%). The second most common comorbidity was heart failure, identified in 27 patients (61.3%), followed by diabetes mellitus, which was present in 15 patients (34.1%) (Figure 4).

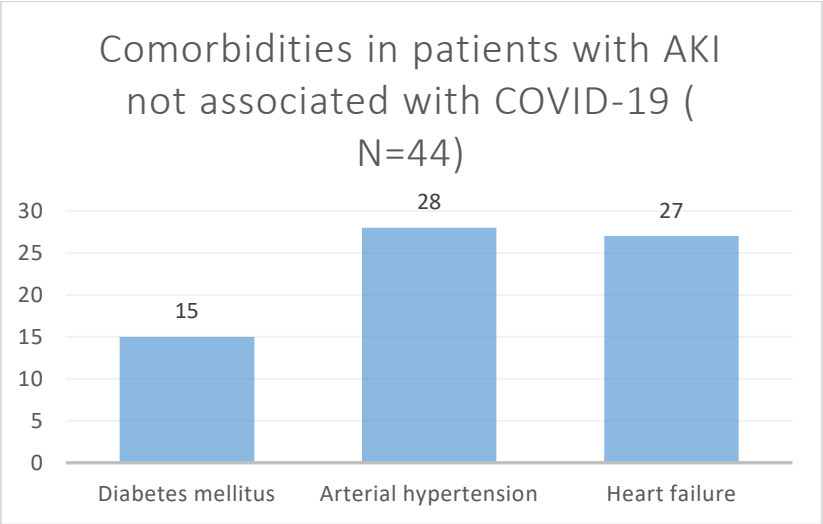

Figure 4. Comorbidities in patients with AKI not associated with COVID-19.

Of the patients with AKI not associated with SARS-CoV2 infection, 39% (17 patients) died. On the other hand, 27 patients (61%) received treatment and were subsequently discharged from the hospital (Figure 5).

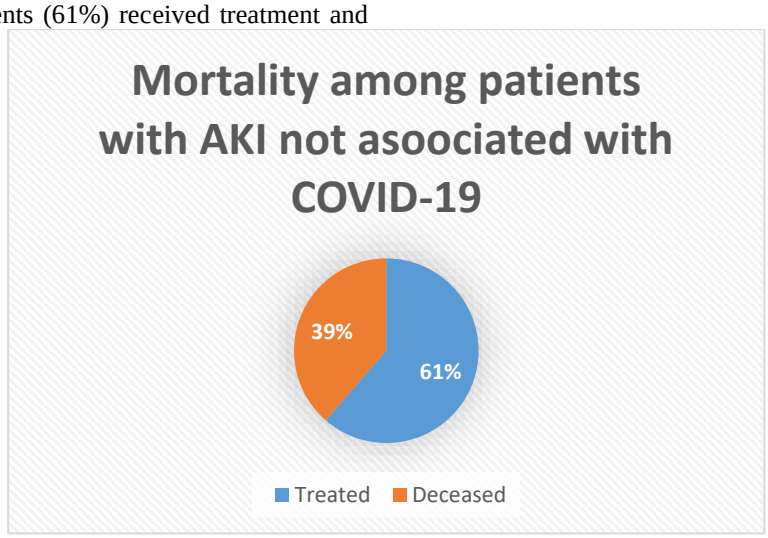

Figure 5. Mortality among patients with AKI not associated with COVID-19.

Patients with AKI associated with COVID-19 infection had an alarming mortality rate, with only 1 patient (5%) out of 22 surviving. The remaining 21 patients (95%) did not survive. The primary cause of death was attributed to multiple organ dysfunction syndrome resulting from the COVID-19 infection (Figure 6).

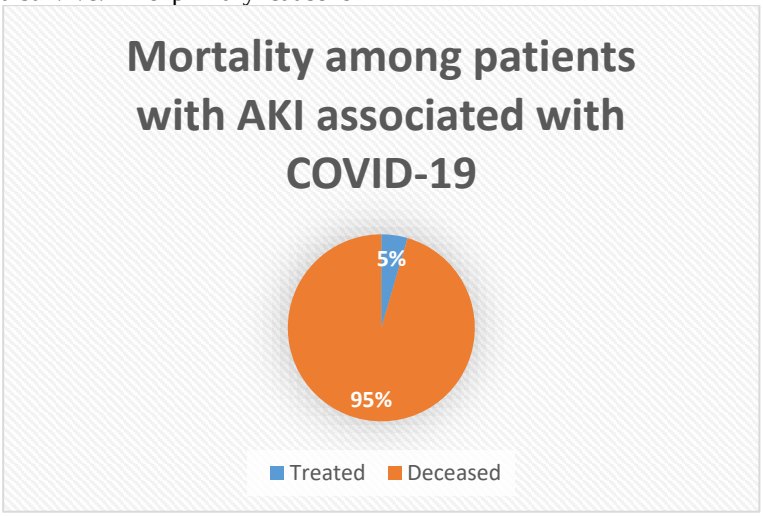

Figure 6. Mortality among patients with AKI associated with COVID-19.

Conclusion

Advanced age is a significant risk factor for developing AKI due to associated comorbidities. The presence of underlying medical conditions renders the kidneys more susceptible to damage and the development of AKI. COVID-19 infection appears to target pre-existing kidney damage, particularly in patients with diabetes or arterial hypertension. Given the high mortality associated with AKI linked to COVID-19 infection in elderly patients, it is essential to carefully monitor biochemical markers of renal function and promptly initiate hemodialysis if necessary.

References

1. Cascella, M., Rajnik, M., Cuomo, A., Dulebohn, S. C., & di Napoli, R. (2022). Features, Evaluation, and Treatment of Coronavirus (COVID-19). StatPearls.

2. Li, H., Burm, S. W., Hong, S. H., Ghayda, R. A., Kronbichler, A., Smith, L., Koyanagi, A., Jacob, L., Lee, K. H., & Shin, J. il. (2021). A Comprehensive Review of Coronavirus Disease 2019: Epidemiology, Transmission, Risk Factors, and International Responses. Yonsei Medical Journal, 62(1), 1–11.

3. Chávez-Valencia, V., Orizaga-de-la-Cruz, C., & Lagunas-Rangel, F. A. (2022). Acute Kidney Injury in COVID-19 Patients: Pathogenesis, Clinical Characteristics, Therapy, and Mortality. Diseases, 10(3), 53.

4. Fabrizi, F., Alfieri, C. M., Cerutti, R., Lunghi, G., & Messa, P. (2020). COVID-19 and Acute Kidney Injury: A Systematic Review and Meta-Analysis. Pathogens, 9(12), 1–16.

5. Nogueira, S. Á. R., de Oliveira, S. C. S., de Carvalho, A. F. M., Neves, J. M. C., da Silva, L. S. V., da Silva Junior, G. B., & Nobre, M. E. P. (2020). Renal changes and acute kidney injury in covid-19: a systematic review. Revista Da Associacao Medica Brasileira (1992), 66Suppl 2(Suppl 2), 112–117.

METHOD OF PERFORMING SELECTIVE PROXIMAL VAGOTOMY

Kosenko P.M.,
Doctor of medical sciences, professor
Far Eastern State Medical University
Russian Federation, Khabarovsk, st. Muravyov-Amursky 35
Vavrinchuk S.A.,
Doctor of medical sciences, professor
Far Eastern State Medical University
Russian Federation, Khabarovsk, st. Muravyov-Amursky 35
Sunozova G.D.
Assistant of the Department of General and Clinical Surgery
Far Eastern State Medical University
Russian Federation, Khabarovsk, st. Muravyov-Amursky 35
DOI: 10.5281/zenodo.7796056

СПОСОБ ВЫПОЛНЕНИЯ СЕЛЕКТИВНОЙ ПРОКСИМАЛЬНОЙ ВАГОТОМИИ

Косенко П.М.
д.м.н., профессор
Дальневосточный государственный медицинский университет
Г. Хабаровск, ул. Муравьева-Амурского 35
Вавринчук С.А.
д.м.н., профессор
Дальневосточный государственный медицинский университет
Г. Хабаровск, ул. Муравьева-Амурского 35
Сунозова Г.Д.
ассистент кафедры общей и клинической хирургии
Дальневосточный государственный медицинский университет
Г. Хабаровск, ул. Муравьева-Амурского 35

Abstract

The objective of the study was to improve the results of surgical treatment of patients with complicated peptic ulcer disease by improving the method of performing selective proximal vagotomy.

Materials and methods. According to the proposed method, 44 patients were operated on. All patients underwent duodenoplasty in combination with selective proximal vagotomy.

Results. The main causes of intraoperative damage to the splenic vessels and pancreas were the transsection of the gastro-splenic and gastro-diaphragmatic ligaments without their preliminary separation from the underlying anatomical formations, as well as the presence of pathological scar-inflammatory changes in this area.

The proposed method of selective proximal vagotomy (patent No. 2717209 dated 03/18/2020) includes isolation of the upper edge of the esophageal hiatus, mobilization of the stomach floor and skeletonization of the left diaphragmatic peduncle transsection of the ascending gastric artery, dissection of the small curvature of the stomach and the cardia in the direction from the angle of the stomach to the cardia with the transsection of transverse neurovascular gastric branches, denervation of the abdominal part of the esophagus, isolation of the right diaphragmatic peduncle and the posterior trunk of the vagus, closure of the exposed muscles of the small curvature of the stomach with serous-muscle sutures up to the cardia, suturing of the esophagus, cardia and the bottom of the stomach by lateral invagination.

Conclusion. The proposed method of selective proximal vagotomy allows to completely exclude intraoperative trauma of the pancreas, spleen and its vessels, as well as to exclude postoperative discoordinated disorders of gastric motility.

The advantages of the proposed method also include a significant reduction in the complexity of the operation, simplification of the execution technique and reduction of the operation time.

The method can be performed by surgeons without experience in SPV operations.

Аннотация

Цель исследования - улучшить результаты хирургического лечения больных с осложненной язвенной болезнью, путем усовершенствования способа выполнения селективной проксимальной ваготомии.

Материалы методы. По предложенной методике было оперировано 44 пациента. Всем больным была выполнена дуоденопластика в сочетании с селективной проксимальной ваготомией.

Результаты. Основными причинами интраоперационных повреждений селезеночных сосудов и поджелудочной железы оказались пересечение желудочно-селезеночной и желудочно-диафрагмальной связок без их предварительного отделения от нижележащих анатомических образований, а также с наличие в этой области патологических рубцово-воспалительных изменений.

Предложенный способ селективной проксимальной ваготомии (патент на изобретение №2717209 от 18.03.2020) включает выделение верхнего края пищеводного отверстия диафрагмы, мобилизацию дна желудка и скелетирование левой ножки диафрагмы, пересечение восходящей желудочной артерии, диссекцию малой кривизны желудка и кардии по направлению от угла желудка к кардии с пересечением поперечных сосудисто-нервных желудочных веточек, денервацию абдоминальной части пищевода, выделение правой ножки диафрагмы и заднего ствола вагуса, закрытие обнажённых мышц малой кривизны желудка серозно-мышечными швами до кардии, сшивание пищевода, кардии и дна желудка методом боковой инвагинации.

Заключение. Предлагаемый способ селективной проксимальной ваготомии позволяет полностью исключить интраоперационную травму поджелудочной железы, селезенки и ее сосудов, а также исключить послеоперационные дискоординированные нарушения моторики желудка.

К преимуществам предлагаемого способа также следует отнести и значительное уменьшение трудоемкости операции, упрощение техники выполнения и сокращение времени операции. Способ может быть выполнен хирургами без опыта операций СПВ.

Keywords: selective proximal vagotomy, complicated peptic ulcer disease
Ключевые слова: селективная проксимальная ваготомия, осложненная язвенная болезнь

Введение. Селективная проксимальная ваготомия (СПВ) до настоящего времени остается в арсенале способов хирургического лечения язвенной болезни (ЯБ) двенадцатиперстной кишки (ДПК) и аксиальных грыж пищеводного отверстия диафрагмы (ГПОД) [1, 3, 4, 5, 8, 9].

Однако, этот способ оперативного лечения является трудоемким, технически сложным и требует высокой квалификации врача-хирурга [4].

К недостаткам известных способов СПВ следует отнести так же высокую вероятность повреждения поджелудочной железы (ПЖ), селезёночных сосудов, нервов и селезёнки [4, 5].

А.Ф. Черноусов указывает, что повреждение ПЖ, селезёночных сосудов и селезёнки является типичным осложнением при выполнении СПВ [7].

Средняя продолжительность выполнения СПВ по данным различных авторов СПВ составляет 180±30 минут [4, 7].

Целью исследования было улучшить результаты хирургического лечения больных с осложненной ЯБ, путем усовершенствования способа выполнения СПВ.

Материалы и методы

Органосохраняющие операции были выполнены у 44 больных с ЯБ, осложненной рубцово-язвенным стенозом (таблица 1).

Таблица 1

Характер выполненных оперативных вмешательств

Характер выполненной операции		**Количество больных**	**%**
Дуоденопластика (ДП) в сочетании с СПВ	Мостовидная ДП +СПВ	40	90,9
	Мостовидная ДП+СПВ+ операция Стронга	1	2,3
	Сегментарная ДП+СПВ	3	6,8
Итого		44	100

Средний возраст больных составил 57,2±9,4 лет (таблица 2)

Таблица 2.

Распределение больных с РЯС ДПК по возрастным группам (по классификации ВОЗ)

Обследованные пациенты	**Молодой возраст (25-44)**		**Средний возраст (44-60)**		**Пожилой возраст (60-75)**	
	n	**%**	**n**	**%**	**n**	**%**
Мужчины (n=34)	10	22,7	11	25	13	29,5
Женщины (n=10)	1	2,2	7	15,9	2	4,5

Всем больным до операции проводилась комплексная оценка моторно-эвакуаторной функции желудка и кишечника и оценка параметров гомеостаза по общепринятым критериям.

Результаты исследования. Проведенный нами анализ причин возникших интраоперационных повреждений селезеночных сосудов и ПЖ показал, что их основной является пересечение желудочно-селезеночной и желудочно-диафрагмальной связок без их предварительного отделения от нижележащих анатомических образований и с анатомическими особенностями расположения ПЖ и сосудов селезёнки относительно желудка, а так же с наличием в этой области патологических рубцово-воспалительных изменений.

Так известно, что тело ПЖ расположено непосредственно за желудком и прилегает к его задней стенке. Между задней поверхностью желудка и поджелудочной железой имеются брюшинные сращения, которые в литературе обозначают как желудочно-поджелудочную связку [2]. Эти сращения

переходят на желудочно-селезёночную и желудочно-диафрагмальную связки, плотно фиксируя поджелудочную железу к задней стенке желудка в зоне непосредственного выполнения мобилизации стенок желудка. Хвост ПЖ расположен между листками желудочно-селезёночной связки и доходит до висцеральной поверхности селезёнки, при этом сосуды селезёнки идут непосредственно по верхнему краю ПЖ впереди неё [6].

Эти способы так же исключают возможность одномоментного пересечения желудочно-селезёночной и желудочно-диафрагмальной связок, что значительно повышает сложность и продолжительность операции, которая составляет около 3,5 часов.

Известно, что рассечение спаек по задней стенке желудка только в области его тела и дна, без их устранения в области антрального отдела, является одной из причин развития послеоперационных дискоординированных нарушений моторики желудка на границе свободного от спаечного процесса тела и фиксированного спайками антрального отдела желудка.

В связи с указанным нами предложен модифицированный способ выполнения СПВ (патент на изобретение №2717209 от 18.03.2020), который позволяет исключить недостатки указанных способов.

Предложенный нами способ СПВ включает выделение верхнего края пищеводного отверстия диафрагмы, мобилизацию дна желудка и скелетирование левой ножки диафрагмы, пересечение восходящей желудочной артерии, диссекцию малой кривизны желудка и кардии по направлению от угла желудка к кардии с пересечением поперечных сосудисто-нервных желудочных веточек, денервацию абдоминальной части пищевода, выделение правой ножки диафрагмы и заднего ствола вагуса, закрытие обнажённых мышц малой кривизны желудка серозно-мышечными швами до кардии, сшивание пищевода, кардии и дна желудка методом боковой инвагинации.

Отличие предлагаемого способа заключается в том, что после выделения верхнего края пищеводного отверстия диафрагмы в бессосудистой зоне рассекаем желудочно-ободочную связку и спайки между задней стенкой антрального отдела желудка и ПЖ до привратника (Рисунок 1).

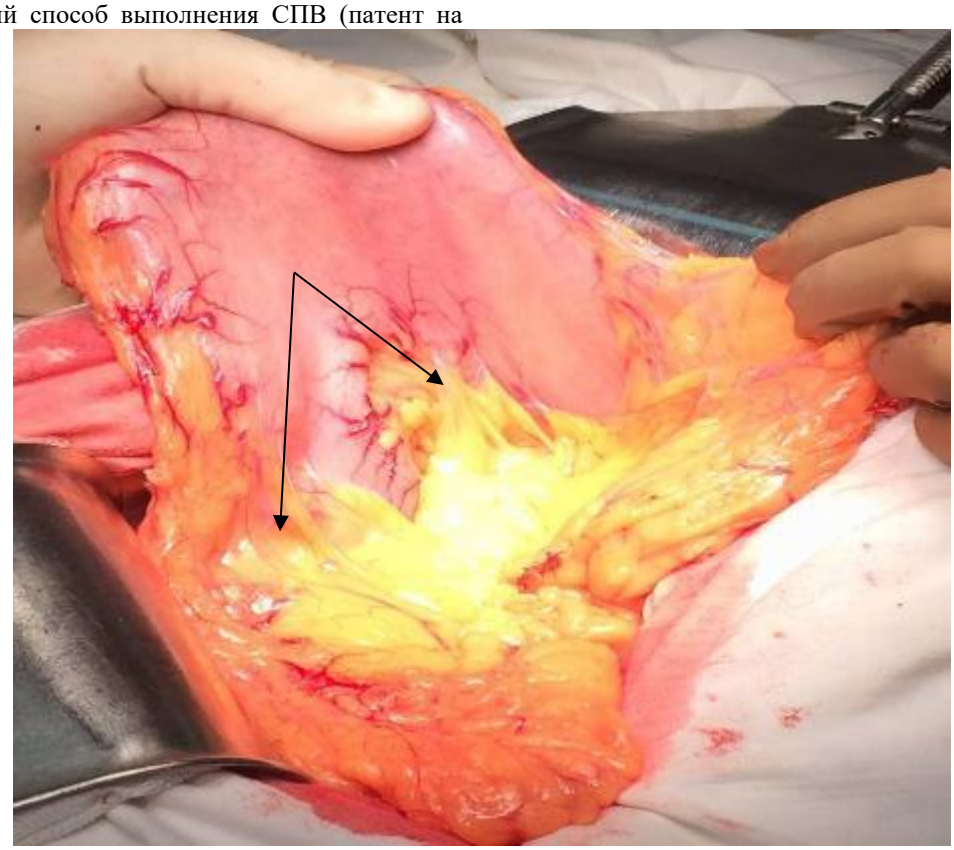

Рис. 1. Множественные спайки между задней стенкой желудка и желудочно-поджелудочной связкой (стрелками указаны спайки)

Затем рассекаем брюшинные сращения между задней стенкой желудка и ПЖ до верхнего края дна желудка и желудочно-поджелудочную связку, полностью отделяем ПЖ с селезёночными сосудами и нервами от задней стенки желудка, желудочно-селезёночной и желудочно-диафрагмальной связок (Рисунок 2).

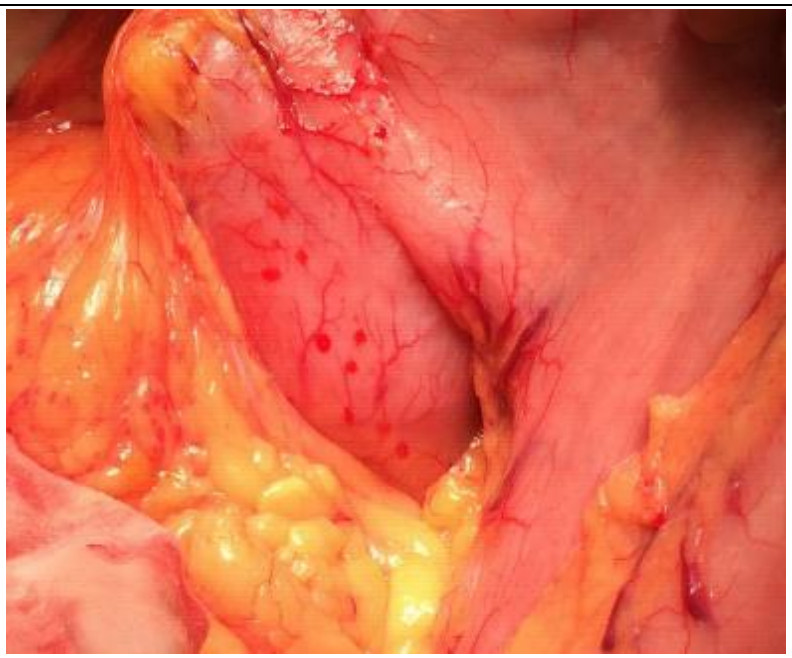

Рис. 2. Рассечены спайки между антральным отделом желудка и поджелудочной железой привратника.

Отличием способа также является и то, что хвост ПЖ выделяем из желудочно-селезёночной связки по направлению от кардии до ворот селезёнки с визуализацией коротких желудочных артерий, после этого желудок натягиваем вниз и вправо (рисунки 3, 4, 5).

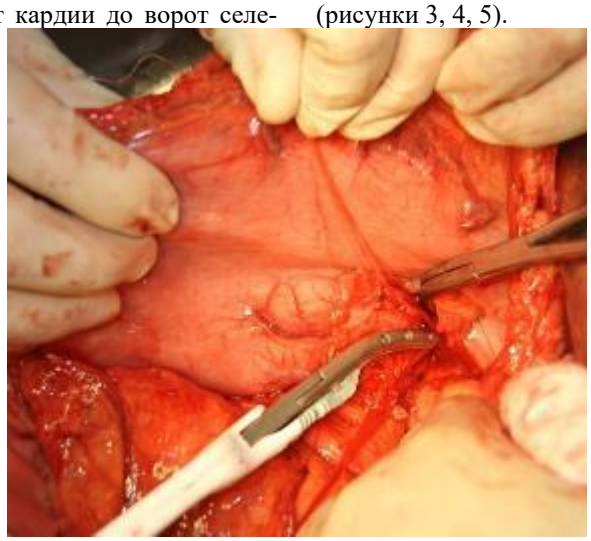

Рис. 3. Рассечение спаек и отделение поджелудочной железы от желудка с использованием аппарата «Liga Sure».

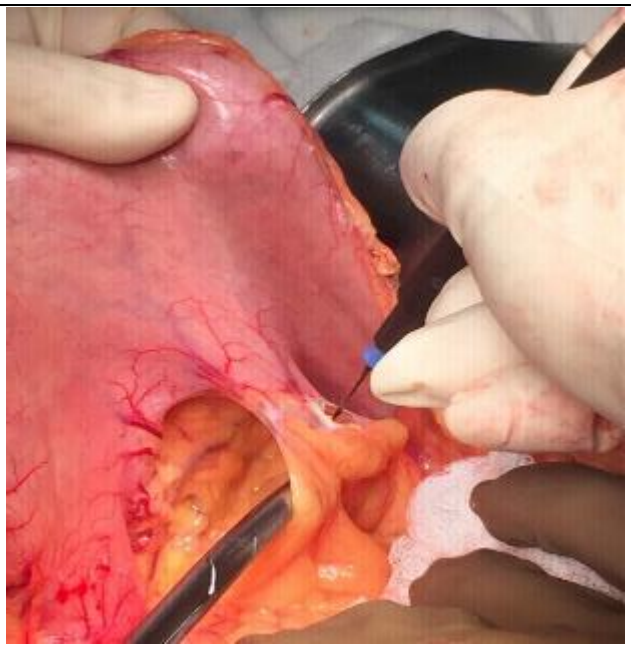

Рис. 4. Рассечение желудочно-поджелудочной связки

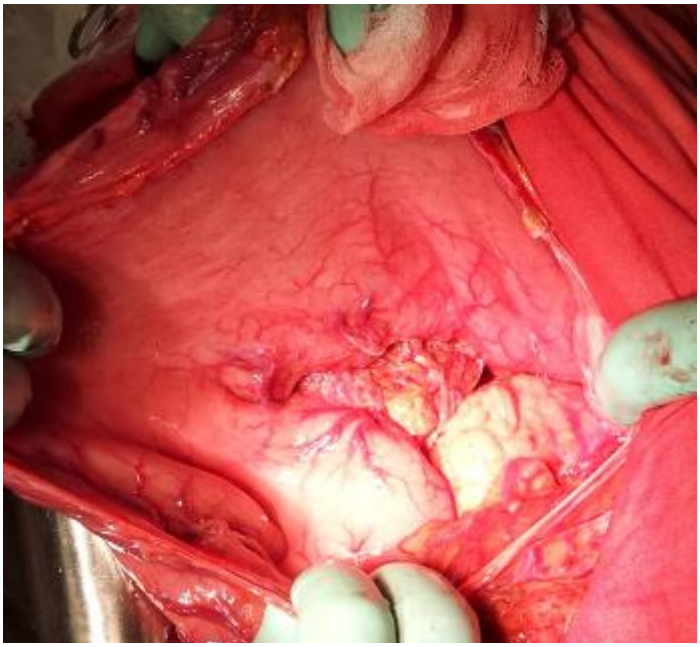

Рис. 5. Поджелудочная железа отделена от желудка

Отличия предлагаемого способа также заключаются и в том, что между задней стенкой желудка и ПЖ хирург вводит кисть руки ладонью к задней стенке желудка, которую проводит до ворот селезёнки и отделяет ею желудок, желудочно-селезёночную и желудочно-диафрагмальную связки от ПЖ с селезёночными сосудами и нервами (Рисунок 6).

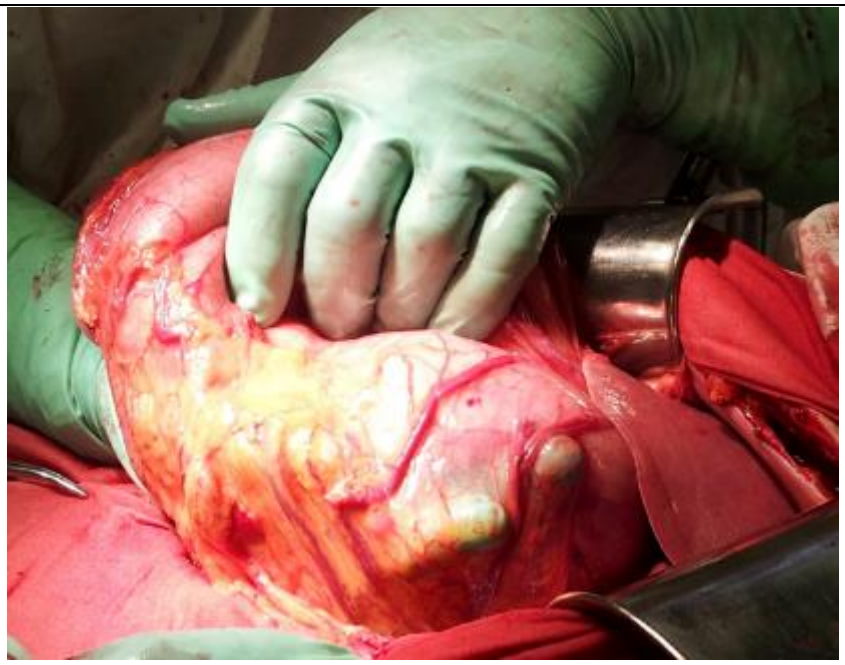

Рис. 6. Кисть руки проведена между задней стенкой желудка и поджелудочной железой. Кончики пальцев визуализируются через желудочно-селезёночную связку в бессосудистой зоне. Видны короткие артерии желудка.

Кончиками пальцев этой же руки хирург захватывает край дна желудка и движением вниз натягивает желудочно-селезёночную связку до визуализации кончиков пальцев руки через неё и через желудочно-диафрагмальную связку. Затем желудочно-селезёночную связку, в бессосудистой зоне средней её части, рассекаем одномоментно продольно от края дна желудка до ворот селезёнки (Рисунок 7, 8).

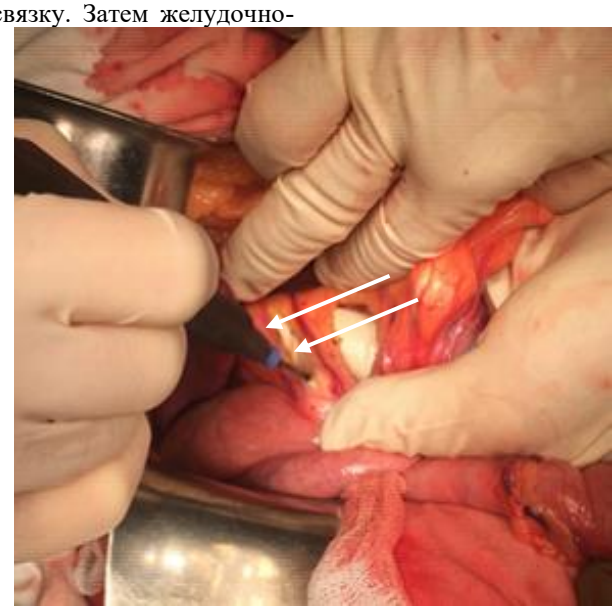

Рис. 7. Пересечение сосудов желудочно-селезеночной связки (стрелками указаны сосуды)

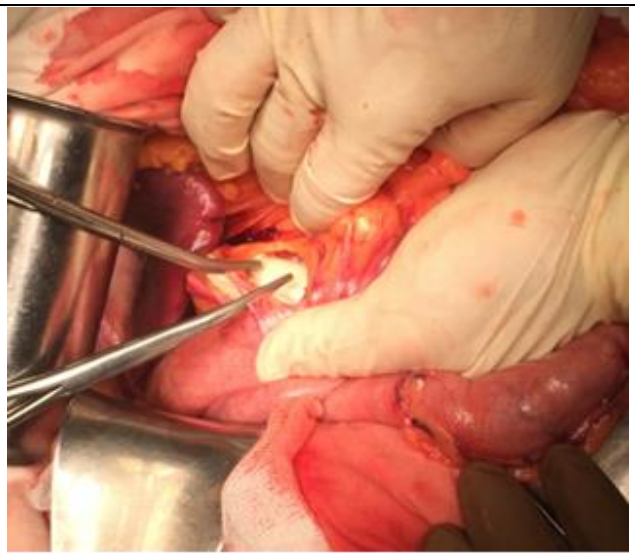

Рис. 8. Выделенные участки связок вместе с расположенными в них короткими артериями, пересекаются между зажимами.

Далее по направлению к пищеводу пересекаем медиальную часть желудочно-селезёночной связки и желудочно-диафрагмальную связку на всю толщину. После этого выполняем скелетирование левой ножки диафрагмы, для этого рассекаем пищеводно-диафрагмальную связку по направлению к пищеводному отверстию диафрагмы и пересекаем восходящую желудочную артерию (Рисунок 9).

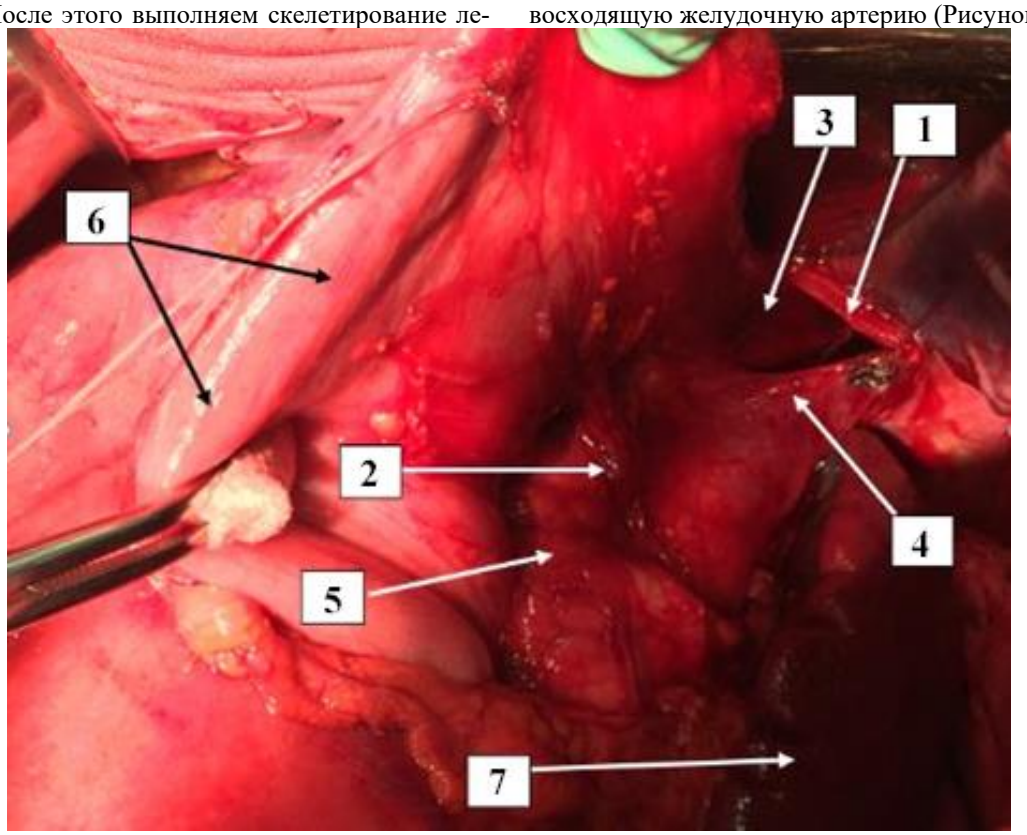

Рис. 9. Вид на область операции после мобилизации дна желудка.
1. - пищеводное отверстие диафрагмы, 2. - восходящая желудочная артерия, 3 - пищевод, 4. - левая ножка диафрагмы, 5 - поджелудочная железа, 6 – мобилизованное дно желудка, 7 – селезёнка.

На заключительном этапе операции проводим денервацию малой кривизны желудка, кардии и абдоминального отдела пищевода, выделяем задний ствол вагуса, закрываем обнажённые мышцы малой кривизны желудка и осуществляем кардиофундопликацию.

При проведении операций СПВ по предложенному способу в течение 11 лет случаев травм ПЖ, селезёночных сосудов и селезёнки не было. По данным послеоперационной рентгеноскопии желудка дискоординированная послеоперационная моторика желудка не регистрировалась.

Обсуждение. Отличительные приемы предложенного нами способа позволили снизить травматичность СПВ за счет исключения возможности интраоперационного повреждения ПЖ, селезёнки и её

сосудов. Это достигается тем, что предварительное механическое отделение желудка с желудочно-селезёночной и желудочно-диафрагмальной связками от ПЖ с селезёночными сосудами и нервами, а также предварительное выделение из желудочно-селезёночной связки и ворот селезёнки хвоста ПЖ полностью исключают возможность их повреждения хирургическим инструментарием при пересечении этих связок.

Введение кисти руки хирурга между желудочно-селезёночной, желудочно-диафрагмальными связками и поджелудочной железой с селезёночными сосудами, и нервами обеспечивает их механическое разделение от этих связок, что позволяет осуществить безопасное одномоментное рассечение и последующее пересечение связок на всю глубину и, следовательно, устранить вероятность их повреждения хирургическим инструментарием.

Натяжение желудка пальцами руки хирурга за край его дна позволяет растянуть желудочно-селезёночную связку и, тем самым, освободить больше места, как для её рассечения, так и для более надежного наложения зажимов для её пересечения, что также снижает риск повреждения селезёнки и кровотечения из коротких артерий желудка.

В то же время рассечение желудочно-селезёночной, желудочно-диафрагмальной и пищеводно-диафрагмальной связок открывает широкий доступ к восходящей желудочной артерии и левой ножке диафрагмы, что обеспечивает хорошую визуализацию этих анатомических образований и значительно упрощает, и ускоряет дальнейшую диссекцию желудка и кардии по малой кривизне с пересечением поперечных сосудисто-нервных желудочных веточек.

Полное рассечение спаек и отсечение поджелудочной железы от задней стенки желудка от привратника до кардии и дна желудка позволяют исключить развитие послеоперационных дискоординированных нарушений моторики желудка.

Выводы. Таким образом, предлагаемый способ СПВ позволяет полностью исключить интраоперационную травму поджелудочной железы, селезенки и ее сосудов, а также исключить послеоперационные осложнения дискоординированные нарушения моторики желудка.

К преимуществам предлагаемого способа также следует отнести и значительное уменьшение трудоемкости операции, упрощение техники выполнения СПВ и сокращение времени операции.

Способ может быть выполнен хирургами без опыта операций СПВ.

References

1. Durleshter V.M. Complex treatment of decompensated cicatricial ulcerative stenosis of duodenum / V.M. Durleshter, M.T. Didigov // Medical Bulletin of the South of Russia. - 2016. - № 3. - C. 54-58.

2. Kovanov, V. V. Operative surgery and topographic anatomy / V. V. Kovanov. - 4. - Moscow: Medicine, 2001. - 167 c.

3. Krylov, N. N. The contribution of the Clinic of Faculty Surgery named after N. N. Burdenko. N.N. Burdenko 1-st Moscow Medical Institute named after I.M. Sechenov in the development of organ preserving operations with vagotomy for peptic ulcer treatment / N.N. Krylov, E.A. Pyatenko. // History of Medicine. - 2016. - № 3. - C. 412-425.

4. Onopriev, V.I. Etudes of functional surgery of peptic ulcer / V.I. Onopriev. - 4. - Krasnodar : Publishing and Polygraphic Production Lease Enterprise, 1995. - 214-271 c.

5. Podoluzhnyj, V.I. The need for pyloroplasty and vagotomy in perforative duodenal ulcer / V.I. Podoluzhnyj, A.B. Startsev, I.A. Radionov. // Bulletin of pancreatology club. - 2020. - № 1. - C. 56-59.

6. Sinelnikov, R. D. Atlas of human anatomy. / R. D. Sinelnikov, J. R. Sinelnikov, A. Y. Sinelnikov. - Moscow : New Wave, 2009. - 351 c.

7. Chernousov A.F. Surgery of gastric and duodenal ulcer / A.F. Chernousov, T.V. Horobrykh, P.M. Bogopolsky. - Moscow : Practical Medicine, 2016. - 250 c.

8. Lagoo J, Pappas TN, Perez A. A relic or still relevant: the narrowing role for vagotomy in the treatment of peptic ulcer disease. Am J Surg. 2014 Jan;207(1):120-6.

9. Seeras K, Qasawa RN, Prakash S. Truncal Vagotomy. 2021 Jan 7. In: StatPearls [Internet]. Treasure Island (FL): StatPearls Publishing; 2021 Jan-. PMID: 30252360.

COAGULOPATHY AND THROMBOSIS IN THE CONSUMPTION OF CONTRACEPTIVES

Maximenco Iulian,
Student at "Nicolae Testemițanu" State University of Medicine and Pharmacy
Saint Stephen the Great Boulevard 165, Chisinau 2004, Moldova
Ambros Ala
PhD, university lector
Department of Biochemistry and Clinical Biochemistry
Nicolae Testemițanu Street 27, Chisinau, Moldova
DOI: 10.5281/zenodo.7796070

Abstract

Hormonal contraceptives exert prothrombotic effects, related to estrogen (intensification of gene expression of coagulation factors II, VII, VIII, X, XII, fibrinogen, von Willebrand factor, heparanase, TAFI, induction of PCa resistance, decrease in expression of antithrombin, factor V, activation inflammation, vasodilatation in non-optimal conditions) as well as antithrombotic effects (activation of PS and TFPI, increase in PAI-1 gene expression and decrease in T-PA gene expression). Progestins activate heparanase, and induce vasodilation. Therefore, contraceptives have diametrically opposite effects, and the pro- or anti-thrombotic result largely depends on the pre-existing coagulant background. Different methods of hormonal contraception have distinct thrombotic risks. The thrombotic effect of estrogen is dose-dependent, diminishing at low doses. But even at doses of 10 μg, the prothrombotic effect persists. There is a difference between the types of estrogens. Thus, the use of estradiol valerate and estradiol decreases the thrombotic risk compared to ethinyl estradiol.

Keywords: hormonal contraception, mechanism of coagulopathy, methods of contraception, coagulation factors, heparanase.

Introduction

Hormonal contraceptives are widely used and effective if used correctly. Since the 1960s, HC have become widespread, and it is now estimated that more than 150 million women use them globally. Deep vein thrombosis and pulmonary embolism, collectively called venous thromboembolism (VTE), occur at an annual rate of 5 cases per 10,000 women of reproductive age, representing approximately 67,000 annual cases of VTE in the European Union, where there are approx. 134 million women between the ages of 15 and 54 [2]. The results of epidemiological studies on the risk of VTE associated with hormonal contraceptives (CH) have varied, with some showing no difference in risk between CH (prospective active surveillance studies) while others showing an increased risk (observational studies or databases) [10]. The aim of the research is the elucidation of the biochemical processes of normal hemostasis, with the determination of the mechanisms by which hormonal contraceptives induce coagulopathies, the description of the types of hormonal contraceptives and their distinct action on coagulation.

Materials and methods

The given work represents a bibliographic study based on current scientific literature to determine the mechanisms that lead to coagulation disorders in the consumption of contraceptives.

Articles, books, websites and scientific publications from 175 bibliographic sources based on data from: PubMed, Medscape, National Library of Medicine, Frontiers, BMJ, WHO, international guidelines and published national and international clinical protocols were used. The period of their publication being primarily 2013-2023.

Results

The coagulation mechanisms of HC are: estrogen administered orally will pass through the liver, inducing changes in blood coagulation and anticoagulant proteins: it increases the synthesis of coagulation factors II, VII, VIII, X, XII, fibrinogen, protein C, protein S, TFPI and thrombin-activatable fibrinolysis inhibitor (TAFI) and decreases the synthesis of others: factor V and antithrombin (AT) [7,11]. It acts on fibrinolysis by increasing the level of tissue plasminogen activator and decreasing the level of PAI-1, but due to TAFI the overall effect is antifibrinolytic. The other mechanisms are: proinflammatory effect at low doses, grow of heparanase activity(increase TF and decrease TFPI), vasodilatory effect of estrogen (compromised veins of the lower limbs) [8,12].

Progestins have also been shown to have a procoagulant effect, even in the absence of estrogen. The first mechanism is also caused by increased heparanase activity. It does this through estrogen receptors. Progestins of the 3rd and 4th generation, which demonstrate more intense procoagulant effects, have been shown to influence heparanase the most. The second mechanism is vasodilatation [9,12].

The correlation of HC methods and the intensity of the procoagulant effect, argued on the basis of clinical studies is represented in table 1. According to clinical studies, COCs of the 1st, 3rd, 4th generation, the vaginal ring and the transdermal patch have the greatest risk. The 2nd generation COC, Norgestimate (GEN 3 COC), medroxyprogesterone injection have an average risk. The intrauterine device, implant, progestin pills and emergency contraception have the lowest risk. The dose difference of ethinylestradiol demonstrates a dose-dependent procoagulant effect. Increasing the dose increases the risk. Among the different types of estrogens, estradiol valerate (E2) and estradiol (E4) have been shown to be less procoagulant and safer.

Table 1.

Correlation between HC method and procoagulant effect

Method of HC	Dose EE	Type of progestine	RR, OR, estimate risk	References
1. OC				
I gen	30-40 µg	Ciproteron	OR 4,0*	Stegeman et al.
II gen	30-40 µg	LNG	OR 2,38*/RR 1,63*	LaVasseur et al. Weill et al.
III gen	30-40 µg 20-30 µg 30-40 µg 20-30 µg	Desogestrol Desogestrol Gestoden Gestoden	OR 4,28 * RR 2,16 ** OR 3,64* RR 2,16*	LaVasseur et al. Weill et al. LaVasseur et al. Weill et al.
	30-40 µg	Norgestimate	OR 2,53*	LaVasseur et al.
IV gen	30-40 µg 30-40 µg	Drosperinonă Drosperinonă	OR 4,0* RR 1,40**	Stegeman et al. Oedingen et al.
2. Vaginal ring	13-15 µg/zi	Etonogestrel	RR 1,90** RR 6,5*	Lidegaard et al.
3. Transdermal patch	30 µg/zi	LNG	OR 2,0*** RR 7,9*	Fleischer et al./ Dore et al. Lidegaard et al.
4. Injection	-	Depo medroxiprogesteron	OR 2,2* RR 3,6*	Bergendal et al. Hylckama et al.
5. Emergency contraception	#	#	#	
6. Progestin pills	-	Noretindrona Drospirenona	OR 1,03*	Tepper et al.
7. IUD	-	LNG	OR 1,03*	Tepper et al.
8. Implant	-	LNG	OR 1,03*	Tepper et al.
The difference between different doses of EE				
	20 µg 30-40 µg	-	RR 0,75**** RR 1****	Weill et al. Weill et al.
The difference between different types of estrogens				
EE și E2 EE și E4	- -	- -	6,9/10.000 9,9/10.000	Grandi et al.

Note: reference variable

* not exposed/ not ill lipsa de expunere/lipsa bolii

** OC with LNG with the same dose of EE

*** OC with Norgestimate 30-40 µg

**** OC with the same type of progestine and 30-40 µg EE

References

1. Bergendal Annica et al. “Association of Venous Thromboembolism With Hormonal Contraception and Thrombophilic Genotypes.” Obstetrics & Gynecology vol. 124 no. 3 Ovid Technologies (Wolters Kluwer Health) Sept. 2014 pp. 600–09. Crossref https://doi.org/10.1097/aog.0000000000000411.

2. Blondon M. Update on Oral Contraception and Venous Thromboembolism. În: “Educational Updates in Hematology Book: 25th Congress of the European Hematology Association Virtual Edition 2020.” HemaSphere vol. 4 Ovid Technologies (Wolters Kluwer Health) June 2020 pp 156-158. Crossref https://doi.org/10.1097/hs9.0000000000000444.

3. Dore David D. et al. “Extended Case-control Study Results on Thromboembolic Outcomes Among Transdermal Contraceptive Users.” Contraception vol. 81 no. 5 Elsevier BV May 2010 pp. 408–13. Crossref https://doi.org/10.1016/j.contraception.2009.12.009.

4. Fleischer K. et al. “Effects of the Contraceptive Patch the Vaginal Ring and an Oral Contraceptive on APC Resistance and SHBG: A Cross-over Study.” Thrombosis Research vol. 123 no. 3 Elsevier BV Jan. 2009 pp. 429–35. Crossref https://doi.org/10.1016/j.thromres.2008.04.022.

5. Grandi Giovanni et al. “Confirmation of the Safety of Combined Oral Contraceptives Containing Oestradiol on the Risk of Venous Thromboembolism.” The European Journal of Contraception & Reproductive Health Care vol. 27 no. 2 Informa UK Limited Feb. 2022 pp. 83–84. Crossref https://doi.org/10.1080/13625187.2022.2029397.

6. Hylckama Vlieg Astrid van et al. “The Risk of Deep Venous Thrombosis Associated With Injectable Depot–Medroxyprogesterone Acetate Contraceptives

or a Levonorgestrel Intrauterine Device." Arteriosclerosis Thrombosis and Vascular Biology vol. 30 no. 11 Ovid Technologies (Wolters Kluwer Health) Nov. 2010 pp. 2297–300. Crossref https://doi.org/10.1161/atvbaha.110.211482.

7. LaVasseur Corinne et al. "Hormonal Therapies and Venous Thrombosis: Considerations for Prevention and Management." Research and Practice in Thrombosis and Haemostasis vol. 6 no. 6 Elsevier BV Aug. 2022 p. e12763. Crossref https://doi.org/10.1002/rth2.12763.

8. Lidegaard O. et al. "Venous Thrombosis in Users of Non-oral Hormonal Contraception: Follow-up Study Denmark 2001-10." BMJ vol. 344 no. may10 3 BMJ May 2012 pp. e2990–e2990. Crossref https://doi.org/10.1136/bmj.e2990.

9. Oedingen Carina et al. "Systematic Review and Meta-analysis of the Association of Combined Oral Contraceptives on the Risk of Venous Thromboembolism: The Role of the Progestogen Type and Estrogen Dose." Thrombosis Research vol. 165 Elsevier BV May 2018 pp. 68–78. Crossref https://doi.org/10.1016/j.thromres.2018.03.005.

10. Sitruk-Ware Regine. "Hormonal Contraception and Thrombosis." Fertility and Sterility vol. 106 no. 6 Elsevier BV Nov. 2016 pp. 1289–94. Crossref https://doi.org/10.1016/j.fertnstert.2016.08.039.

11. Stegeman B. H. et al. "Different Combined Oral Contraceptives and the Risk of Venous Thrombosis: Systematic Review and Network Meta-analysis." BMJ vol. 347 no. sep12 1 BMJ Sept. 2013 pp. f5298–f5298. Crossref https://doi.org/10.1136/bmj.f5298.

12. Tepper Naomi K. et al. "Progestin-only Contraception and Thromboembolism: A Systematic Review." Contraception vol. 94 no. 6 Elsevier BV Dec. 2016 pp. 678–700. Crossref https://doi.org/10.1016/j.contraception.2016.04.014.

13. Weill Alain et al. "Low Dose Oestrogen Combined Oral Contraception and Risk of Pulmonary Embolism Stroke and Myocardial Infarction in Five Million French Women: Cohort Study." BMJ BMJ May 2016 p. i2002. Crossref https://doi.org/10.1136/bmj.i2002. [Original source: https://studycrumb.com/alphabetizer]

MODIFICATION IPOM - PLASTIC SURGERY IN PATIENTS WITH UMBILICAL HERNIAS

Molchanov M.A.,
Surgeon of the Samara City Hospital № 7, Russia.
443112, Samara, Kraynyaya street, 17.
Krivoschekov E.P.,
MD, professor of department of surgery of institute of professional education
Samara State Medical University, Russia.
443095, Samara, Tashkentskaya street, 159
Shorin S.A.,
Surgeon, head of department of surgery of the
Stavropol Central District Hospital
445004, Samara region, Togliatti, Avtozavodskoe highway, 5
Sadchikov S.V.,
Surgeon of the Stavropol Central District Hospital
445004, Samara region, Togliatti, Avtozavodskoe highway, 5
Trubnikov A.A.
Surgeon of the Stavropol Central District Hospital
445004, Samara region, Togliatti, Avtozavodskoe highway, 5
DOI: 10.5281/zenodo.7796126

Abstract

In the conditions of modern, constantly progressive medicine, it is a hopeless option to isolate the hernial sac from the subcutaneous tissue to the level of the hernial gate and remove it. This is too traumatic stage of the operation, which is accompanied by detachment of subcutaneous tissue, dissection of aponeurosis, damage to the lymphatic collectors, and bleeding of tissues. When suturing the wound, the synthetic prosthesis remains in contact with subcutaneous tissue, cavities form in the wound, and lymphorrhea persists for a long time. All this requires constant monitoring of the wound and does not exclude the development of complications, the number of which reaches 25%.

Keywords: IPOM plastic surgery, umbilical hernias, prevention of complications.

The aim of our study was to evaluate the effectiveness of the method of intraoperative prevention of wound complications and reducing the trauma of operations in patients with IPOM - plastic surgery in patients with umbilical hernias. During the study period, 82 patients with umbilical hernias were operated on. The size of the defect was from 3 cm^2 up to 875 cm^2. There were 37 males and 451 females. The patients age ranges from 18 to 67 years.

Operation technique. Access to the abdominal cavity was performed through an incision in the upper dome of the hernial sac. The implant was fixed along the perimeter of the muscular-aponeurotic contour of the hernial gate from the inside. Through U-shaped sutures were applied with the prosthesis going beyond the edges of the defect by 3-5 cm. With this approach, there is no trauma in the release of the hernial sac, there is no wide detachment of subcutaneous tissue and additional dissections of the aponeurosis. The U-sutures included the omentum tissue, which became a protection against contact injury between the intestine and the prosthesis. Did not allow contact of the reticular prosthesis with subcutaneous tissue. The peritoneal surface of the hernial sac sheets was de-epithelized and stitched over a fixed prosthesis, creating a dense presentation between them. Such techniques significantly reduce the volume of surgical trauma and avoid the accumulation of fluid in the wound.[1]

Operations were performed without isolation of the hernial sac and its removal, which resulted in significantly reduces the traumatic nature of interventions. Operations are not accompanied by a wide detachment of subcutaneous tissue, the network of lymphatic collectors remains intact, direct contact of the synthetic prosthesis with subcutaneous tissue is completely excluded, and fluid accumulation in the wound does not occur.[5] Treatment of the hernial sac is atraumatic.

Through the cut the anterior wall of the hernial sac was inserted into the abdominal cavity and all subsequent stages of the operation were performed. The leaves of the hernial sac were separated on clamps and a cavity was created, the work inside of which is convenient, visually controlled and can be carried out with maximum compliance with the conditions of asepsis - there is no overhang of loose fiber, and intestinal loops are easily held in the created cavity and do not fall out on the abdominal wall. From the inside of the hernial sac, it is easier to approach the areas where the soldered organs and the scarring process are most pronounced and are associated with the separation of the intestines from adhesions after possible incomplete infringements in the anamnesis. Preparation for intraperitoneal plastic surgery consisted in freeing the hernial gate from fixed organs and adhesions. There were no additional dissections of the aponeurosis. The condyle-aponeurotic contour of the hernial gate is easily determined by a tight roller on the side of the abdominal cavity.

The prosthesis was fixed using a true muscular-aponeurotic contour of the hernial gate, which is repre-

sented by rectus abdominis muscles in a state of diastasis. The application of U-shaped sutures along the perimeter of the hernial gate with the prosthesis going beyond the edges of the defect at least 3-5 cm excluded the fixation of the implant "edge to edge". The U-sutures also included the omentum tissue, which became a protective pad between the intestinal loops and the prosthesis.[4] Muscle-aponeurotic prosthetic plastic surgery creates conditions that combine the properties of elastic decompression along the suture line due to contractile the ability of the muscles, and high resistance of the aponeurosis to mechanical loads. Creating conditions for damping unloading is extremely important, since it increases the reliability of fixing the prosthesis, reduces postoperative pain and allows patients to be activated early.

Sheets of the preserved hernial sac were sewn over the surface of the prosthesis, the prosthesis was placed between the sheets of the hernial sac from above and the omentum from below, the produced fluid is absorbed by the peritoneum and its accumulation in the wound does not occur.

Special surgical techniques formulated in terms of "peritoneal desquamation" and "peritoneodesis of the hernial sac" have been developed.[2] They were used during surgery as an alternative to removing the hernial sac, and were of particular importance not only in the prevention of wound complications, but also in stimulating reparative processes. During the operation, special physiological properties of the peritoneum were used - traumatization of the mesothelial cover of the peritoneum is accompanied by the release of exudate, which is immediately permeated with fibrin filaments. Formed fibrin adhesions keep the surfaces close together fabrics between each other. Then they form strong connective tissue splices. This mechanism is a protective, physiologically determined property of the peritoneum. It is purposefully used during surgery to improve healing conditions and activate reparative processes.

Mechanical destruction and desquamation of the epithelium (desquamation) of the peritoneal surface of the hernial sac was performed intraoperatively with a special technical device. Destruction of functionally active mesothelial cells suppresses the production of fluid and its accumulation in the wound does not occur. In addition, and most importantly, desquamation creates conditions for the formation of fibrin adhesions and early germination of connective tissue cellular elements (fibroblasts, collagen and elastic fibers). The formulated concept of peritoneodesis of the herniated sac means the creation of a tight connection of its peritoneal parts. surfaces with fabrics. The herniated sac sheets were stitched over the implant in such a way that their de-epithelized peritoneal surfaces fit snugly to the surface of the fixed implant. Between the connected surfaces, active germination of connective tissue elements occurs, which freely penetrate through the implant cells and, fusing with it, create strong adhesions with the formation of the so-called "prosthetic aponeurosis". The use of" desquamation "and" peritoneodesis " of the hernial sac creates special, most favorable conditions for the course of reparative processes and is the most effective treatment for the patient. a preventive measure for the development of complications.[7]

The use of intraperitoneal plastic surgery makes it possible to perform operations from smaller incisions. When choosing access, the incision length was determined by the size of the hernial gate and in accordance with them. Surgery through the hernial sac cavity creates quite comfortable conditions for performing intraperitoneal plastic surgery from an incision corresponding to the size of the hernial gate. Such calculations significantly reduced the size of the section. In particular, they used variable access. It was used in patients with large hernial defects and minor soft tissue excesses that do not require extensive excision. Two small incisions were made, from which the entire volume of the intervention was performed. A certain area of the hernial gate was opened through one of the incisions and U-shaped sutures were applied to the implant from the abdominal side. The implant was inserted through one incision, then the prosthesis was moved inside the abdominal cavity and fixed through the aperture of another incision. Soft tissue dislocation allows tunneling of the implant and its gradual fixation under visual control. Removal of excess soft tissues in patients with large hernias was performed according to pre-planned reference lines. It is important that the fabrics after excision can be sewn without tension. To get more accurate landmarks, it is advisable to use the middle line of the abdomen, applied from the xiphoid process to the womb. The hernial sac was shifted laterally without significant tension and a line was drawn on the skin at the base of the hernial sac coinciding with the midline of the abdominal wall. Then, the hernial sac was shifted in the opposite direction and the middle line on the skin of the removed hernial sac was also marked. When excising tissues along these lines, the opposite edges of the wound correspond to the middle line and are located in a state of adequate matching and tension.[3]

The distance between the middle and posteroaxillary lines on each side was measured. From the posterior-axillary line, a centimeter tape was placed, going to the side of the laterally removed hernial sac and making marks on the skin. The marks correspond to the midline of the abdomen. The same marks were made on the hernial sac, which was taken in the opposite direction. After excision along these reference lines, the edges of the wound coincide with the middle line and do not experience tension during stitching.

This approach simplifies the selection of the cut line and direction. For hernial gates that are wider than their length, cross-sections are recommended. As the wound heals, such incisions do not acquire an aesthetic appearance. In cosmetic terms, median incisions look more preferable. When working from the inside of the hernial sac, there is no such dependence, since there is no need to isolate the hernial sac, and its cavity provides quite adequate conditions for fixing the implant in any form of hernial gate. The use of median access becomes a working standard and method of choice. Cross sections no access rights were used. Figural incisions were

used in cases where significant excess adipose skin tissue was removed.

Conclusions. Wound healing took place by primary tension. No significant tissue edema was observed. Wound complications were noted in 3 patients. There were no intra-abdominal complications. There were no relapses during follow-up of patients for up to 6 months. Patients are active and functional. The intraperitoneal approach to umbilical hernia repair expands intraoperative opportunities for the prevention of wound complications.

References

1. Molchanov M. A.. Intraperitoneal plasty of postoperative and umbilical hernias / / Postgraduate Bulletin of the Volga region No. 1-2, Samara, Medicine, 2015, pp. 157-162.

2. Grigoriev S. G., Krivoshchekov E. P., Grigorieva T. S., Dmitrieva I. A. Desquamation and periotenodesis of the hernial sac during plastic surgery of postoperative hernias // Bulletin of Surgery of Kazakhstan: Tez. III Congress of Surgeons of Kazakhstan with international participation "Innovations in Surgery". - 2012. - p. 248.

3. Zhebrovsky V. V. Atlas of operations in abdominal hernias / V. V. Zhebrovsky, F. N. Ilchenko. Simferopol, 2004, 315 p. (in Russian).

4. Krivoshchekov E. P., Grigorieva T. S., Grigoriev S. G., Kostin A. Yu. Zashchita kishechnika ot kontaktnoy travmy pri intraperitoneal plastike [Protection of the intestine from contact trauma in intra-abdominal plastic surgery]. III Congress of Surgeons of Kazakhstan with international participation "Innovations in Surgery". - 2012. - p. 252.

5. Krivoshchekov E. P., Molchanov M. A. et al. Krivoshchekov E. P., Grigoriev S. G., Molchanov M. A., Grigorieva T. S. Sposob snizheniya intraoperatsionnoy travmy pri intraperitoneal plastike umbilical and ventral hernias. Fundamental'nye issledovaniya No. 1 chast 5, 2015, pp. 980-983.

6. Chevrel J.P., Rath A.M.Classification of incisional herniaso of abdominal wall // Hernia. 1999. Vol. 4. P. 7-11.

7. Krivoshchekov E. P., Molchanov M. A. et al. Intraoperative prevention of postoperative complications in the method ipom- plasty of the ventral and umbilical hernias / Krivoshchekov E. P., Molchanov M. A., Grigoriev S. G., Romanov V. E., Grigorieva T. S. / Post-graduate Bulletin of the Volga region No. 1-2, Samara, Meditsina Publ., 2017, pp. 103-107.

THE IMMUNE SYSTEM OF THE ORAL CAVITY

Postovoi E.,
Student, Department of Histology, Cytology and Embryology,
Nicolae Testemitanu State University of Medicine and Pharmacy, Chisinau, Republic of Moldova
Fulga V.
university lecturer, scientific adviser
DOI: 10.5281/zenodo.7796140

ИММУННАЯ СИСТЕМА РОТОВОЙ ПОЛОСТИ

Постовой Е.,
Студентка, Кафедра Гистологии, Цитологии и Эмбриологии, USMF „Nicolae Testemitanu", Кишинев, Республика Молдова
Фулга В.,
преподаватель университета, научный руководитель

Abstract

The oral cavity has a multicomponent system of protection against adverse environmental influences. The oral mucosa, lamina propria, submucosa, lymphoepithelial ring Pirogov-Waldeyer and saliva contain cellular and humoral factors that can respond autonomously to various antigens, chemical, mechanical and other influences.

Аннотация

Ротовая полость имеет многокомпонентную систему защиты от неблагоприятных воздействий окружающей среды. Слизистая оболочка полости рта, собственная пластинка, подслизистая оболочка, лимфоэпителиальное кольцо Пирогова-Вальдейера и слюна содержат клеточные элементы и гуморальные факторы, которые могут автономно реагировать на различные антигены, химические, механические и другие воздействия.

Keywords: oral cavity, oral mucosa, epithelium, saliva, tonsils, dendritic cells, Langerhans cells, oral immunity, cellular immunity, humoral immunity, oral tolerance.

Ключевые слова: ротовая полость, слизистая ротовой полости, эпителий, слюна, миндалины, дендритные клетки, клетки Лангерганса, иммунитет рта, клеточный иммунитет, гуморальный иммунитет, толерантность ротовой полости.

Вступление

Ротовая полость является основными воротами для большинства антигенов. Условия окружающей среды, которые влияют на слизистую оболочку полости рта, включают: механические нагрузки, изменения температуры, обработку пищи и защиту от микроорганизмов или токсинов (например, никотина) [34]. Иммунный статус полости рта определяет целостность ее тканей, участвует в нейтрализации нежелательных чужеродных антигенов, опосредует формирование защитных иммуновоспалительных реакций против внедрения патогенов и снижает колонизацию различных микроорганизмов [11, 30].

В первые часы после проникновения антигена иммунный ответ опосредуется факторами врожденного иммунитета в две фазы: немедленный ответ и ранний индуцибельный ответ. При высокой начальной функциональной активности гуморальных и клеточных факторов врожденного иммунитета любой патоген может быть уничтожен очень быстро в месте проникновения до развития адаптивного иммунного ответа. Врожденный иммунитет также участвует в уничтожении некротических и апоптотических клеток и в восстановлении поврежденных тканей [28].

Врожденный и приобретенный иммунитет осуществляются тканями, клетками и эффекторными молекулами, которые защищают организм от заболевания путем распознавания потенциальных патогенов или поврежденных тканей. Защитные механизмы полости рта делятся на неспецифические и специфические [4, 20].

Основными структурными компонентами, ответственными за неспецифическую резистентность, являются: слизистая и подслизистая оболочки полости рта; эмаль, пелликула и дентин зуба; слюна (ротовая жидкость), содержащая гуморальные (ферменты, лизоцим, комплемент и др.) и клеточные (фагоцитарные клетки) неспецифические факторы защиты. Специфические факторы защиты делятся на гуморальные (Ig) и клеточные (Т и В лимфоциты) [23].

Морфо-функциональные и иммунологические аспекты слизистой ротовой полости

Иммунная функция слизистой оболочки ротовой полости зависит от состояния неспецифических и специфических механизмов иммунной защиты [15]. Эпителиальный барьер ротовой полости является механическим фактором неспецифического иммунитета [20]. Защитный механизм зависит от структуры эпителия, наличия в эпителии иммунокомпетентных клеток, таких как лимфоциты и

клетки Лангерганса (LC), и функции эпителиальных клеток в обнаружении патогенов [9].

Покоящиеся эпителиальные клетки не обладают свойствами иммуноцитов, но в условиях воспаления они способны представлять антиген Т-хелперам (Th) и стимулировать пролиферацию Т-цитотоксических клеток [23].

Микроорганизмы и продукты их распада мгновенно и эффективно распознаются различными APC, включая эпителиальные клетки, через различные рецепторы опознавания паттерна (PRRs). PRRs активируют врожденную иммунную систему, которая "увлекает" адаптивные клетки, мигрирующие в дренирующие лимфатические узлы, где, в свою очередь, индуцируется сильный иммунный ответ. Распознавание микроорганизмов осуществляется в основном 3 типами PRR: TOLL-подобными рецепторами (TLR), NOD-подобными рецепторами (NLR) и RIG-подобными рецепторами (RIL). TLR распознают широкий спектр вирусных и бактериальных агентов, демонстрируя варианты сплайсинга при таких заболеваниях, как болезнь Бехчета. Это может привести к аберрантной сигнальной трансдукции и индукции хронического воспаления, характерного для таких заболеваний. Распознавание TLR также встречается при красном плоском лишае (OLP) [1, 4, 27, 28, 29].

PRR распознают патоген-ассоциированные молекулярные паттерны (PAMPs), которые одинаковы у разных микроорганизмов. Процесс распознавания включает связывание PAMPs с PRR, что приводит к трансформации внутриклеточной доменной структуры PRR. Эта биохимическая реакция активирует цепь ферментов и генов в APC для выработки провоспалительных цитокинов, которые могут регулировать функцию интраэпителиальных лимфоцитов (IEL) [13, 26, 28]. Эти клетки располагаются вблизи базовой мембраны, между другими эпителиальными клетками [1, 28].

Большинство IEL являются Т-лимфоцитами, причем обнаруживаются как Th (CD4+), так и супрессорные (CD8+) лимфоциты. Соотношение Th:Т-цитотоксических клеток составляет приблизительно 5:1. Повышение IEL выше 5% во всех эпителиальных клетках указывает на хронический воспалительный процесс или продолжающийся иммунный процесс. IEL участвуют в иммунологическом надзоре, уничтожая инфицированные вирусом клетки или клетки-мутанты [20].

Клетки Лангерганса (LC) полости рта являются миелоидными дендритными клетками. В эпителии слизистой оболочки дендритные клетки (DC) и LC выходят в виде "пальцевидных" выростов, которые проникают из собственной пластинки непосредственно через эпителиальный слой и вступают в контакт с веществами в просвете ротовой полости [4, 5, 11]. Когда слизистая оболочка полости рта инвазирована микроорганизмами, LC вызывают иммунный ответ, действуя как APC и экспрессируя MHC II. Чтобы обеспечить немедленную защиту от вторжения патогенов, DC должны быстро реагировать на бактериальные структуры. Для этого используются TLRs, Fc-γ, лектиновые рецепторы С-типа и рецепторы комплемента [11, 31].

Иммунологическая и защитная роль собственной пластинки

Барьерно-защитная функция собственной пластинки подразделяется на неспецифические и специфические механизмы. Неспецифические механизмы формируются за счет основного вещества и механических свойств волокон собственной пластинки, которые имеют специфическую архитектуру в различных частях слизистой оболочки полости рта. Специфические механизмы включают иммунокомпетентные клетки, расположенные в собственной пластинке [20]. Макрофаги, к примеру, могут участвовать в обработке и презентации антигена в качестве APC. Эти клетки выделяют иммунные химические мессенджеры, хемокины и цитокины, стимулирующие пролиферацию фибробластов. Фибробласты в свою очередь производят фиброкины, которые регулируют различные иммунокомпетентные клетки, а также вырабатывают вещества, способные подавлять активность и пролиферацию Т-лимфоцитов. Т-клетки, активированные в собственной пластинке слизистой оболочки полости рта, присутствуют в большом количестве. Имеется много CD8+ и CD4+ Th2 клеток. Большое количество CD4+ Th2 клеток выделяют IL-3, IL-4, IL-5, IL-6, IL-13, GM-CSF. Также могут образовываться адаптивные регуляторные Т-клетки (Treg) [20, 28].

Морфо-функциональные и иммунологические особенности слюны

Слюна выполняет ряд важных функций, необходимых для поддержания здоровья полости рта. Она является доступной биожидкостью, содержащей многочисленные компоненты, участвующие в иммунном ответе и защите полости рта [24].

Строма малых слюнных желез содержит тучные клетки, лимфоциты, макрофаги и плазматические клетки, которые синтезируют IgA и биологически активные вещества. Эпителиальные клетки экскреторных протоков синтезируют секреторный компонент, который захватывает и переносит Ig через эпителий в слюну. Количественный и качественный состав Ig в слюне, выделяемой малыми слюнными железами, может значительно отличаться. Скорее всего, это связано с различными условиями в разных частях ротовой полости [7, 18]. sIgA характеризуется повышенной устойчивостью к протеолитическим ферментам в секретах, а его концентрация в слюне в 1000 раз выше, чем в сыворотке. Гетеротипическая функция sIgA с лизоцимом обеспечивает дополнительную защиту слизистой оболочки полости рта антителами, которые активно секретируются в просвет, а также присутствующими в собственной пластинке и внутриклеточно, и комплексами антител, прикрепленными к эпителию [6, 23].

В последние годы проводятся исследования по разработке вакцин, которые вызывают мукозальный иммунитет посредством иммунного ответа

sIgA. Антитела, образующиеся после иммунизации, могут быть эффективны против внеклеточных организмов и их токсинов. Антитела могут препятствовать проникновению вирусов и бактерий в клетки хозяина и предотвращать инфекцию. Способность антител нейтрализовать токсины может предотвратить вредные последствия таких инфекций, как дифтерия [4, 10].

Химические факторы естественной резистентности слюны включают лизоцим, пероксидазу, лактоферрин и другие ферменты в ротовой жидкости, а также компоненты системы комплемента, интерферон и другие белки [20]. Только фракция C3 системы комплемента содержится в слюне в небольшом количестве. Остальные фракции отсутствуют или обнаруживаются в небольшом количестве, поэтому условия для активации системы комплемента в слюне менее благоприятны, чем в крови. sIgA может активировать и связывать комплемент по альтернативному пути. IgM и IgG обеспечивают активацию комплемента по классическому пути [20, 23]. Фагоцитарные клетки в большом количестве попадают в полость рта через десневые щели. 80% из них составляют моноциты и нейтрофилы. В десневой жидкости количество макрофагов составляет 18%, а в нормальной десневой ткани - около 2%. Считается, что такой высокий процент фагоцитарно активных клеток создает барьер для проникновения патогенов. Однако, как только лейкоциты вступают в контакт с гипотонической слюной, они в значительной степени теряют свою фагоцитарную функцию. Если бы фагоцитарная функция не была настолько нарушена, вся резидентная микрофлора полости рта была бы уничтожена за короткий промежуток времени. Местная фагоцитарная активность может повышаться, когда в полости рта появляются очаги воспаления с повышенным осмотическим давлением. Так осуществляется их защитное действие против конкретного патогена [23].

Анатомо-гистологические и функциональные аспекты миндалин ротовой полости

Миндалины, будучи частью кольца Пирогова-Вальдейера, являются лимфоэпителиальными органами, благодаря тесному взаимодействию между лимфоцитами, соединительной тканью и эпителием [4]. Различают нёбные, трубные, язычные и глоточные миндалины. Кроме того, в желудочке гортани находятся гортанные миндалины [20].

Наружная фиброзная поверхность нёбной миндалины соединена с нижележащей тканью и покрыта слоем плотной волокнистой соединительной ткани - тонзиллярной капсулой. Собственная пластинка содержит лимфоидную ткань, представленную: лимфоидными узелками (фолликулами), диффузной межузелковой и надузелковой лимфоидной тканью [20].

Крипты миндалин содержат разнообразные антигенные вещества, которые являются источником постоянной антигенной стимуляции. Лимфоциты вступают в контакт с антигенами крипт, обладая способностью к трансэпителиальной миграции. В результате миграции и реакции трансформации в бластные клетки лимфоциты дифференцируются либо в плазматические клетки (В-лимфоциты), либо в Т-лимфоциты. В свою очередь, -лимфоциты дифференцируются в плазматические клетки и В-клетки памяти, а Т-лимфоциты дифференцируются в эффекторные Т-лимфоциты и Т-клетки памяти [17, 20, 21].

В-клетки памяти в лимфатических узлах остаются в состоянии покоя в течение определенного периода времени, а затем выходят в гемоциркуляцию, попадая в другие периферические органы иммуногенеза. Они возвращаются в миндалины через посткапиллярные венулы, заселяя близлежащие участки слизистой оболочки. Здесь они обеспечивают местный иммунитет, превращаясь в плазматические клетки после антигенной стимуляции [20].

Иммунологическая толерантность ротовой полости

В норме в полости рта нет воспаления, а различные грибковые и бактериальные инфекции встречаются довольно редко. Это свойство развивается благодаря адаптации иммунной системы полости рта к патогенам, характеризующейся толерантностью к различным комменсальным микроорганизмам [10, 15, 16]. Иммунологическая толерантность полости рта является результатом либо отсутствия активации Т-клеток в ответ на иммуногенную презентацию, либо подавления активности эффекторных Т-клеток клетками Treg. В то время как зрелые DC являются мощными активаторами адаптивных Т-клеточных иммунных ответов, незрелые DC не способны генерировать такие ответы; но через среду Treg-клеток они опосредуют анергию или иммунные ответы низкого уровня, что в целом приводит к иммунной толерантности [11, 12].

Основная функция Treg-клеток заключается в регуляции функций других Т-лимфоцитов во избежание чрезмерной иммунной активации, аутовоспалительных реакций и аутоиммунных заболеваний. Было установлено, что перорально введенные антигены могут индуцировать все типы Т-клеток с регуляторными свойствами и даже Treg-клетки фенотипа CD8. Характерна также активация Th3 Tregs, которые продуцируют TGF-β и IFN-γ, обладают регуляторной функцией и экспрессируют на своей поверхности LAP. TGF-β может индуцировать дифференцировку Th17 и участвует в аутоиммунитете [8, 14]. Вместе с ингибирующими лигандами, такими как CTLA-4, который экспрессируется в Treg, перечисленные цитокины ограничивают ответы Th-клеток, которые вызывают иммунные реакции на антигены, нанесенные на поверхность слизистой в нормальных ситуациях. Treg-клетки избирательно подавляют иммуновоспалительные ответы на комменсальные микроорганизмы, способствуя регуляции иммунных реакций [2, 4, 11, 32, 33].

Недавно сублингвальная область была исследована как потенциальный путь десенсибилизации в терапии аллергии и животных моделях аутоиммунных заболеваний [4, 16]. Экстракты аллергенов помещаются сублингвально, что приводит к им-

мунной толерантности к аллергену, отсюда и название сублингвальная иммунотерапия (СЛИТ) [12]. Существуют исследования, демонстрирующие, что местные DC слизистой оболочки полости рта связывают аллергены во время СЛИТ. Это приводит к сдвигу иммунного ответа с Th2 на Th1, наряду с индукцией Treg и IgG [3].

Дискуссия

Неиммунные клетки (например, фибробласты и эпителиальные клетки) и клетки врожденного иммунитета (макрофаги, нейтрофилы, базофилы, эозинофилы, тучные клетки, DCs, γδ-Т-лимфоциты, NK-клетки), а также гуморальные факторы (цитокины, антитела, хемокины, белки системы комплемента), синтезируемые этими клетками, участвуют в начальных защитных реакциях. Помимо защитного ответа, все эти клетки индуцируют развитие адаптивного иммунитета без видимого воспаления или признаков воспаления. Развитие любой инфекции можно остановить, если повысить активность ранних стадий защитных реакций. В этом случае инфекция не будет проявляться клиническими признаками. Ранний и индуцированный иммунный ответ может быть незаметен для человека. В защите от внеклеточных микроорганизмов основную роль играют фагоциты (нейтрофилы и моноциты) и опсонины, а от внутриклеточных - NK, макрофаги и цитокины, которые синтезируются Т-лимфоцитами [28]. Все элементы врожденного иммунитета взаимосвязаны с врожденным гуморальным иммунитетом, который действует через образование антител [6].

Слюна поддерживает здоровье полости рта, выполняя ряд защитных функций, таких как: секреция антибактериальных веществ; размягчение пищи; буферные свойства; содействие ускоренному заживлению ран слизистой оболочки полости рта; минерализация зубов; увлажнение поверхности слизистой оболочки полости рта и влияние на микробиом полости рта.

Существует баланс между экологической системой полости рта, иммунным процессом и толерантностью к патогенам. Конечный ответ, по-видимому, зависит от количества и интенсивности воздействия антигена [25].

Заключение

1. Слизистая рта защищает организм от неинфекционных и инфекционных антигенов, так как она первой встречает большинство антигенов в окружающей среде.

2. Слюна содержит множество факторов неспецифической защиты: лизоцим, пероксидазу, лактоферрин, нуклеазу, IgG, IgA, IgM, различные белки с противогрибковыми, противовирусными и антибактериальными агентами, а миндалины участвуют в активации лимфоцитов для защиты организма.

3. LC, являясь APC, участвуют в регуляции иммунного гомеостаза в полости рта, изменяя иммунную систему полости рта не только в отношении проникновения патогенов, но и толерантности к собственным антигенам и комменсальным микробам.

4. sIgA, являясь основным иммуноглобулином в слюне, помогает поддерживать баланс между комменсальными микроорганизмами и защитными механизмами, находящимися в слизистой оболочке полости рта.

5. Treg-клетки являются основным механизмом, вызывающим толерантность полости рта.

References

1. Abbas A.K, Lichtman A.H., Pillai S. Cellular And Molecular Immunology. 8th edition. ELSEVIER Saunders, 2014;

2. Aggor, F.E.Y., Break T.J., Trevejo-Nunez Glraldina et al. Oral epithelial IL-22/STAT3 signaling licenses IL-17-mediated immunity to oral mucosal candidiasis. In: Science Immunology, 2020, 5(48), pp. 1–15;

3. Allam, JP; Novak N. Immunological mechanisms of sublingual immunotherapy. In: Current Opinion in Allergy and Critical Immunology, 2014, 14(6), pp. 564–569;

4. Bergmeier, L.A. Immunology of the Oral Mucosa. In: Oral Mucosa in Health and Disease: A Concise Handbook, Springer International Publishing, Cham, London, 2018, pp. 53–67;

5. Berkovitz B.K.B., Holland G.R.,Moxham B.J. Oral Anatomy, Histology and Embryology. 5th edition. Elsevier, 2017;

6. Brandtzaeg P. Secretory immunity with special reference to the oral cavity. In: Journal of Oral Microbiology, 2013, 5(1), pp. 1–24;

7. Bykov V.L. Histology and Embryology of Human Oral Cavity Organs: Textbook, second revised edition, Special Literature, St. Petersburg, 1998, 248;

8. Castro-Sanchez P., Martin-Villa J-M. Gut immune system and oral tolerance. In: British Journal of Nutrition, 2013, 109(S2), pp. 3–11;

9. Cruchley, A.T., Bergmeier, L.A. Structure and functions of the oral mucosa. In: Oral Mucosa in Health and Disease: A concise handbook. Springer International Publishing, Cham, London, 2018, pp. 1–18;

10. De Sousa-Pereira, P., Woof, J.M. IgA: Structure, Function, and Developability. In: Antibodies, 2019, 8(4), 57, pp. 1–30;

11. Feller L., Altini M., Khammissa R.A.G. et al. Oral mucosal immunity. In: Oral Surgery, Oral Medicine, Oral Pathology and Oral radiology, 2013, 116(5), pp. 576–583;

12. Gemonov V.V., Lavrova A.N., Falin L.I. Histology and embryology of oral cavity organs and teeth: textbook, GEOTAR-Media, Moscow, 2019, 320;

13. Groeger S, Meyle J. Oral Mucosal Epithelial Cells. In: Frontiers in Immunology, 2019, 10(208), pp. 1–22;

14. Hovav, AH. Dendritic cells of the oral mucosa. In: Mucosal Immunology, 2014, 7(1), pp. 27–37;

15. Kirichuk V.F., Ponukalina E.V., Chesnokova N.P. Structural and functional features of the oral mucosa. In: Scientific Review, Abstract Jornal, 2018, 1, pp. 56-59;

16. Kraan H., Vrieling H., Czerkinsky C. et al. Buccal and sublingual vaccine delivery. In: Journal of Controlled Release, 2014, 190(28), pp. 580–592;

17. Kumar G.S. Orban's Oral Histology and Embryology. 14th edition. Elsevier, 2015;

18. Kuznetsov S.L. Histology of the oral organs: textbook, GEOTAR-Media, Moscow, 2014, 624;

19. Moutsopoulos N.M., Konkel J.E. Tissue-Specific Immunity at the oral Mucosal Barrier. In: Trends in Immunology, 2018, 39(4), pp. 276–287;

20. Myadelets O.D., Kichigina T.N., Bobr O.L. Morphophysiological bases of barrier-protective function of oral cavity: textbook for students of the Faculty of Dentistry, VGMU, Vitebsk, 2005, 120;

21. Opravin A.S. Ulianovskaya S.A. Clinical morphology of the oral cavity: training manual, Publishing house of the Northern State Medical University, Arkhangelsk, 2011, 306;

22. Park J-Y, Chung H, Choi Y et. al. Phenotype and Tissue Residency of Lymphocytes in the Murine Oral Mucosa. In: Frontiers in Immunology, 2017, 8(250), pp. 1–10;

23. Pravosudova N.A. Microbiology of the oral cavity: textbook, Penza, 2013, 89;

24. Proctor G.B. The physiology of salivary secretion. In: Periodontology 2000, 2015, 70(1), pp. 11–15;

25. Ron G.I., Balyan L.N. Ecological System And Immunity Of An Oral Cavity. In: Actual Problems Of Stomatology, 2012, 2, pp. 8-12;

26. Savichuk N.O., Oleynik O.E., Nazar O.V. Oral mucosa as part of mucosal-associated lymphatic tissue: local (cellular) immunity factors. In: Actual Problems of the Modern Medicine: Bulletin of Ukrainian Medical Stomatological Academym 2009m 9(3), pp. 211-215;

27. Seoudi N, Bergmeier LA, Hagi-Pavli E. et. al. The role of TLR2 and 4 in Behçet's disease pathogenesis. In: Innate Immunity, 2014, 20(4), pp. 412–422;

28. Shabashova N.V., Danilova E.U. Mucosal Immunity And Oral Microbiota (Review). In: Problems in medical mycology, 2015, 17(4), pp. 4-13;

29. Sinon S.H., Rich A.M, Parachuru V.P.B. et al. Downregulation of toll-like receptor-mediated signalling pathways in oral lichen planus. In: Journal of Oral Pathology and Medicine, 2015, 45(1), pp. 28–34;

30. Tsarinsky M.M., Tsarinskaya N.M. Current Views On Mechanisms To Maintenance Immunity In The Oral Cavity. In: Kuban Scientific Medical Bulletin, 2012, 2(131), pp. 183-186;

31. Upadhyay J., Upadhyay R.B., Agrawal P. et al. Langerhans Cells and Their Role in Oral Mucosal Diseases. In: North American Journal of Medical Sciences, 2013, 5(9), pp. 505–514;

32. Wang, X., Sharp, J. S., Handel, T. M et. al. Chemokine Oligomerization in cell signaling and migration. In: Progress in Molecular Biology and Translational Science, 2013, 117, pp. 531–578;

33. Wu RQ., Zhang, DF., Tu E. et al. The mucosal immune system in the oral cavity – an orchestra of T cell diversity. In: International Journal of Oral Science, 2014, 6(3), pp. 125–132;

34. Yakubov, G.E., Gibbins, H., Proctor, G.B. et. al. Oral Mucosa: Physiological and Physicochemical Aspects. In: Mucoadhesive Materials and Drug Delivery Systems, 2014, pp. 1–37;

ASSESSING KIDNEY FUNCTION IN ELDERLY

Stițiuc Irina,
Student, Faculty of General Medicine,
State University of Medicine and Pharmacy "Nicolae Testemiţanu"
Republic of Moldova, Chisinau
Boris Sasu
Doctor of medical sciences, Associate professor,
The Discipline of Rheumatology and Nephrology,
State University of Medicine and Pharmacy "Nicolae Testemiţanu"
Republic of Moldova, Chisinau
DOI: 10.5281/zenodo.7796143

Abstract

In recent years, due to the increase in life expectancy in Western societies, there has been such an unprecedented phenomenon - a sharp increase in the proportion of elderly people aged 65 years and older. The main direction that will significantly affect the daily professional life of nephrologists in the 21st century is the progressive aging of the world's population. Therefore, plans to integrate nephrology with gerontology and geriatrics will allow these sciences to adapt to this inevitable phenomenon of increasing demographic pressure and manage health and care at all levels - from the individual patient to the general population and global health systems.

Aim of the study: To study the prevalence and characteristics of functional changes in the kidneys in elderly and senile people for the early implementation of preventive actions.

Keywords: Aging, Kidney function, Glomerular filtration rate, Chronic kidney disease

Introduction

Aging is a comprehensive process that is caused by many factors and their action, in turn, is repeated and accumulated throughout life. These are stress, past illnesses, accumulation of toxins and free radicals, depletion of stem cells, exposure to xenobiotics (foreign substances), temperature damage, insufficient excretion of protein breakdown products, lack of vitamins and microelements, hypoxia, and others [5,6].

In addition, aging is a multifocal process that occurs in different cell structures: in the nucleus, membranes, in different types of cells: nervous, secretory, immune, renal, and others [4].

Undoubtedly, aging is associated with a decrease in physiological homeostasis. This multidimensional phenomenon encompasses physical, psychological and social changes. In higher organisms, aging homeostasis is regulated by the interaction of many organs. With age, dysfunction of one organ can lead to functional failure of many organs [5].

It is well known that both the number of past diseases and chronic diseases increase with age. Urological diseases such as nephropathy (such as pyelonephritis, polycystic kidney disease, diabetic or hypertensive nephropathy, etc.), adenoma and prostate cancer, urinary incontinence, etc occupy a large percentage of them. In an aging body, damage to various structures occurs: collagen, cell membranes, DNA and other molecules, cells and tissues [2,3,7].

Aging is an inevitable process of life for all living beings. However, data from longitudinal studies suggest that one third of all healthy people aged 23–97 years are practically not affected by changes in kidney function throughout their lives [1].

Materials and methods

To achieve the goal of the study, a group of 50 patients was retrospectively selected, of which 34 were women and 16 were men. Their age ranged from 60 to 90 years, the average age was 71.8 ± 7 years. Patients were treated in the Department of Nephrology at the IMSP SCM "Holy Trinity", Chisinau, in 2022.

The following data was extracted from the observation sheets:

- Clinical data (medical history, BMI, sex, age, main diagnosis, concomitant diagnosis, presence of hypertension, risk factors for BCR)
- Paraclinical data (general blood test, biochemical blood test, urinalysis, calculation of GFR, results of ultrasound of the kidneys).

Research methods

The study is based on the following research methods: historical, descriptive. Primary data collection methods are based on medical records (patient records) using official statistics. Statistical processing of the results of the study was carried out by computerized methods of analysis of variations using special programs (Microsoft Excell 2013 for Windows).

Results

In both age groups, approximately the same percentage of men and women with pathology of the nephro-urinary system appears.

- 67.64% of women are aged 60-74,
- 32.35% belong to the age group of 75-90 years,
- 0% of women are in the 90+ age group.
- 68.75% of the men who underwent the study were aged 60-74 years,
- 31.25% - in the age group of 75-90 years,
- 0% of men are in the 90+ age group.

1. Characteristics of diseases of the urinary system in the elderly and senile age

Among the nephropathologies that patients of elderly and senile age suffered from, the most common was chronic pyelonephritis in the acute stage - 92%. In 28% of 50 patients, solitary or multiple cysts were

found on echography. And 8% of patients had uni-/bilateral hydronephrosis. Glomerulonephritis was rarely detected - only 2% of cases.

Among all concomitant diseases, the prevalence of arterial hypertension is 48%, various forms of heart disease (ischemic, hypertensive or mixed) - in 40% of patients. 32% of patients had anemia of renal or other origin. Diabetes mellitus type 2 was in the stage of compensation or undercompensation in 30% of patients. There is obesity of class 1 and 2 in 20% of patients, nephrolithiasis confirmed by ultrasound - in 8%. Hyperuricemia was present in 4% of cases, cystitis - in 4% (Fig. 1).

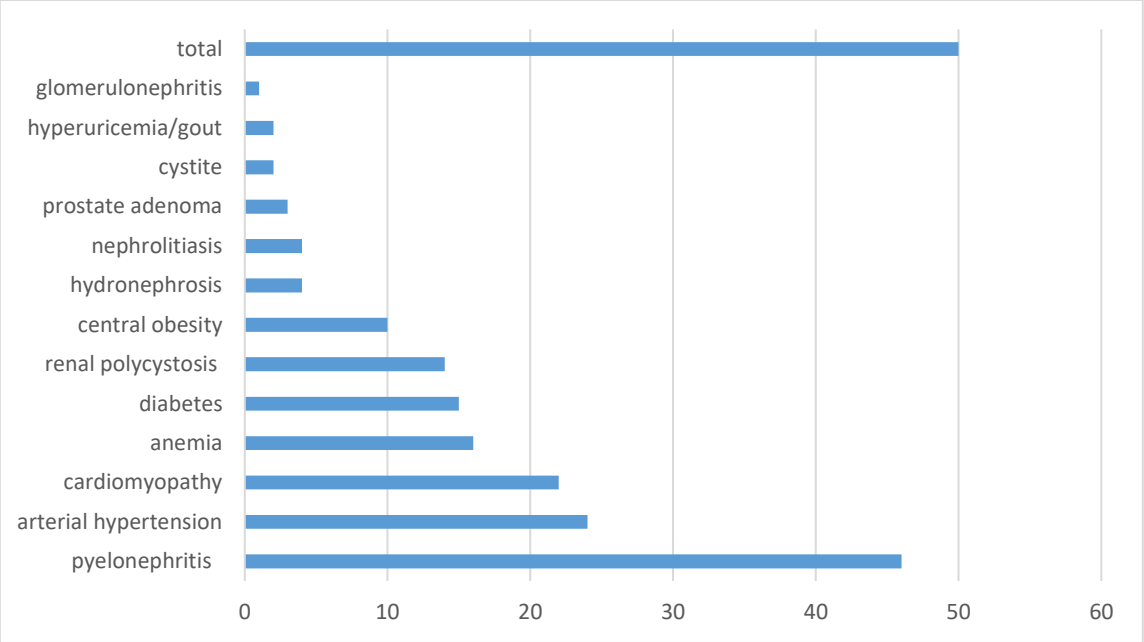

Figure 1. Disease prevalence by age and sex 1

2. Prevalence of the disease by age and sex

The diagram below shows the prevalence of diseases that are risk factors for the development and progression of BCR (Fig. 2).

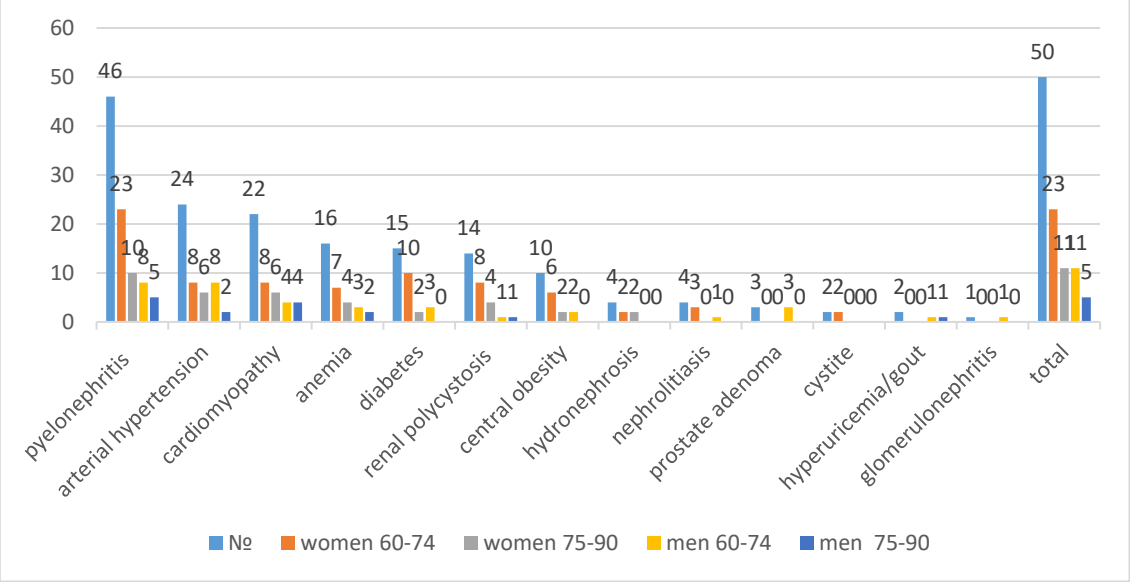

Figure 2. Distribution by diseases that elderly and senile patients suffered from

3. Estimated GFR < 60 ml/min over 1.73 m^2

Glomerular filtration rate (GFR) is estimated using an equation developed by the Collaborative Organization for the Epidemiology of Chronic Kidney Disease (CKD-EPI).

Of the 50 patients, only 18 people, including 5 elderly and 13 senile patients, had GFR > 60 ml/min over an area of 1.73 m^2. The prevalence of reduced kidney function (estimated GFR < 60 ml/min per 1.73 m^2) was in 32 patients.

Moreover, the trend of increasing prevalence of renal dysfunction with age was observed mainly in women. Thus, GFR < 60 ml/min per 1.73 m^2 was determined in 69% of women and 63% of elderly men and in 91% of women and 60% of men of senile age.

4. Prevalence of CKD

Among patients with chronic kidney disease (CKD), the stage of the disease should be determined by the level of renal function according to the KDOQI CKD classification.

Overall, 64% of participants had CKD and were predominantly in CKD stages III (11 women and 2 men) and IV (6 women and 5 men), with a female predominance. The prevalence of CKD stage V according to KDOQI was 4 women and 4 men, of which 2 men and only 1 woman of senile age (Fig. 3).

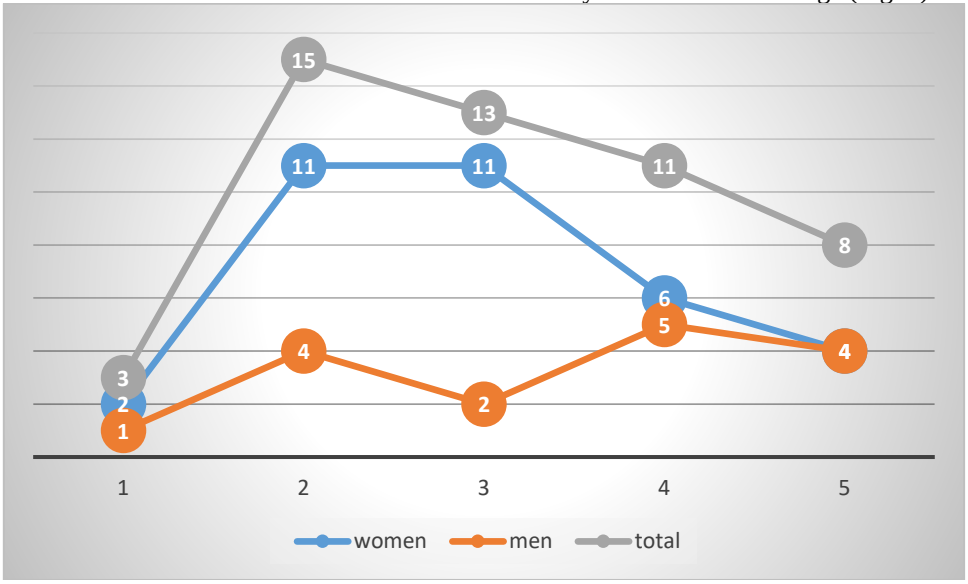

Figure 3. Prevalence of CKD in elderly and senile patients

Conclusion

The population of the planet is rapidly aging, and with age, the functionality of the kidneys proportionally fades. It is also clear that GFR itself is an indicator of accelerated aging. In this sense, the practical benefits of research work are important for the medical community, whose goal is to ensure the prevention and diagnosis of renal pathology at any age, especially in the elderly, the prevention of concomitant complications and, thus, the prolongation of the quality of care in old age and active life.

References

1. Baba M, Shimbo T, Horio M, Ando M, Yasuda Y, Komatsu Y, Masuda K, Matsuo S, Maruyama S. Longitudinal Study of the Decline in Renal Function in Healthy Subjects. PLoS One. 2015 Jun 10;10(6):e0129036.

2. Budylev S.A., Selivanov A.N., Perelygin K.V., Mudrakovskaya E.V., Fundamental research-2014.-No.10(part 10)-1902-1906

3. Denic A, Glassock RJ, Rule AD. Structural and Functional Changes With the Aging Kidney. Adv Chronic Kidney Dis. 2016 Jan;23(1):19-28.

4. Di Micco R, Krizhanovsky V, Baker D, d'Adda di Fagagna F. Cellular senescence in ageing: from mechanisms to therapeutic opportunities. Nat Rev Mol Cell Biol. 2021 Feb;22(2):75-95.

5. Pomatto LCD, Davies KJA. The role of declining adaptive homeostasis in ageing. J Physiol. 2017 Dec 15;595(24):7275-7309.

6. Rahal A, Kumar A, Singh V, Yadav B, Tiwari R, Chakraborty S, Dhama K. Oxidative stress, prooxidants, and antioxidants: the interplay. Biomed Res Int. 2014;2014:761264.

7. Weinstein JR, Anderson S. The aging kidney: physiological changes. Adv Chronic Kidney Dis. 2010 Jul;17(4):302-7.

PHYSICAL SCIENCES

GEOPHYSICAL RESEARCHES OF PORTALS WILL ALLOW TO PROVE THE EXISTENCE OF INVISIBLE UNIVERSES AND TO EXPLORE THEM[1]

Antonov A.A.
PhD, HonDSc, HonDL, ResProf., H.ProfSci
Independent researcher, Kyiv, Ukraine
DOI: 10.5281/zenodo.7796151

Abstract

The article proves that the version of the special theory of relativity (STR) presented in physics textbooks is incorrect. This is because in the early 20th century science lacked experimental knowledge required for the STR to be created, and the postulate (called the principle of light speed non-exceedance) that replaced the knowledge turned out to be incorrect and has been experimentally refuted in the 21st century. It is explained that tsunami and piano music would not exist, church bells would not ring and even swings would not swing on playgrounds, if the generally accepted version of the STR were true. Moreover, this version of the STR also implies that Ohm's law as interpreted by Steinmetz used daily by millions of radio and electrical engineers in their practice does not exist, and therefore radio engineering and electrical engineering should not exist either.

That is why, an alternative version of the STR has been created instead of the incorrect one. It follows from this that there is an invisible Multiverse whose universes are interconnected by numerous portals, including those located on Earth. And at least some of anomalous zones are entrances to portals. Geophysical exploration of portals are very necessary, as they will allow us to obtain new valuable knowledge about our Multiverse and confirm the correctness of the alternative version of STR.

Keywords: portals, parallel universes, Multiverse, special theory of relativity, physical reality of imaginary numbers, dark matter, dark energy

1. Introduction

Portals, sometimes also called 'star gates' [1], understood as transitions from some universes to others, are the subject of research in the article. Therefore, it is clear that one can speak of portals only if there are at least two universes, i.e. Multiverses. The term 'Multiverse' meaning two and more universes was proposed by the American philosopher-psychologist William James in 1895 and introduced to practice by the English science fiction writer Michael John Moorcock. To date, a large number of Multiverse hypotheses have been proposed. The most informative of them are [2]-[13].

But the special theory of relativity (STR) [14]-[16] recognized in physics as the greatest scientific achievement of the 20th century, denies existence of Multiverses at all and claims that there is only our visible universe.

Yet, there are a very large number of the so-called anomalous zones [17]-[20] planet. They are fraught with phenomena incapable of being explained by modern science. At least some of them are supposedly entrances to portals. Geophysical exploration of portals will allow visiting them safely and solving some important problems of modern astrophysics successfully.

2. The version of the special theory of relativity presented for study in physics textbooks is incorrect

The alternative version of the STR states the generally recognized version of the STR studied in physics textbooks to be incorrect [21]-[32], because:

- the relativistic formulas obtained therein are incorrect;
- the relativistic formulas have been incorrectly explained using the incorrect principle of light speed non-exceedance;
- the relativistic formulas have entailed wrong conclusions consisting in physical unreality of imaginary numbers and existence of only our visible universe.

Hence the alternative version of the STR thereby asserts exactly what we need – the existence of other universes, besides our universe, which together form the Multiverse. This follows from its relativistic formulas that are different from those in the generally accepted version of the STR. In order to understand the relativistic formulas of the alternative version of the STR better, let us first consider the simpler relativistic formulas of the generally accepted version of the STR. They are as follow

$$m = \frac{m_0}{\sqrt{1-(v/c)^2}} \quad (1)$$

$$\Delta t = \Delta t_0 \sqrt{1-(v/c)^2} \quad (2)$$

[1] This is reprint of the article "Antonov A. A. Geophysical exploration of portals will provide new knowledge about space. Proceedings of the III International Scientific Conference. The modern vector of the development of science. Philadelphia, USA. 2023. pp. 85-101."
DOI https://doi.org/10.5281/zenodo.7709801

$$l = l_0\sqrt{1-(v/c)^2} \qquad (3)$$

where m is the relativistic mass of a moving body;

m_0 is the rest mass of a moving body;

Δt is the relativistic time of a moving body;

Δt_0 is the rest time of a moving body;

l is the relativistic length of a moving body;

l_0 is the rest length of a moving body;

v is the velocity of a moving body;

c is the speed of light.

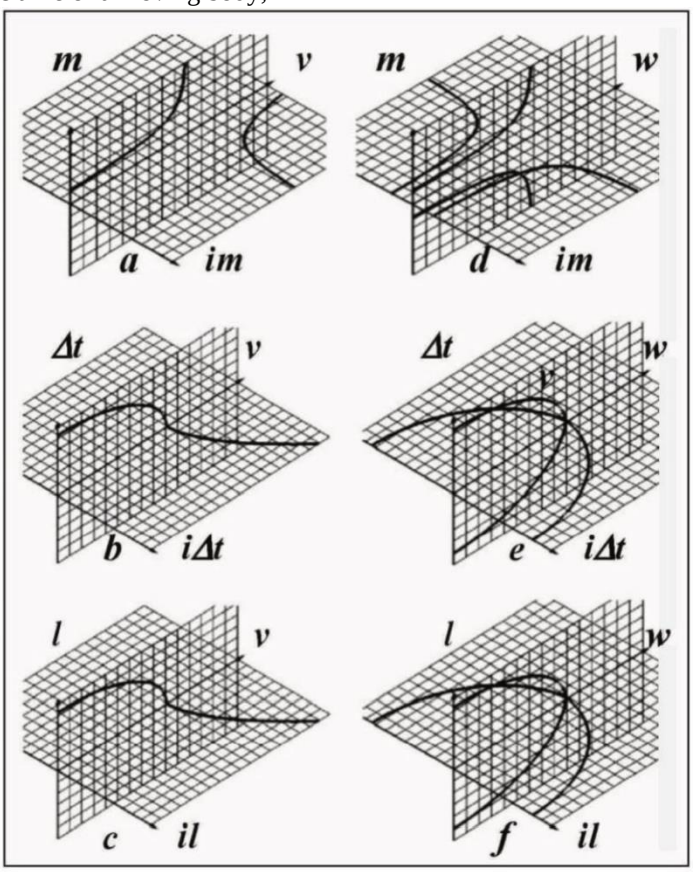

Fig. 1. Graphs of functions $m(v)$, $\Delta t(v)$ and $l(v)$ corresponding to the existing and alternative versions of the STR in the subluminal $v < c$ and hyperluminal $v > c$ ranges

Fig. 1a,b,c presents the graphs of the formulas. As can be seen, all formulas for $v < c$ lead to results measured by real numbers, and for $v > c$ to results measured by imaginary numbers. This circumstance greatly discouraged authors of the generally accepted version of the STR, since until very recently no one could explain physical sense of the results measured by imaginary numbers discovered 500 years ago. And no one would need a theory whose results could not be explained even by its creators. The fate of the generally accepted (but it's only now, not then) version of the STR hung in the balance in the early 20th century. It was saved by introducing a postulate, i.e. an unproven assumption, called the principle of light speed non-exceedance, the sense of which is clear from its name. The postulate looked quite acceptable, since in the early20th century physics knew no phenomenon, in which any physical entity would move with superluminal velocity. This is how the STR has begun to be studied and still been studied even in the most prestigious universities

But in 1934, Cherenkov radiation was discovered [33]. The radiation is emitted when electrically charged particles are moving at speeds faster than that of light. In 1958, Pavel Alekseevich Cherenkov, Igor Evgenievich Tamm and Ilya Mikhailovich Frank received the Nobel Prize for the discovery and explanation of this radiation. The fate of the STR hung in the balance again. And the STR was saved once again. This time it was saved by making a clarification that the principle of light speed non-exceedance had implied the speed of light exclusively in a vacuum.

In the 21st century, one more attempt to refute the STR was undertaken. This time it was the OPERA experiment at the Large Hadron Collider. It was supposed to register superluminal neutrinos and thereby prove physical reality of imaginary numbers. A sensational report about successful completion of the very complex and expensive experiment was published on September 22, 2011. However, six months later, the OPERA experiment was refuted by the ICARUS experiment. Therefore, the STR again failed to be refuted.

Nevertheless, in 2008-2010, i.e. before publication of the OPERA experiment results, the results of alternative studies of special processes in linear electric circuits [34]-[38], were published. They proved that resonance, discovered by Galileo in 1602, occurs at complex frequencies, rather than at real ones, which has

still been stated in textbooks on the theory of linear electric circuits. Thus, physical reality of imaginary numbers has been finally proved and the unsuccessful OPERA experiment has become useless. And since mathematics is the language of all exact sciences, the principle of physical reality of imaginary numbers proven experimentally in the theory of linear electric circuits has become generally scientific. Therefore, this time the principle of light speed non-exceedance has been refuted.

At the same time, it has been also proved that if the outdated version of the STR presented in physics textbooks were true, then tsunami, bell ringing and music of piano or other musical instruments would be impossible; swings would not swing in a playground; Ohm's law as interpreted by Steinmetz used daily by millions of radio engineers all over the world would not work; and there would be no radio and electrical engineering at all. However, authors of the incorrect version of the STR did not know this when they created their theory at the beginning of the 20th century, but later physicists-relativists did not want to know this. Moreover, they did everything so that no one knew about it. For example, they staged a misleading and very expensive advertising action in the form of OPERA and ICARUS experiments at the Large Hadron Collider.

Nevertheless, physical reality of imaginary numbers has already been proven and the truth of this statement is beyond doubt. And therefore, in accordance with the relativistic formulas (1)-(3), something must exist in nature at $v > c$. However, analysis of the formulas has shown that the universes corresponding to such a situation should be physically unstable and therefore self-liquidating, i.e. could not exist. Thus, the relativistic formulas (1)-(3) are incorrect as well as the generally accepted version of the STR.

The generally accepted version of the STR turned out to be incorrect because, due to the lack of necessary scientific knowledge in the early 20th century, relativistic formulas were derived incorrectly. Postulates were used instead of missing scientific knowledge. However, the principle of light speed non-exceedance turned out to be wrong. Derivation errors were not timely detected and corrected. In subsequent years, following the inertia of competitive struggle (after all, within the framework of a market economy, science is a kind of business), the STR turned out to be so canonized that it became poorly receptive to new knowledge. As a result, the relativistic formulas have not yet been corrected.

3. Alternative version of the special theory of relativity

3.1. There is a hidden Multiverse in nature, not a Monoverse

Actually, relativistic formulas obtained in the generally accepted version of the STR not only were not, but could not be explained, because functions (1)-(3) vary in significantly different ways (see Fig. 1a,b,c) in the subluminal (for $v < c$) and superluminal (for $v > c$) velocity ranges. As has been shown above, universes corresponding to the formulas (1)–(3) are physically unstable in the superluminal velocity range (for $v > c$) and, therefore, cannot even exist. That is why the formulas (1)-(3) are incorrect. In order for the same regularities to take place in the subluminal (for $v < c$) and superluminal (for $v > c$) velocity ranges and, therefore, formulas describing the corresponding processes could be explained, the graphs $m(v)$, $\Delta t(v)$, $l(v)$ should take the form shown in Fig. 1d,e,f. This requires introduction of the function i^q into the corrected relativistic formulas of the STR corresponding to them

$$m(q) = \frac{m_0 i^q}{\sqrt{1-(v/c - q)^2}} = \frac{m_0 i^q}{\sqrt{1-(w/c)^2}} \quad (4)$$

$$\Delta t(q) = \Delta t_0 i^q \sqrt{1-(v/c - q)^2} = \Delta t_0 i^q \sqrt{1-(w/c)^2} \quad (5)$$

$$l(q) = l_0 i^q \sqrt{1-(v/c - q)^2} = l_0 i^q \sqrt{1-(w/c)^2} \quad (6)$$

where $q(v) = \lfloor v/c \rfloor$ – is the 'floor' function of discrete mathematics (Figure 2a);

$w = v - qc$ is its own local velocity for each universe (Fig. 2b).

And the function i^q is the simple and clear function convenient for this situation, since, for integers of the argument q, it takes on only the proper values +1, $+i$, –1, $-i$ and in the proper sequence. These values correspond to four different universes alternating in space. However, its values are unknown for non-integers of the argument. This is not actually a problem, since we can replace the function i^q in the formulas (4)-(6) by the Euler's formula $e^{iq\pi/2} = cos(q\pi/2) + i\,sin(q\pi/2)$ that takes on the same values +1, $+i$, –1, $-i$ for integers of the argument q and, therefore, can completely replace it

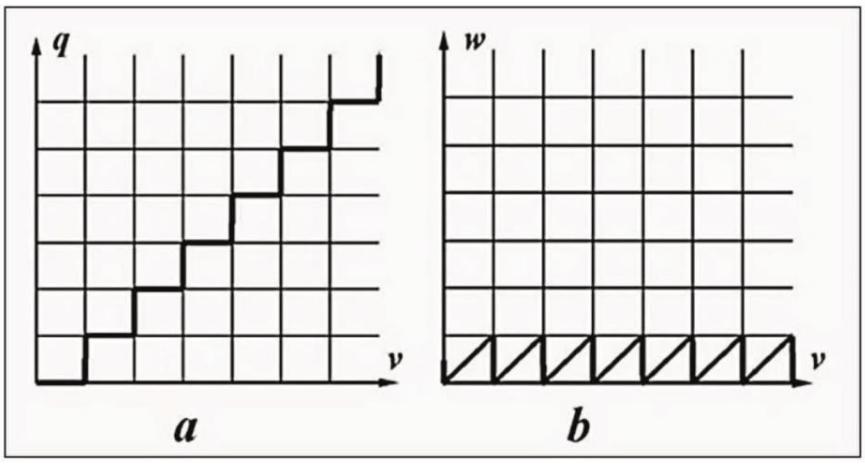

Fig. 2. *Graphs of functions* $q(v)$ *and* $w(v)$
illustrating the meaning of the 'floor' function of discrete mathematics

$$m(q) = \frac{m_0 e^{iq\pi/2}}{\sqrt{1-(v/c-q)^2}} = \frac{m_0[\cos(q\pi/2)+i\sin(q\pi/2)]}{\sqrt{1-(w/c)^2}} \quad (7)$$

$$\Delta t(q) = \Delta t_0 e^{iq\pi/2}\sqrt{1-(v/c-q)^2} = \Delta t_0[\cos(q\pi/2)+i\sin(q\pi/2)]\sqrt{1-(w/c)^2} \quad (8)$$

$$l(q) = l_0 e^{iq\pi/2}\sqrt{1-(v/c-q)^2} = l_0[\cos(q\pi/2)+\sin(q\pi/2)]\sqrt{1-(w/c)^2} \quad (9)$$

Thus the corrected relativistic formulas (4)-(6) and (7)-(9) imply that the quantity q takes on integers[2] (see Fig. 2a), determined by the discrete 'floor' function $q(v) = \lfloor v/c \rfloor$. The integers correspond to different universes. Thus, the quantity $q = 0$ corresponds to our visible universe (for which $i^0 = 1$) and the quantity $q = 1$ corresponds to another universe (for which $i^1 = i$) that is invisible for us by virtue of the condition $v > c$, because it is located beyond the event horizon. Stephen William Hawking wrote about imaginary time in such a Multiverse: *"Imaginary time is a new dimension, at right angles to ordinary, real time".* Thus, his research confirmed the validity of the hypothesis of the hidden Multiverse considered below.

[2] It takes non-integer values in the portals considered below, in which, from their entrance to exit, under the influence of physical factors that have not yet been studied, the value changes by one

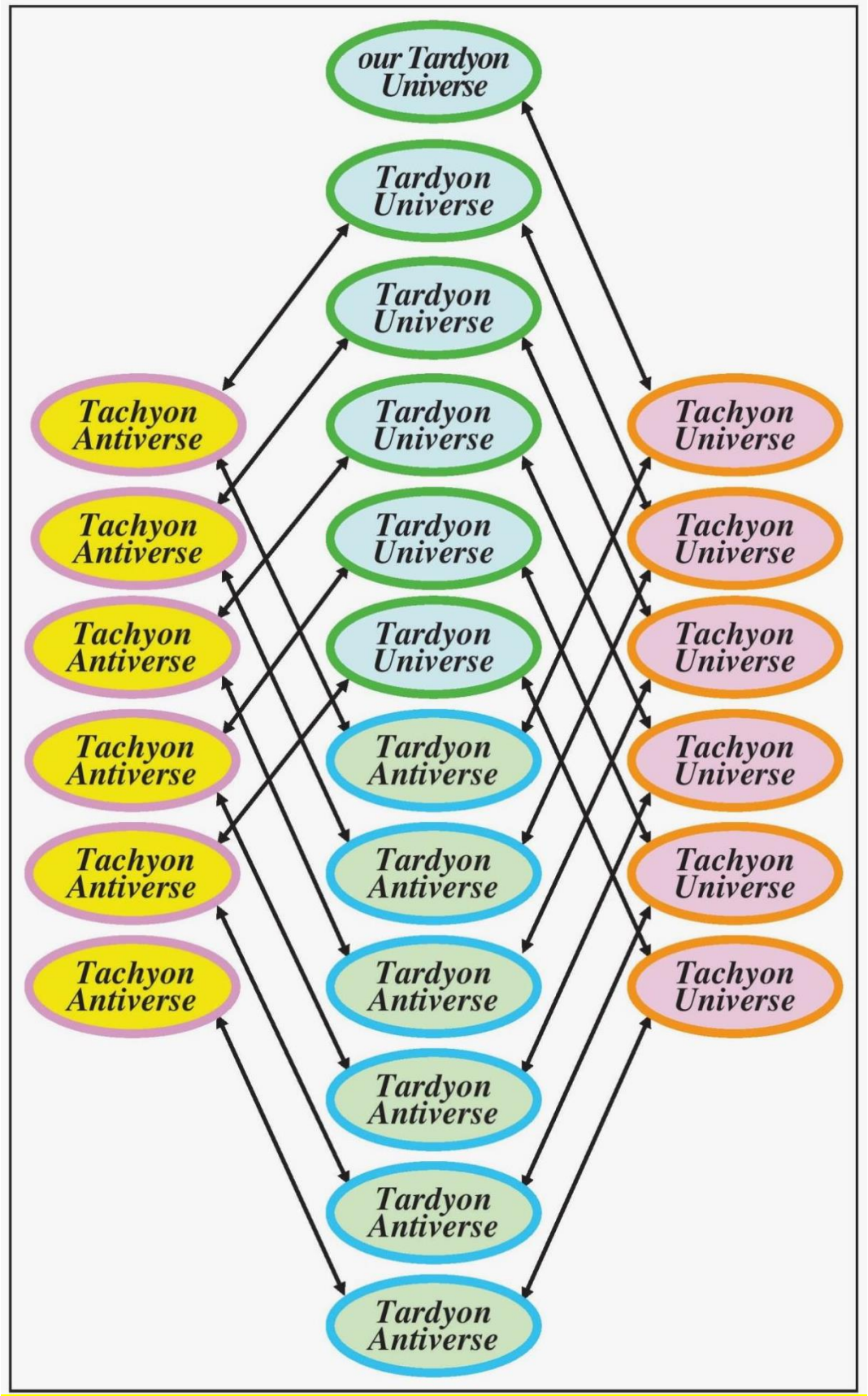

Fig. 3. Estimated helical structure of the hidden Multiverse

Let us, for definiteness, call the universe corresponding to $q = 1$ a tachyon universe, since it contains tachyons [39]-[40] that are understood to be subatomic particles moving at a speed faster than that of light. Therefore, many physicists believe that they should not exist in nature (by which they mean a Monoverse corresponding to the generally accepted interpretation of the STR), since they violate the principle of causality. However, since tachyons are actually in a tachyon universe (or antiverse), rather than

in our universe, they do not violate the principle of causality.

For similar reasons, let us call our universe a tardyon universe. Then it would be logical to assert that the quantity $q = 2$ corresponds to a tardyon antiverse (for which $i^2 = -1$), the quantity $q = 3$ corresponds to a tachyon antiverse (for which $i^3 = -i$), the quantity $q = 4$ corresponds to another tardyon universe (for which $i^4 = 1$), the quantity $q = 5$ corresponds to another tachyon universe (for which $i^5 = i$), etc.

Consequently, such a Multiverse has a helical structure (Fig. 3). Moreover, since $v = w + qc$ follows from the formula $w = v - qc$, then $v > c$ is for all universes, except for ours, and therefore they are beyond the event horizon, i.e. are invisible. The entire Multiverse is also invisible, which is why it is called hidden [41]-[47]. Universes of the hidden Multiverse do not intersect, which is why they can be called parallel. However, drifting in the fourth spatial dimension q they sometimes touch each other and even slightly penetrate into each other, forming some transitional zones called portals [48],[49] (they are shown by double-headed arrows in Fig. 3).

3.2 Dark matter and dark energy phenomena are generated by the existence of the Multiverse

But shown in Fig. 3 structure of the hidden Multiverse has the significant drawback that it does not take into account the existence of the phenomena of dark matter and dark energy, which are not explained. So what are dark matter and dark energy? And why is it so important to explain them? This is because, according to the data obtained by the WMAP spacecraft, the entire universe (actually, the entire hidden Multiverse) consists of 22.4% of dark matter, 73.0% of dark energy and only 4.6% of baryonic matter [50]. And according to more recent data obtained by the Planck spacecraft, the entire universe (again, actually, the entire hidden Multiverse) consists of 26.8% of dark matter, 68.3% of dark energy and only 4.9% of baryonic substances [51]. That is, according to these data, almost the whole of nature is not at all what we have understood it to be in our visible universe. It is rather different. Thus, without understanding physical sense of dark matter and dark energy, understanding of our visible universe does not seem to be quite reliable. However, despite all the efforts of scientists to solve this important problem, dark matter and dark energy have been defied explanation for almost a hundred years. Michio Kaku wrote in this regard: *"Of course, a whole bunch of Nobel Prizes is waiting for the scientists who can reveal the secrets of the 'dark energy' and 'dark matter'".*

But all these efforts have actually so far been undertaken within the framework of the generally accepted version of the STR. Therefore, considering the remark of Albert Einstein *"Insanity: doing the same thing over and over again and expecting different results"*, let us now try to seek for such an explanation within the framework of the alternative version of the STR. We should assume what could not be assumed within the framework of the generally accepted version of the STR – to seek for the explanation in the macrocosm, rather than in the microcosm. That is, we should assume that the phenomena of dark matter and dark energy are evoked in our visible universe by the rest of invisible universes of the hidden Multiverse. We should as well assume that the phenomena of dark matter and dark energy [52]-[60] are a kind of optical shadow of these invisible universes on our universe (however, it is gravitational or some other shadow, rather than an electromagnetic one). This will make it possible to understand why, until now, no material carriers of these phenomena have been found by research at the Large Hadron Collider. After all, no optical image (including a shadow) has ever contained any physical components of such an image.

Then, having made such an assumption, it might be argued that:

- the phenomenon of dark matter is evoked by invisible universes of the hidden Multiverse adjacent to our visible universe, and
- the phenomenon of dark energy is evoked by the rest of invisible universes of the hidden Multiverse, more distant from our visible universe.

Herewith, since these universes do not intersect anywhere, they are parallel. However, floating in space, they inevitably touch and even slightly penetrate into each other in many spots, generating portals. Adjacent universes exchange their material content through these portals. Therefore, over billions of years of their existence, parameters of all universes have substantially averaged. And this allows you to determine the number of universes in the hidden Multiverse. Assuming that our visible universe has such averaged parameters, we can find the following:

- the total number of universes in the hidden Multiverse is 100% / 4.6% = 21.74 according to the above data obtained by the WMAP spacecraft, and 100% / 4.9% = 20.41 according to the data obtained by the Planck spacecraft. Consequently, their real number is supposedly equal to 20…22 universes;
- the number of universes in the hidden Multiverse that are adjacent to our universe and evoke the phenomenon of dark matter is 22.4% / 4.6% = 4.87 according to the above data obtained by the WMAP spacecraft, and 26.8% / 4.9% = 5.47 according to the data obtained by the Planck spacecraft. Consequently, their real number is supposedly equal to 5…6 universes.
- the number of universes in the hidden Multiverse that evoke the phenomenon of dark energy is 73.0% / 4.6% = 15.87 according to the above data obtained by the WMAP spacecraft, and 68.3 % / 4.9% = 13.94 according to the data obtained by the Planck spacecraft. Consequently, their real number is supposedly equal to 14…16 universes.

3.3 Dark matter and dark energy phenomena allow to determine the structure of the hidden Multiverse

And immediately striking is the discrepancy between the obtained calculation results and the one

shown above in Fig. 3 supposed structures of the hidden Multiverse, which cannot be explained in any way by the inaccuracy of the measurements of the WMAP and Planck spacecraft, since the difference between the results of calculations and experimental data is too large. There has been found to be five or six other parallel universes adjacent to our universe, rather than two. However, this number does not fit within the structure shown in Fig. 3.

Hence, it is logical to assume that there has been some mistake in the previous reasoning. This mistake, most likely, is that earlier, for simplicity, we have supposed the existence of only one extra dimension q in the hidden Multiverse, and, therefore, its correspondence to physically real complex numbers containing only one imaginary unit. In order for six other parallel universes to be adjacent to our universe (i.e. three tachyon universes and three tachyon antiverses), there should be three extra dimensions q, r, s, determining their position in space. Therefore, the structure of the hidden Multiverse should be described by quaternions $\sigma + i_1\omega_1 + i_2\omega_2 + i_3\omega_3$, i.e. hypercomplex numbers [61], containing three imaginary units i_1, i_2, i_3 connected by the relations

$$i_1^2 = i_2^2 = i_3^2 = -1 \quad (10)$$

$$i_1 i_2 i_3 = i_2 i_3 i_1 = i_3 i_1 i_2 = -1 \quad (11)$$

$$i_1 i_3 i_2 = i_2 i_1 i_3 = i_3 i_2 i_1 = 1 \quad (12)$$

That is why, the relativistic formulas (4)-(6) and (7)-(9) must be corrected again as follows

$$m(q,r,s) = \frac{m_0 i_1^q i_2^r i_3^s}{\sqrt{1-[v/c-(q+r+s)]^2}} \quad (13)$$

$$\Delta t(q,r,s) = \Delta t_0 i_1^q i_2^r i_3^s \sqrt{1-[v/c-(q+r+s)]^2} \quad (14)$$

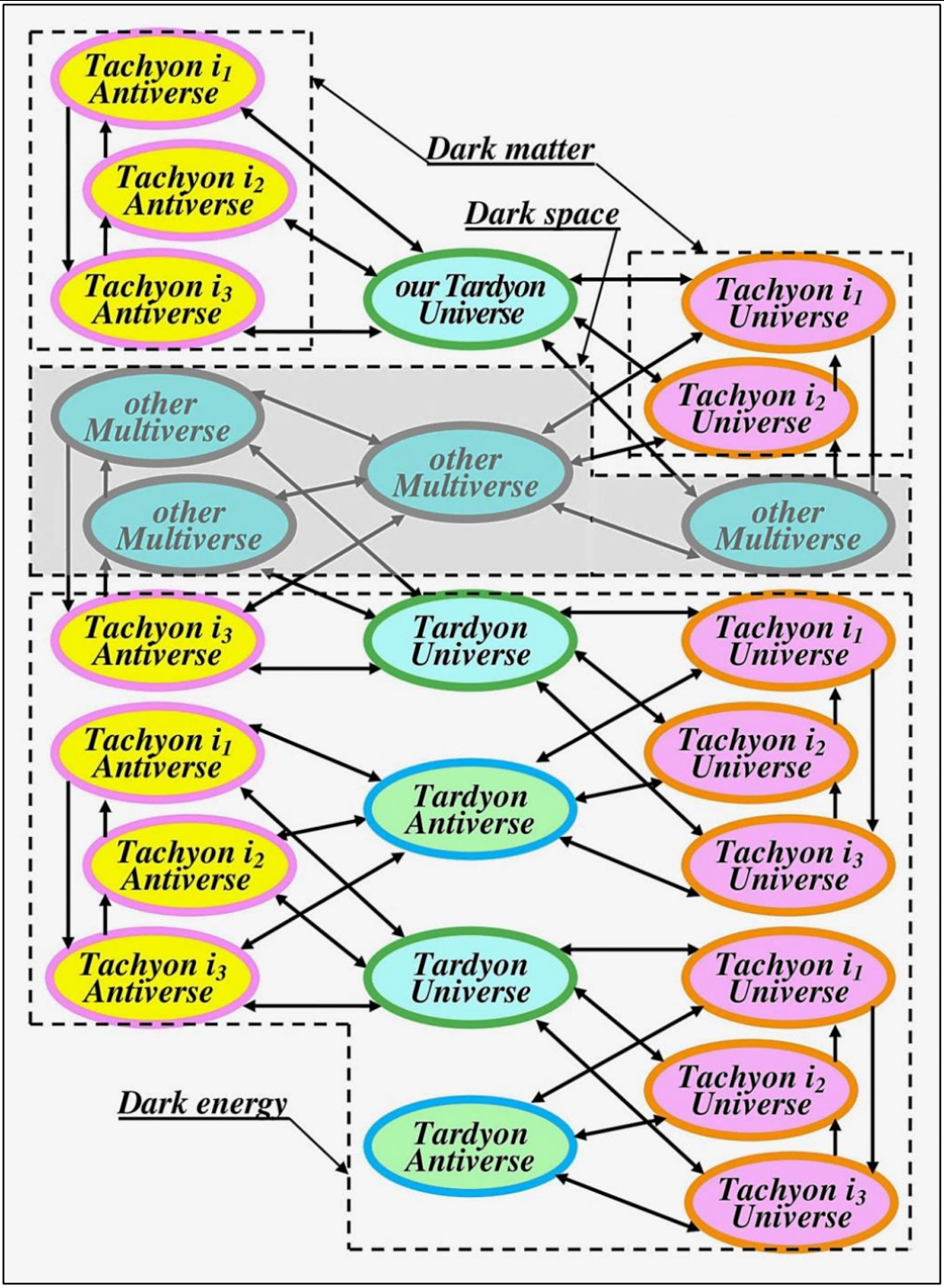

Fig. 4. *Probable structure of the hidden Multiverse corresponding to the data obtained by the WMAP and Planck spacecraft*

$$l(q,r,s) = l_0 i_1^q i_2^r i_3^s \sqrt{1-[v/c-(q+r+s)]^2} \tag{15}$$

or

$$m(q,r,s) = \frac{m_0 e^{iq\pi/2} e^{ir\pi/2} e^{is\pi/2}}{\sqrt{1-[v/c-(q+r+s)]^2}} \tag{16}$$

$$\Delta t(q) = \Delta t_0 e^{iq\pi/2} e^{ir\pi/2} e^{is\pi/2} \sqrt{1-[v/c-(q+r+s)]^2} \tag{17}$$

$$l(q) = l_0 e^{iq\pi/2} e^{ir\pi/2} e^{is\pi/2} \sqrt{1-[v/c-(q+r+s)]^2} \tag{18}$$

where m is the relativistic mass of a moving body;

Δt is the relativistic time of a moving body;

l is the relativistic length of a moving body;

q, r, s are the coordinates of the universe in which a moving body is located.

These formulas implies that our Multiverse has a quaternion structure in six-dimensional space [62]-[64] and its structure is described by the function $f_{q,r,s}(x, y, z) + i_1 q + i_2 r + i_3 s$, where the real summand $f_{q,r,s}(x, y, z)$ describes distribution of physical content in the universe with coordinates q, r, s, and the imaginary summand $i_1 q + i_2 r + i_3 s$ describes the position of this universe in the space of the Multiverse.

According to the formulas (4)-(6), for integers[3] of the coordinates of the universes q, r, s in the hidden Multiverse

- we get $i_1^q i_2^r i_3^s = 1$ for $q + r + s = 0$, that corresponds to our visible universe, which we shall call it a tardyon universe, since we have $0 \le v < c$ in this case;
- we get either $i_1^q i_2^r i_3^s = i_1$ or $i_1^q i_2^r i_3^s = i_2$ or $i_1^q i_2^r i_3^s = i_3$ for $q + r + s = 1$, which corresponds to one of the invisible universes adjacent to our universes; we shall call them tachyon universes, since we have $v > c$ in this case;
- we get either $i_1^q i_2^r i_3^s = -1$ for $q + r + s = 2$, which corresponds to one of the invisible universes; we shall call them tardyon antiverses, since we have $v > c$ in this case;
- we get either $i_1^q i_2^r i_3^s = -i_1$ or $i_1^q i_2^r i_3^s = -i_2$ or $i_1^q i_2^r i_3^s = -i_3$ for $q + r + s = 3$, which corresponds to one of the invisible universes; we shall call them tachyon antiverses, since we have $v > c$ in this case;
- etc.

Examples of the structural diagrams of the hidden Multiverses corresponding to the calculations are shown in fig. 4-6. As can be seen, the universes contained in these Multiverses are interconnected not only by bidirectional portals corresponding to the formula (10), but also by unidirectional portals corresponding to the formulas (11) and (12). Besides, some universes of the hidden Multiverse, including our visible universe, it appears, can be connected through portals with universes of other Multiverses that together form a Hyperuniverse[4], generating the phenomenon of dark space [65], [66].

[3] And non-integer values q, r, s are taken in portals

[4] By analogy with the term 'Multiverse', hereinafter, instead of 'Hyperuniverse', we will use the term 'Hyperverse'.

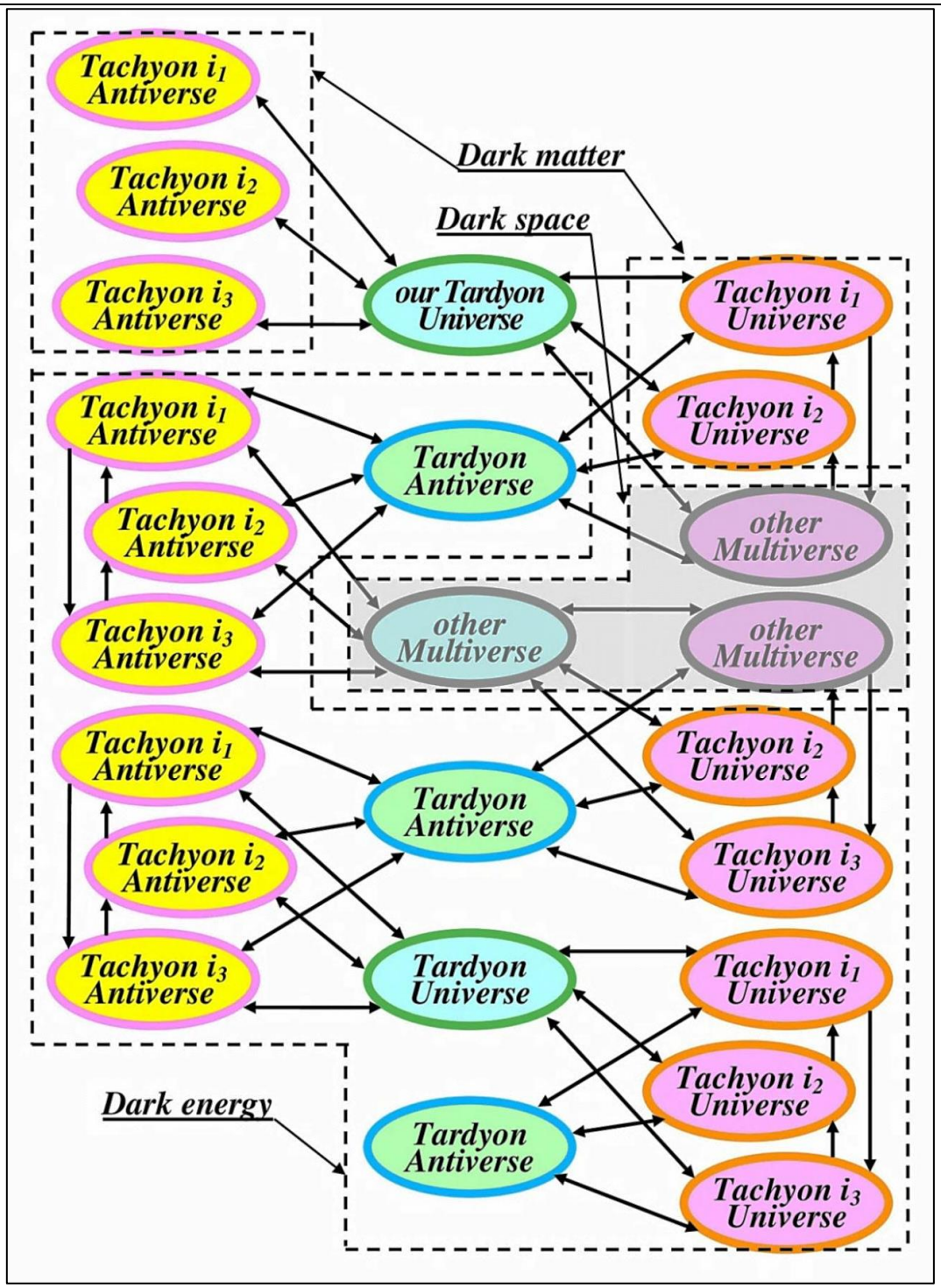

Fig. 5. *Another probable structure of the hidden Multiverse corresponding to the data obtained by the WMAP and Planck spacecraft*

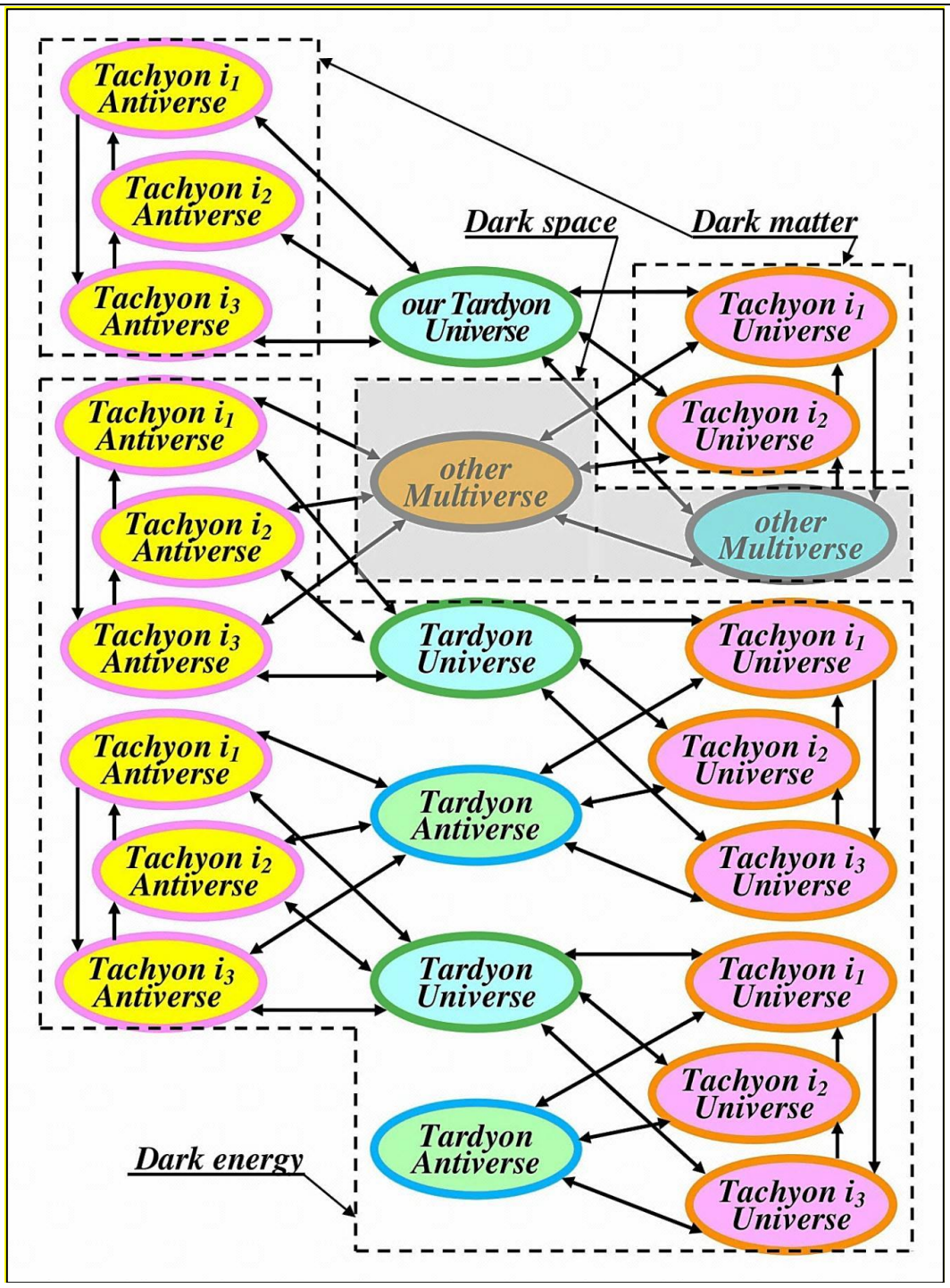

***Fig. 6**. One more probable structure of the hidden Multiverse corresponding to the data obtained by the WMAP and Planck spacecraft*

4. How to see invisible universes

So, the alternative version of the STR successfully solves the problems that turned out to

be unsolvable for the generally accepted version. Nevertheless, it will remain but a hypothesis until it finds experimental confirmation. What experimental confirmations of its truth will be authoritatively convincing and how can they be obtained?

Experimental confirmations of real physical existence of the hitherto undetected invisible universes would obviously be the most authoritative evidence. It turns out that one can see [67]-[71], or, in other words, discover them. This requires placing a telescope in a portal[5] and comparing its observations of the starry sky with the observations of telescopes located outsidethe portals (Fig. 7). Constellations in the skies of other universes would actually be completely different. Therefore, once a hypothetical telescope is moved through a portal from our universe (i.e. from the earth's surface) to an adjacent universe invisible on Earth, all

[5] Similarly, to see the invisible neighbouring room of our dwelling, you need to look into it from the corridor connecting these rooms

the known constellations in the starry sky would gradually be replaced by the constellations of the adjacent universe. This would be the most obvious and indisputable evidence of existence of other universes. And such an experiment will be much less expensive than a similar experiment a hundred years ago by the President of the Royal Astronomical Society, Sir Arthur Stanley Eddington [72], [73].

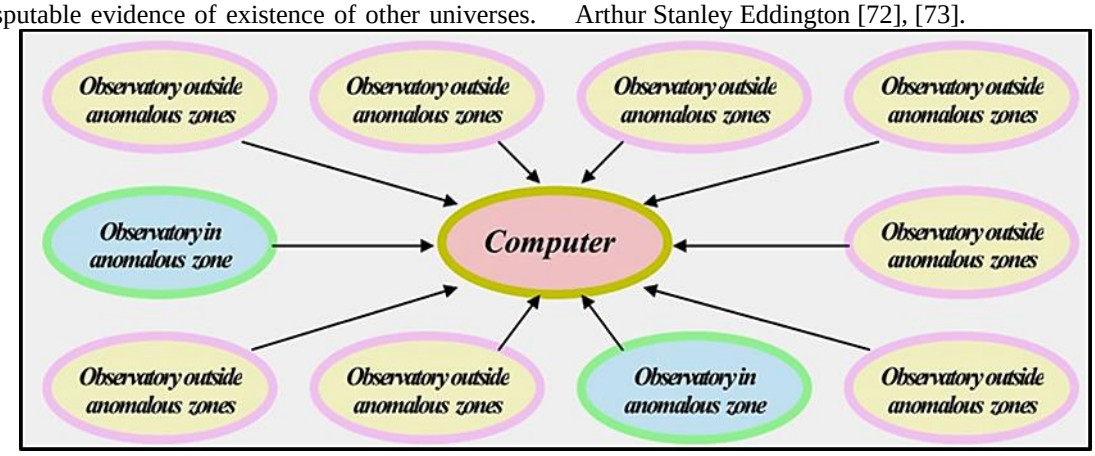

Fig. 7. Diagram of an astronomical experiment on invisible universe detection

Fig. 8. The Main Astronomical Observatory of the National Academy of Sciences of Ukraine located in an anomalous zone

Moreover, some observatories, such as, for example, the Main Astronomical Observatory of the National Academy of Sciences of Ukraine (Fig. 8) located in the Holosiivskyi forest, just 12 km from the centre of Kyiv, the capital of Ukraine, are already in anomalous zones, presumably being entrances to portals. Other observatories also located in anomalous zones can be identified by similar comparative studies of high-precision astronomical observations of all observatories. It is also desirable to subject all anomalous zones to such an examination so that to determine passport data of all portals available on Earth. Their comparative analysis will reveal how many adjacent invisible universes there are on the Earth and determine whether there are universes among these invisible universes that are not the part of the hidden Multiverse. Exploration of such universes would be the most interesting, as it makes possible to discover the Hyperverse.

In the future, when the portals are explored and people learn how to navigate through them safely, people can visit adjacent universes that are currently invisible. This would be another proof of their existence.

5. The relevance of geophysical researches of portals

At present, portals are absolutely unexplored. This even raises doubts as to their existence. Herewith, although there are a lot of anomalous zones supposedly being the entrances to portals, people avoid visiting them. And they are right. This is unsafe, because portals are a kind of invisible labyrinths, three-dimensional labyrinths. So, naturally, finding a way out of a portal is not easy without knowing this and taking special precautions in advance (for example, the Ariadne's thread mentioned in ancient Greek mythology). Even more difficult is to successfully move from entrance to exit through a portal (the Ariadne's thread would not help here) and get into an adjacent universe. To do this, you need to create special tools for orientation in the portals.

But all the means used for a serious portal research, including portal orientation tools, vehicles (including unmanned vehicles), communications equipment and everything else, are much less

expensive than people's flights to the Moon or Mars and much more effective in terms of quantity and quality of new expected knowledge, both astrophysical and geophysical. From the standpoint of scientific, as well as political and economic consequences for human civilization development this would appear to be much more crucial than, for example, the discovery of America by Columbus.

6. Conclusion

Thus, because the fallacybility of the universally recognized version of STR stated in physics textbooks, which asserts the existence in nature of our only visible universe, is experimentally proven in the most indisputable way, and the alternative version of this theory states that there are many parallel universes, it has also been proven that there are portals between these universes.

And these portals need to be explored. This is very important from a practical point of view, since one must know how one can safely visit neighboring universes. This is no less important from a scientific point of view, as it will prove the existence of anti-space and anti-time and the possibility of traveling through the hidden Multiverse not only in space, but also in time. Moreover, time travel can be not only in the past, but also in the future [74]-[78].

Acknowledgments

The author gratefully acknowledges the insights, comments, and assistance of Olga Ilyinichna Antonova

References

1. Antonov A. A. 2016. Stargate of the Hidden Multiverse. Phylosophy & Cosmology. 16. 11-27.
2. Lewis D. (1986). On the Plurality of Worlds. Basil Blackwell, Oxford.
3. Deutch D. (1998). The Fabric of Reality: The Science of Parallel Universes and Its Impli-cations. Penguin Books, New York.
4. Ellis, G.F.R., Kirchner U. and Stoeger, W.R. (2004). Multiverses and physical cosmology, Monthly Notices of the Royal Astronomical Society. 347(3), 921 – 936.
5. Vilenkin A. (2007). Many Worlds in One: The Search for Other Universes. Hill and Wong. NY.
6. Carr B. ed. (2009). Universe or Multiverse? Cambridge University Press. Cambridge. UK..
7. Gribbin J. (2010). In Search of the Multiverse: Parallel Worlds, Hidden Dimensions, and the Ultimate Quest for the Frontiers of Reality. Wiley & Sons Inc. Hoboken. NJ.
8. Lucash V.N. and Mikheyeva, E.V. (2010). Physical cosmology, Physmathlit, Moscow.
9. Ellis G.F.R. (2011). Does the Multiverse Really Exist? Scientific American. 305, 38 – 43.
10. Greene B. (2011). The Hidden Reality: Parallel Universes and the Deep Laws of the Cosmos. Vintage. NY.
11. Hawking S., Mlodinow L. (2012). The Grand Design. Reprint Edition. Bantam. NY.
12. Tegmark M. (2014). Our Mathematical Universe: My Quest for the Ultimate Nature of Reality. Vintage. NY.
13. Kaku M. (2005) Parallel Worlds: A Journey Through Creation, Higher Dimensions, and the Future of the Cosmos. Doubleday.
14. Einstein A. (1920) Relativity: The Special and General Theory. H. Holt and Company. NY.
15. Bohm D. (2006). The Special Theory of Relativity. Routledge, Abingdon-on-Thames.
16. Penrose R. (2010). The Nature of Space and Time. Princeton University Press. Princeton.
17. Chernobrov V. 2001. Encyclopedia of the mysterious places of the Earth. Armada press. Moscow. (In Russian)
18. Chernobrov V. 2004. Encyclopedia of mysterious places in Russia. Veche. Moscow. (In Russian)
19. Chernobrov V. 2007. Encyclopedia of the mysterious places of the Earth and Space.. Veche. Moscow. (In Russian)
20. Chernobrov V. 2009. The Ultimate Encyclopedia of mysterious places in Moscow and Moscow region. Geleos. Moscow. (In Russian)
21. Kalinin S. A. 2003. Einstein's cardinal mistakes. Publishing house Editorial URSS. M. (In Russian)
22. Artekha S. N. 2007. Criticism of the foundations of the theory of relativity. 2nd ed. Publishing house LKI. M. (In Russian)
23. Antonov A. A. 2013. Refutation of the special theory of relativity. International Journal of Physical and Social Sciences. 3(5). 192-210.
24. Antonov A. A. 2014. Correction of the special theory of relativity: physical reality and nature of imaginary and complex numbers. American Journal of Scientific and Industrial Research. 5(2). 40-52. doi:10.5251/ajsir.2014.5.2.40.52
25. Antonov A. A. 2021. Special theory of relativity, which is studied in physics textbooks, is incorrect. German International Journal of Modern Science. 16, 49-53.
DOI: 10.24412/2701-8369-2021-16-49-53
26. Antonov A. A. 2021. Version of the special theory of relativity that is studied in all physics textbooks is incorrect. Österreichisches Multiscience Journal. (Insbruck, Austria). 43(1). 17-22. http://osterr-science.com
27. Antonov A. A. 2021. Special theory of relativity presented in physics textbooks is wrong. Norwegian Journal of development of the International Science 68(1). 3-7. DOI: 10.24412/3453-9875-2021-68-3-7.
28. Antonov A. A. 2021. Experimental evidences for the fallacy of the STR version in the physics textbooks. European Journal of Applied Sciences. Services for Science and Education. UK. 9(6). 349-364. DOI:10.14738/aivp.96.11304.
29. Antonov A. A. 2022. The existence of radio engineering refutes the physics textbooks' version of STR. The scientific heritage. 83(1). 19-22. DOI: 10.24412/9215-0365-2022-83-1-19-22
30. Antonov A. A. 2022. The version of STR presented in physics textbooks is incorrect, since it follows from it that radio engineering should not exist.

European Journal of Applied Sciences. Services for Science and Education. UK. 10(1). 440-445.

DOI://doi.org/10.14738/aivp.101.2022

31. Antonov A. A. 2022. The existence of radio engineering refutes the physics textbooks' version of STR. The scientific heritage. 83(1). 19-22. DOI: 10.24412/9215-0365-2022-83-1-19-22

32. Antonov A. A. 2022. Why the physics textbooks tech am incorrect version of the special theory of relativity which denies the existence of radio- and electrical engineering. Challenges and problems of modern science. Proceedings of the III International Scientific and Practical Conference. London, UK. 78-86. https://conference-w.com/

33. Tamm I. E. (1959). General properties of radiation emitted by systems moving at superlu-minal velocities and some applications to plasma physics. Advances in Physical Sciences. 68(3). 387-396. doi:10.3367/UFNr.0068.195907c.0387

34. Antonov A. A. (2008). Physical Reality of Resonance on Complex Frequencies. European Journal of Scientific Research. 21(4). 627-641. http://www.eurojournals.com/ejsr.htm

35. Antonov A. A. (2009), Resonance on Real and Complex Frequencies. European Journal of Scientific Research. 28(2). 193-204. http://www.eurojournals.com/ejsr.htm

36. Antonov A. A. (2010). New Interpretation of Resonance. International Journal of Pure and Applied Sciences and Technology. 1(2). 1-12.

http://doi.org/10.17686/sced_rusnauka_ 2010-888

37. Antonov A. A. (2010). Oscillation processes as a tool of physics cognition. American Journal of Scientific and Industrial Research. 1(2). 342 – 349.

doi:10.5251/ajsir.2010.1.2.342.349

38. Antonov A. A. (2010). Solution of algebraic quadratic equations taking into account transitional processes in oscillation systems. General Mathematics Notes. 1(2). 11-16.

http://doi.org/10.17686/sced_rusnauka_2010-887

39. Tanaka S. (1960). Theory of matter with superlight velocity. Progress of Theoretical Physics (Kyoto). 24(1). 171-200. doi: 10.1143/PTP.24.171

40. Hill J.M., Cox B.J. (2012). Einstein's special relativity beyond the speed of light. Proceeding of Royal Society A.: Mathematical, Physical and Engineering sciences. 468(2148). 4174-4192. doi:10.1098/rspa.2012.0340.

41. Antonov A.A. (2012). Discovery of the real multiverse. Encyclopedia of Russian Thought, Reports to the Russian Physical Society. 16(3). 3-20. (In Russian)

http://doi.org/10.17686/sced_rusnauka_2012-1115

42. Antonov A.A. (2013). Knowledge of the multiverse as a factor in accelerating the development of human civilization. Journal of Russian Physical Thought. 1-12, 6-77.

http://doi.org/10.17686/sced_rusnauka_2011-1117 (In Russian)

43. Antonov A.A. (2015). The astrophysical phenomenon of dark matter and dark energy proves the existence of the hidden Multiverse. American Journal of Modern Physics. 4(4). 180-188. doi: 10.11648/j.jamp.20150404.14

44. Antonov A. A. (2015). Hidden Multiverse. International Journal of Advanced Research in Physical Science. 2(1). 25-32. http://doi.org/10.17686/sced_rusnauka_2015-903.

45. Antonov A. A. (2016). What Physical World do We Live in? Journal of Modern Physics. 7(14). 1933-1943.

http://dx.doi.org/10.4236/jmp.2016.714170

46. Antonov A. A. (2016). Verifiable Multiverse. Global Journal of Science Frontier Research: A Physics and Space Science. 16(4) 4-12 doi: 10.17406/GJSFR

47. Antonov A. A. (17 February 2017) Verifiable hidden Multiverse. Global Journal of Science Frontier Research. Research blog.

48. Antonov A. A. (2012), Earth, portals, parallel universes. American Journal of Scientific and Industrial Research. 3(6). 464-473. doi:10.5251/ajsir.2012.3.6.464.473

49. Antonov A. A. (2015). Where to look for alien civilisations. Cosmology. Commentaries: Stephen Hawking's Aliens. The Search for Intelligent Extraterrestrial Life. Project Break-through Liste. http://cosmology.com/Aliens1.html

50. Hinshaw G., Larson D., Komatsu E., et al. (2013) Nine Year Wilkinson Anisotropy Probe (WMAP) Observations: Cosmological Parameter Results. arXiv:1213.5226 [astro-ph/CO].

51. Adam R., Ade P.A.R., Aghanim N., et al. (2015). Plank 2015 Results. 1. Overview of Products and Scientific Results. arXiv:1502.01582v2 [astro-ph.CO].

52. Antonov A. A. (2015). Why dark matter and dark energy are invisible? Optics. 4(6), 43-47. doi: 10.11648/j.optics.20150406.12

53. Antonov A. A. (2015). Hidden Multiverse: explanation of dark matter and dark energy phenomena. International Journal of Physics. 3(2). 84-87. doi:10.12691/ijp-3-2-6

54. Antonov A. A. (2015). Explanation of dark matter and dark energy phenomena. Journal of Science Frontier Research: A Physics and Space Science. 15(1). 33-38.

http://doi.org/10.17686/sced_rusnauka_2015-902

55. Antonov A. A. (2015). Hidden Multiverse: explanation of dark matter and dark energy phenomena. Cosmology. 19. 40-61.http://cosmology.com/AntonovMulyiverse.pdf

56. Antonov A. A. (2015). Review of A. A. Antonov's publications on the problem of explaining the phenomenon of dark matter and dark energy. Journal of the Russian Physical and Chemical Society. 87(3) 63-76. (In Russian)

57. Antonov A. A. (2016). Explaining the Phenomenon of Dark Matter and Dark Energy by Existence of the Hidden Multiverse. Frontiers of Astronomy, Astrophysics and Cosmology. 2(1). 1-9. doi: 10.12691/faac-2-1-1

58. Antonov A. A. (2016). Hypothesis of the Hidden Multiverse: Explains Dark Matter and Dark Energy. Journal of Modern Physics. 7(10), 1228-1246. doi: 10.4236/jmp.2016.710111

59. Antonov A. A. (2017). Nature of dark matter and dark energy. Journal of Modern Physics. 8(4). 567-582. doi: 10.4236/jmp.2017.84038

60. Antonov A. A. (2017). Hypothesis of the hidden Multiverse explains the phenomenon of dark matter and dark energy. Applied Physics Research. 9(2). 30-41.

doi: https://doi.org/10.5539/apr.v9n2p30

61. Kantor I. L., Solodovnikov A. S. 1989. Hypercomplex Numbers: An Elementary Introduction to Algebras. Springer.

62. Antonov A. A. (2011), Structure of the Multiverse. British Journal of Science. 2(2). 51-60. http://doi.org/10.17686/sced_rusnauka_2011892

63. Antonov A. A. (2015). Quaternion structure of the hidden Multiverse: explanation of dark matter and dark energy. Global Journal of Science Frontier Research A: Physics and Space Science. 15(8). 8-15.

64. Antonov A. A. (2015). Principles and structure of the real Multiverse: explanation of dark matter and dark energy phenomena. American Journal of Modern Physics. 4(1). 1-9.

doi:10.11648/j.ajmp.20150401.11

65. Antonov A. A. (2018) Discovery of Dark Space. Journal of Modern Physics, 9, 14-34. https://doi.org/10.4236/jmp.2018.91002

66. Antonov A. A. (2018). Physical Reality and Essence of Imaginary Numbers in Astrophysics: Dark Matter, Dark Energy, Dark Space. Natural Science. 10(1). 11-30.

doi:10.4236/ns.2018.101002

67. Antonov A. A. 2020. How to See Invisible Universes. Journal of Modern Physics. 11(05), 593-607. DOI: 10.4236/jmp.2020.115039

68. Antonov A. A. 2020 Can invisible universes be seen? International independent scientific journal. 21(2). 51-60. http://www.iis-journal.com

69. Antonov A. A. 2020. Universes Being Invisible on Earth outside the Portals Are Visible in Portals. Natural Science. 12(8). 569-587. https://doi.org/10.4236/ns.2020.128044

70. Antonov A. A. 2021. Invisible universes can be seen in anomalous zones. International independent scientific journal. 23(1). 28-44. http://www.iis-journal.com

71. Antonov A. A. 2020. Invisible universes can be seen in anomalous zones. Danish Scientific Journal. 43(1). 9-24. http://www.danish-journal.com

72. Dyson F.W, Eddington A.S., Davidson C. 1929. A determination of the deflection of light by the sun's gravitational field, from observations made at the total eclipse of May 29, 1919. Philosophical transactions of the Royal Society A. 220. 291-333.

https://doi.org/10.1098/rsta.1920.0009

73. Eddington A. S. 1923. The Mathematical Theory of Relativity. 2nd Ed. Cambridge University Press. London.

74. Antonov A. A. 2021. Experimental refutations of the STR version contained in physics textbooks and confirmations of the truth of its alternative version. German International Journal of Modern Science. 22. 52-61.

75. Antonov A. A. 2021. Antimatter, Anti-Space, Anti-Time. Journal of Modern Physics, 12(05), 646-660. DOI: 10.4236/jmp.2021.125042.

76. Antonov A. A. 2021. Antipodes in space. German International Journal of Modern Science. 11(1). 15-25. DOI: 10.24412/2701-8369-2021-11-1-15-25

77. Antonov A. A. 2021. There is not only antimatter, but also anti-space and anti-time. Journal of science. Lyon. 21. 22-30. https://www.joslyon.com/

78. Antonov A. A. 2021. Do antimatter, anti-time and anti-space exist in nature. Annali d'Italia. 20(1). 14-24. https://www.anditalia.com/

UNCERTAINTY OF A CRITICAL POINT ON THE FREEZING CURVE

Beycan İbrahimoğlu
Anadolu Plasma Technology Centre, Ankara-Turkey
DOI: 10.5281/zenodo.7796155

Abstract

P. W. Bridgman developed a method to measure the force acting on a moving piston of known area and conducted experiments on gases, liquids and solids at high pressures. He reported that there is no critical point on the freezing curve in his experiments on various materials. Researchers working in universities and laboratories in the USA, France, England, Germany, Russia, the Netherlands and other universities and laboratories have reported that there is no critical point on the melting curve at high pressures in their experiments on gases, liquids and solids with this method developed by P. W. Bridgman.

The main method of research in physical chemistry is experience. The new physical chemistry is an experimental science. A real physicochemical experiment is of great importance in the study of physical laws and processes. The method and methodology applied in determining the hypothesis put forward is the most important factor. Experiments are key to propose a hypothesis and solve a problem. Although the existence of a critical point on the melting curve seems theoretically and graphically possible, P. W. Bridgman and other researchers have reported that there is no critical point.

In our opinion, it is not possible to determine the existence of a critical point on the freezing curve by the method applied by P. W. Bridgman and other researchers in their experiments. With this method it was possible to determine the pressure and temperature dependent melting curve. For nearly a century, the presence or absence of a critical point on the freezing curve has been a matter of debate.

In the experiments conducted by P. W. Bridgman and other researchers, it was found that there was no critical point, but it is possible to determine the existence of a critical point by the experimental results of the intermittent metastable state on the freezing curve at high pressures or by applying the geometric method depending on the thermodynamic parameters of the substance.

Keywords: benzene, intermittent metastable state, graphical method, computer calculations, freezing curve, critical pressure.

Introduction

Phase transitions are one of the most interesting phenomena in physical chemistry. They differ by their nature and the Ehrenfest criteria are commonly used to classify them. The first type of phase transitions with a intermittent metastable state when pressure is applied can be called structural phase transitions. Changes in important physical properties of crystalline, electronic, dielectric-metal, dielectric-semiconductor and other materials during phase transitions occur at high pressure and contribute to the understanding of the physicochemical nature of matter. And recently, they were even able to obtain a boron-doped superconducting diamond. This will contribute greatly to the development of future electronics. On the other hand, the application of pressure gives rise to the practical possibility of synthesizing new materials with specific properties. The fundamental problem of high pressure physics is the study of the T-P diagram of a substance and the establishment of its crystal structure under certain T/P conditions.

High-pressure applications cover the automobile, aerospace, semiconductor and pharmaceutical industries, food and other sectors in physical, chemical and technical matters. The role of high pressure in achieving unique physical and chemical properties of materials in advanced high-tech industries and in basic and applied research is indisputable. The experimental setup developed for the study of solids, liquids and gases at high pressures and the experimental setup and experimental techniques used on the freezing curve are examined by summarizing the work of P.W. Bridgman and other researchers [1] on the freezing curve.

Experimental setup and experimental technique

Although P. W. Bridgman and other researchers have developed some constructive modifications on a device that allows the creation of very high pressure, in general, the measurement methods are the same and the results are close to each other. For example: in the Keyes laboratory of Massachusetts Institute of Technology, fifty measuring instruments with a free piston pressure system have been in wide use for more than twenty years [1,3-11]. In conclusion, P.W. Bridgman divided his own work into two parts. First, by increasing the measurement technique to 12,000 kg/cm2 and second, by increasing the pressure field to 50,000 bar/cm2. Performed by the moving piston method, which makes it possible to determine all the necessary parameters. The general nature of the results is that the melting curve increases continuously with temperature and pressure, in combination no parameter changes, there is no reason to expect anything other than infinite growth of the melting curve. In experiments by Beatty and Bridgman, it was reported that there was no critical point [12]. The absolute values of the volumes of liquids and solids decrease along the melting line and the effect of pressure prevails over the effect of temperature. They also reported that the two most important results of measurements on more than 50 liquids are the reversal of the sign of $(d^2V/dT^2)p$ with increasing temperature at a constant pressure of several thousand

kg/cm^2 and that (dP/dT)v is not only a function of volume [9,13,14].

Based on experiments conducted by P.W. Bridgman, Simon et al. [2] reported that the melting curve probably ends at a critical point. Rayet and Bridgman explicitly argue on liquid-solid equilibrium for argon up to 10,000 kg/cm^2 that the critical point cannot be ignored in any way. Several papers on this subject have come out of myBridgman laboratory. Later, new data on the melting curves of nitrogen and argon up to 5000 kg/cm^2 reported unlimited growth in the melting curve [3]. There are studies by Leiden and Kizom [4-8] in which the melting of certain stationary gases is determined over a much smaller pressure range than in Simon, but with greater accuracy. The Simon and Glatzel equation turned out to be applicable and its constants were determined. They reported that the Tait equation has wide applicability for volumes of liquids as a function of pressure:

$$V = V_0 - C \log [(B+P) / B]$$

According to Tammann and Moritz volume change the maximum pressure should return to zero at some final pressure:

$$\Delta v = a - b \log (C + \rho). \Delta v.$$

According to this equation, it should occur at 40,000 kg/cm^2 for CO [15].

In our studies, the CO2 critical pressure of carbon dioxide was determined as 5700bar. Figure 0.

Although most of the studies devoted to melting at high pressure aim to solve the problem of the nature of the melting curve, the method applied in experiments has generally identified the existence of a critical point in the melting curve that depends on pressure and temperature. However, as determined above, many theoretical studies have reported that it is possible to have a critical point at high pressures. Experimentally applied at high pressures, the method has been the main subject of dispute whether the melting curve ends at the critical point, whether it has a maximum.

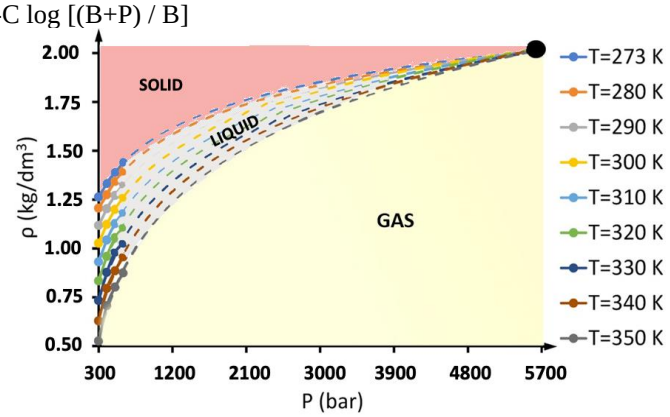

Figure 0. Isotherms in the density-pressure (ρ-p) phase diagram and the intersection point of their extensions

Metastable state

From a physical point of view, matter is in a state of thermodynamic equilibrium. Metastability, then, is the non-equilibrium state of matter. Phase transitions in the equilibrium curves of evaporation, freezing and sublimation end in metastable states. Overall, the study of phase transitions under high pressure is very interesting and important for our future. Especially in the production of new types of materials.

The most commonly considered phase transitions are those with a change in temperature and pressure, under a constant pressure. Abrupt change in temperature and pressure at constant pressures is clearly visible on the melting curve with dashed metastable state. It has been reported that the metastable state determines the presence of a critical point on the liquid-solid equilibrium curve, just as it determines the presence of a critical point on the liquid-vapor equilibrium curve[16-21]. For this purpose, a special experimental setup was designed and experiments were carried out to obtain a intermittent metastable state at high pressures [22]. The abrupt temperature- and pressure-dependent change in the intermittent metastable state at constant pressures decreases with increasing pressure and becomes zero on the freezing curve. The point on the melting curve of benzene where the metastable state is reset at 2200atm pressure and 356K temperature is defined as the critical point of benzene [23-30].

As mentioned above, this change in the properties of matter due to temperature and pressure is visible with a sudden jump. During a phase transition of the first type, the most important, primary comprehensive parameters change abruptly: specific volume (i.e. density), the amount of internal energy stored and the concentration of components. This change always occurs at a certain rate, which means that a limited amount of time is needed to "close" the entire gap in density or specific internal energy. During this time, the phase transition does not occur immediately in the entire volume of the substance, but gradually. In the first type of phase transitions, the abrupt jump and gradual transition occur stably at temperature and pressure values with the presence of a discontinuous metastable state.

Freezing of liquid benzene during cooling time at constant pressures, first in the discrete metastable state and then in the isothermic freezing process is completed. The point defining the system "freezes", pressure and temperature remain constant. The phase transformation completed by the first, second and super-type metastable state spontaneously formed under constant pressure by cooling benzene at 500atm pressure and 286.7K temperatures on the freezing curve is shown in Figure 1 and the I, II and III thermograms are given schematically.

The first thermogram (figure 1. I) shows the isothermic freezing time t of benzene cooled at point *a* between points *d* and *c* depending on the pressure and the completion of isothermic freezing at point c and the transition to solid phase along the *d* line. This thermogramma is only the first type of phase transition resulting in a sustained metastable state.

The second thermogram (figure 1. II) shows that benzene cooled at point *a* supercools from freezing at point *b* to point *c* during t_1, depending on the pressure. Suddenly rises from point *c* to point *d* during t_2. Isothermic freezing between points *d-e* of temperature for time t_3, terminating at point *e* and representing the solid phase along line *f*. This thermogram is the first type of phase transition resulting in isothermic freezing after the intermittent metastable state.

Third (figure 1. III), thermogramma Super phase transformation and super metastabel state, although this phase transformation is still not realized in the defined experiments, it is graphically shown to be possible [31]. In the thermogram, benzene cooled at point *a* supercools between points *b* and *c* during t_1, rises abruptly from point *c* to point *d* during t_2 and ends only in a metastable state without isothermic process. This phase transformation from the liquid phase to the solid phase with only metastable state characterizes the second type of phase transition.

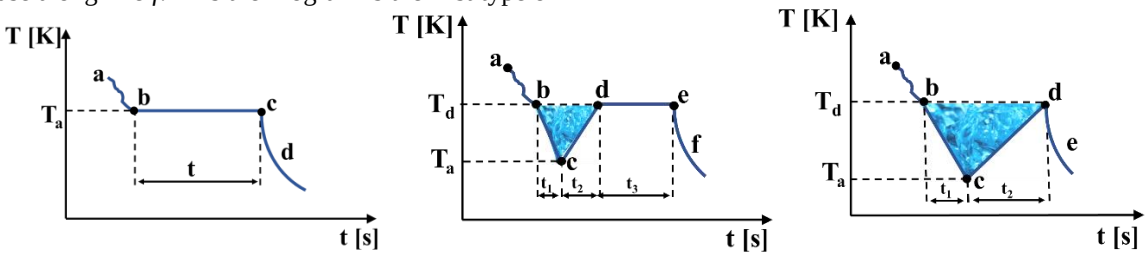

I *II* *III*

Figure 1. Thermograms representing metastable states I, II and III.

The intermittent metastable state shown schematically on the freezing curve of liquid benzene at constant pressures of 500atm pressure and 286.7K temperature at constant pressures (Figure 1, II) is given in detail in Figure 2.

Figure 2. It was determined by experiments that the intermittent metastable state obtained on the freezing curve of liquid benzene is the sudden rise (adiabatic rise) of the liquid with supercooling under constant pressure -ΔT, and Δp: isenthalpic pressure drop, which decreases with increasing pressure and becomes zero at 2200atm pressure and 356K temperature.

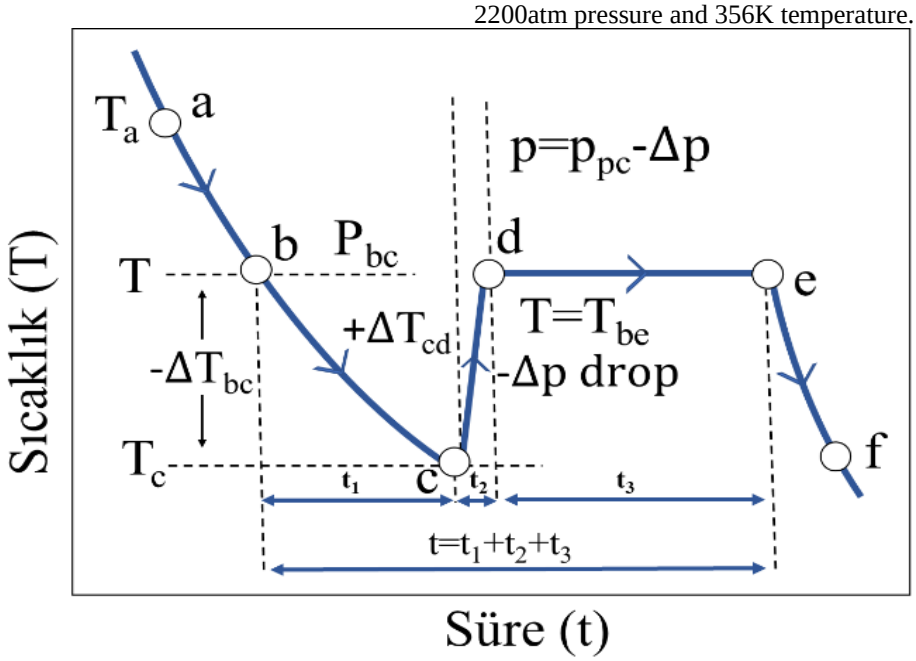

Figure 2. Freezing through metastable liquid formed by cooling the liquid-solid equilibrium graph of benzene, ab: isobaric cooling of stable liquid with temperature T_a, bc: isobaric supercooling of stable liquid with temperature T, -ΔT: temperature drop during supercooling, cd: adiabatic and (isenthalpic) change of supercooled liquid with temperature T_c, ΔT= (-ΔT): isenthalpic temperature rise, Δp: isenthalpic pressure drop, bcd: formation of metastable liquid, de: isothermic ($T = T_{be}$) and isobaric ($p = p_{bc}-\Delta p$) freezing, e: metastable solid, f: stable solid, $t_1+t_2+t_3=t$: step times and total time to complete the batch metastable state

Computer results of the intermittent metastable state

The most promising way to create state diagrams is the optimal combination of experimental, theoretical and graphical methods followed by computer calculations. In this study, the experimentally obtained parameters of the intermittent metastable state are evaluated using the Tayt equation of state [45].

$$\rho = \frac{\rho_0}{1 - A \cdot ln\left(\frac{B + P}{B + P_{атм}}\right)}$$

Where ρ0 is the density at atmospheric pressure P_{atm} and temperature T, ρ is the density at some pressure P and temperature T.

P-T phase diagrams of benzene were drawn as a result of computer calculations considering intermittent metastable regions [45]. In addition, the diagrams are constructed by considering discrete metastable regions, and for benzene [53-55], the experimental and theoretical values of p-T in the subcritical region of the phase diagram do not exceed 1%. On the P-V diagram for a wide range of pressure variations in the high pressure region, the isotherm of the T= 356 K endpoint of the metastable state and the isotherm of the T= 278.5 K triple point of benzene are exactly very close at pressures in the range of 220 MPa and above. In this study, the experimental presence of the endpoint of the discontinuous metastable state at P = 220 MPa and temperature T = 356 K indicates the transformation of a liquid into a solid around this point.

The phase transition takes place in stages, from a disordered phase (liquid) to a less ordered phase and so to the most ordered phase (solid). That is, the transition develops through a series of intermittent metastable state-enhancing phases.

The experimental results determined with the discrete metastable state on the freezing curve of benzene at high pressure were found to coincide with the computer drawings and the confirmation equation.

Graphical method in geometry.

The main research topic of geometric thermodynamics, which is the basis of Gibbs' scientific papers, is the relationship between the physical and chemical properties of material bodies, their transformation into geometrically shaped images, their study and interpretation, which helps to precisely determine certain laws. The essence of geometric thermodynamics is not only to represent the state of thermodynamic systems using geometric images. These images are the subject of research, not the goal itself. Geometry establishes certain physical laws by applying methods. Geometry studies spatial relationships and shapes with graphics. Graphics is the only way to solve many technical problems. It is the only method of determining the physical and chemical properties of substances that have been reliably incorporated into the research methodology..

I. The dependence of *(dV/dT)p=const* is based on the postulates that were later recognized as the postulates of the ideal gas law in determining the absolute temperature. The physical and theoretical importance of absolute temperature cannot be disputed.

II. The dependence of *(dρ/ dT)p=const bağlılığı,* the point where the isobars meet on the (T) axis, indicated the ionization temperature for monatomic gases and the dissociation temperature for polyatomic gases [34-46]. This rule does not apply to Hydrogen gas [47-52].

It is also possible to apply the graphical method to liquid and solid phases of matter.

III. The dependence of *(dρ/ dT)p=const bağlılığı*, applied to benzene in the liquid phase, determined the point at which the sublimation curve of the isobars ends. Figure 3. In addition, since experimental studies on the sublimation equilibrium curve involve technical requirements, it is important to graphically determine the point where the sublimation equilibrium curve ends. Applied to the test results of liquid benzene at T=298K and T=498K (ρ-T), p=constant dependence, 168K temperature where the solid ⇋ vapor equilibrium curve ends and ρk=1200 kg/m^3 critical density point were evaluated. The pressure of the critical density was determined as Ps = (Püç/Tüç) x Ts = 0.023bar.

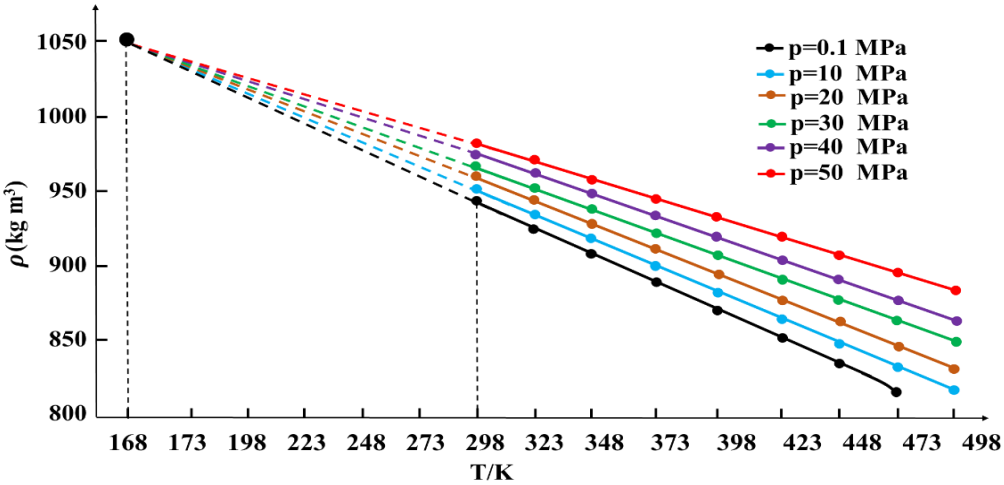

Figure 3. ρ-T, p=const dependence of benzene.

IV. The dependence of *(dρ/dP)T=const* is applied to the liquid phase of benzene and the isotherms converge at one point at high pressure [24-31]. The parameters obtained by applying the graphical method to benzene and other substances are given in table 1.

Table1.

Critical temperature, critical pressure, critical density and sublimation curve endpoint values obtained graphically for various substances.

Matter	Chemical Name of Matter	Critical temperature K	Critical denstiy kg /m^3	Critical pressure MPa	desubduction curve ends temperature, K
M-Toloudin	C7H9N	436	1085	200	178
O- Toloudin	C7H9N	303.15	1115	140	153
Benzen	C6H6	562.7	1200	220	160
Benzonitril	C7H5N	700	1150	185	198
N-Dekan	C10H22	617.6	839	130	140
O-Ksilen	C8H10	630	990	205	120
N-hepten	C6H17	540	885	425	80

The pressure-temperature phase diagram of benzene was drawn using the values given in table 1 obtained by experimental and graphical methods. The p-T phase diagram of benzene is given in figure 4.

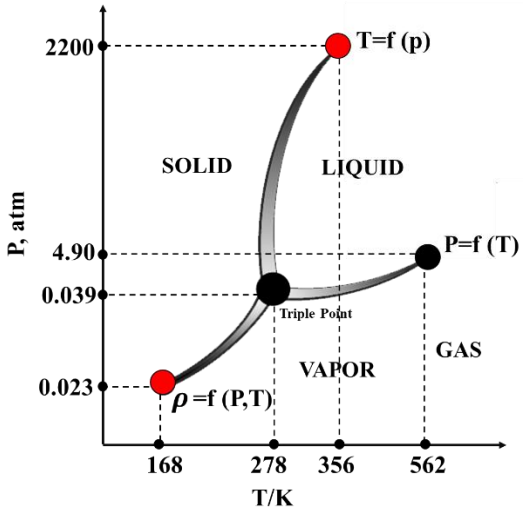

Figure 4.

In the liquid phase of benzene, the isotherms converge at a pressure of 2200atm, which is a critical point on the melting curve. The point determined by experimental, computer and graphical methods at 2200atm pressure represents the critical point on the freezing curve of benzene. The critical point determined by the dashed metastable state on the freezing curve of benzene at high pressure is drawn in Figure 5.

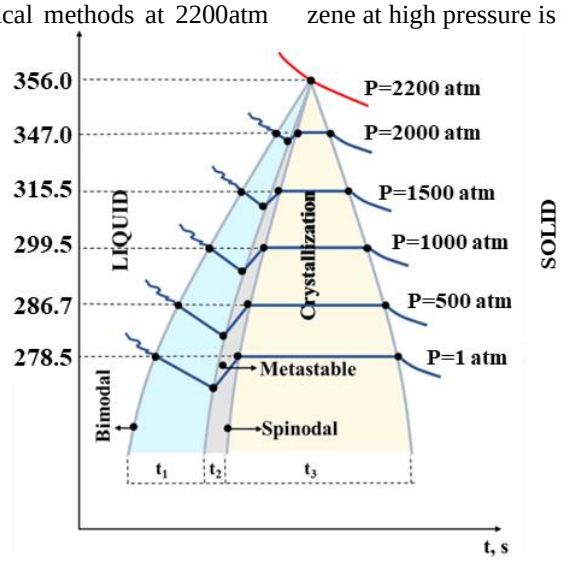

Figure 5. Temperature and time diagram of the critical point on the freezing curve of benzene

According to the theory of L. D. Landau [12], during phase transitions of the first kind, the distribution function over the energy or density of the system has two **bimodal** maxima. At the first-order phase transition point, the density distribution is indeed bimodal. In this case, the greater the number of particles in the system, the higher and narrower the peaks on the bimodal curve. The highest maximum corresponds to the most favorable, stable state of the system and the second maximum corresponds to a less favorable, metastable state. At the transition point, the heights of the maxima become the same and the system can coexist in both states at the same time. This is illustrated in the temperature versus time diagram on the freezing curve of benzene. Figure 5.

Conclusion

At high pressures and temperatures, it is very difficult to determine the intermittent metastable burst of melting by experiments. Although the existence of a critical point on the melting curve is theoretically possible, it cannot be determined experimentally by measuring the volume with the force acting on the moving piston whose area is known.

In experiments, the absolute values of the volumes of liquids and solids decrease along the melting line and the effect of pressure dominates the effect of temperature. The compressibility of the solid phase at the melting point is never greater than the compressibility of the liquid phase at the melting point, usually less than 25% and not much more.

These approaches and a phase transition of the first kind imply the existence of metastable states for each of the phases: evaporation, melting and sublimation.

By obtaining a discrete metastable state on the liquid-solid equilibrium curve of benzene, the existence of a base point at a pressure of 2200atm and a temperature of 356K was determined by computer investigations and graphical method and this point was defined as the critical pressure.

Our metastable and graphic research highlights the following issues.

1. The first type of phase transitions, achieved by continuous or discontinuous metastable state, are completed by an isothermic process.
2. The second type of phase transformation is the "super metastable phase transformation", which represents the transformation from a metastable state to a solid phase without an isothermic process, plotted graphically.
3. Critical temperature at the point on the liquid-vapor equilibrium curve where the metastable state ends under constant pressure with increasing temperature T_{cr},
4. The point pressure at which the metastable state ends under constant pressure by cooling the liquid-solid equilibrium curve p_{cr},
5. The point at which the metastable state ends under constant pressure by cooling the solid-vapor equilibrium curve is represented by the critical density ρ_{cr}
6. With the transition of the liquid phase to the solid phase, the density of the substance between the liquid and solid phases is equalized $\rho_L = \rho_s$
7. The evaporation equilibrium curve is a function of temperature, the freezing curve is a function of pressure, the sublimation equilibrium curve is a function of density.

References

1. P. W. Bridgman , Rev. of. Modern Physics 18, № 1, 1 (1946)
2. F. Simon , M. Ruheman n an d W. A. M. Edwards , Zschr. f. phys. Chem, B 6, 331 (1930). Кривые плавления водорода, неона, азота и аргона.
3. O. K. Rice, J. Chem. Phys. 6, 472 (1938). Equilibrium solid-liquid for argon.
4. W. H. K e e s om a. K. C1 u s i и s, Proc. Amst. Acad. Sci. 34, 605 (1931). Переход жидкого гелия 1 в жидкий гелий II под давлением.
5. W. H. K e e s om a. J. H. C. L i s m a n, Kon. Akad. van. Wetens. Amst.Proc. 34, 598 (1931). Кривая плавления водорода до 450 *кг/см²*.
6. W. H. K e e s om a. J. H. C. L i s m a η, Kon. Akad. van Wetens. Amst.Proc. 35, 605 (1932). Кривая плавления-водорода до 610 *кг/см2.*
7. W. H. K e e s om a. J. H. C. L i s m a n, Kon. Akad. van Wetens. Amst.Proc. 36, 378 (1933). Кривая плавления неона до 200 *кг/см²*.
8. J. H. C. L i s m a n a. W. H. Keesom, Physica 2, 901 (1935). Кривая плавления кислорода до 170 *кг/см²*.
9. P. W. Bridgman , J. Chem. Phys. 9, 794 (1941): a) Замерзание и сжатие до 50 000 kg/cm2 ; Proc. Am. Acad. Arts Sci. 74, 399 (1942): b) Параметры замерзания и сжатия 21 вещества до 50 000 кг\см2
10. F r e d e r i c k G. K e y e s , Ind. Eng. Chem. 23, 1375 (1931). Техника высоких давлений.
11. F r e d e r i c k G. K e y e s , Proc. Am. Acad.68,505 (1933). Методика и тех. ника, применяемые при выполнении программы Массачузетского технологического института по исследованию *P—V* зависимости для воды до 460° С.
12. J. A. B e a t t i e a. O. C. B r i d g m a n, Ann. d. Physick 12, 827 (1932). Об измерениях с поршневым манометром. II. Влияние старения и вязкости масла на константу манометра; зависимость между истинным и эффективным диаметром поршня.
13. P. W. B r i d g m a n , Proc. Am. Acad. Arts Sci. 66, 185 (1931). Объёмы восемнадцати жидкостей как функции давления и температуры.
14. P. W. B r i d g m a n , J. Chem. Phys. 9, 794 (1941): a) Замерзание и сжатие до 50 000 *kg/cm2;*Proc. Am. Acad. Arts Sci. 74, 399 (1942):
b) Параметры замерзания и сжатия 21 вещества до 50 000 *кг\см²*
15. O. T a m m a n n u. G. Mor i t z, Zschr. f. anorg. allgem. Chemie 218, 60 (1934). О ходе кривых плавления.
16. V. G. Baidakov & S. P. Protsenko. Metastable phase equilibria in a Lennard-Jones system. *Journal of Engineering Thermophysics* volume 16, pages249–258 (2007).

17. V.G. Baidakov, Singular point of a system of lennard-jones particles at negative pressures. V.G. Baidakov, S.P. Protsenko, Phys. Rev. Lett. 95(1) (2005), 015701–1–015701–4

18. V.G. Baidakov, Metastable extension of the sublimation curve and the critical contact point.V.G. Baidakov, S.P. Protsenko, J. Chem. Phys. 124(23), 231101–231103 (2006)

19. Gregg Jaeger. The Ehrenfest Classification of Phase Transitions: Introduction and Evolution. May 1998Archive for History of Exact Sciences 53(1):51-81. DOI:10.1007/s004070050021

20. Landau L.D., Lifshitz E.M. Statistical physics. Part 1. M.: Nauka, 1976.

21. M. SKVORTSOV. USUAL AND UNUSUAL PHASE TRANSITIONS. Soros educational journal N 8, 1996. st.103-108. (http://stat.phys.spbu.ru/Metod/Faz-perex2.pdf)

22. B.I. Farzaliev, A.M. Ragimov. Investigation of phase transitions in liquids. BAKU 1984 Preprint №1 Institute of Physics of the Academy of Sciences of Azerbaijan.

23. M. Azreg-Aïnou, A. Huseynov, B. Ibrahimoglu, Phase equilibrium and metastabilityof liquid benzene at high pressures, J ChemPhys, 124 (2006). https://doi.org/10.1063/1.2198808

24. M. Azreg- Aïnou, B. Ibrahimoglu, High-pressure eff ects on the benzene pre-crystallization metastable states, Eur. Phys. J. E, 42 (2019) 1-10. https://doi.org/10.1140/epje/i2019-11863-2

25. V. D. ALEXANDROV,. B.IBRAGIMOGLY, A. E. POKINTELITSA, PRESSURE FALLING EFFECTS ACCOMPANIING PHASE TRANSFORMATIONS OF BENZENE UNDER THE ACCESSION OF COMPREHENSIVE COMPRESSIONUDC 541.64: 542.62: 546.23 Modern Building Materials Edition 2015 1 (111) UKRAİNA

26. B.Ibrahimogly, Chidem Kanbesh, I.M.Ahmedov PHASE TRANSFORMATIONS OF BENZENE IN TERMS OF LOW TEMPERATUES AND HIGH PRESSURES23, Chemistry Problems N4-2015,p 367-371 UDK-541,64; 546-13. Baku Azerbaijan

27. Beycan Ibrahimoglu , Deniz Uner, Ayfer Veziroglu , Fuat Karakaya , Beycan Ibrahimoglu. Construction of phase diagrams to estimate phase transitions at high pressures: A critical point at the solid liquid transition for benzene. International Journal of Hydrogen Energy. Volume 46, Issue 29, 26 April 2021, Pages 15168-15180

28. B. İbrahimoğlu, B İbrahimoğlu, T. Gasimiva, B.C. Askerli. A new type of phase diagram of pure substances. News of the Azerbaijan national academy of elites. Physics-texnika and piyaziyat hands series, physics and astronomy 2022. No 2. YDK 536 539. p.107-114

29. B. İbrahimoğlu, B İbrahimoğlu, T. Gasimiva, B.C. Askerli. A new type of phase diagram of pure substances. News of the Azerbaijan national academy of elites. Physics-texnika and piyaziyat hands series, physics and astronomy 2022. No 2. YDK 536 539. p.107-114

30. Beycan IBRAHIMOGLU, Yüksel SARIKAYA and Beycan IBRAHIMOGLUJR. Utilization of Graphical Method to Determinethe Characteristics of Desublimation Equilibrium Curve of Benzonitrile . " International Journal of Modern Engineering Research (IJMER), vol. 12(08), 2022, pp 01-07.

31. Beycan Ibrahımoglu, Fuat Karakaya, Tarana Gasımova, Beycan IBRAHIMOGLU, Super phase transıtıon and super metastabel state, Chemical Physics, 2021ya). Contents lists available at ScienceDirect Chemical Physics journal homepage: https://doi.org/10.1016/j.chemphys.2021.11131

32. J. H. Dymond & .R. Malhotra .The Tait equation: 100 years on. International Journal of Thermophysics volume 9, pages941–951 (1988)

33. Safarov, M.M. Khasanova, S.S. Gulomov, M.M. Radzhabova, D.Sh. Davlatov, R.Dzh.Khakimov, D.Sh. Rafiev, S.S. Radzhabov, A.R. Oymatova, Khusainov, Z.Kh. Analysis of applicability of Tate type equation to different classes of substances in a condensed state on the example of density. II. Density calculation Vestnik Natsionalnogo Universiteta; ISSN 1993-6923;CLASSICAL AND QUANTUM MECHANICS, GENERAL PHYSICS (S71)

34. B.I.Farzaliev., A.M.Ragimov, A.T. Hajiyev. Graphical definition of the parameters of the triple equilibrium point. UDC 533.77. "OIL AND GAS" 24. June 1985. Baku, Azerbaijan).

35. Farzaliev B. I, Aliev N. F On benzene phase transitions at high pressures // Thermodynamic and transport properties. substances. Themed. Science. Work. - Baku, AzPU, 1989. - pp.61-65.

36. Farzaliev B.I, Aliev N.F., Determination of gases by graphical analytic method. Proceedings of a Scientific Conference Az TU, Baku, 1992. P. 21 (Russian).

37. Ibrahimoglu B., Grafoanalytical of Critical Pressure in Gas. Finding with the method, vol. 17, 2. Ankara: Journal of Turkish Journal of Science and Technology of Turk; 1994.

38. Ibrahimoglu B.İ, Ataer O.E., Determination of a Node on the Melting Curve, ULIBTK-97,11 th National Congress of Business Science and Technology, Edirne,1997.P.33.

39. B. İbrahimoglu, Karakaya, F., Ibrahimoglu, B. (2021). Determination of the Real Critical Pressure and Critical Density of Substances. Academia Letters, Article 2704. https://doi.org/10.20935/AL2704.

40. Beycan Ibrahimoglu, B.A. Grigoryev, Berk Gökbel, Beycan Ibrahimoglu jun.. Phase transitions and the phase diagramsA case of benzene.Научно-технический сборник · ВЕСТИ ГАЗОВОЙ НАУКИ. № 4 (49) / 2021.UDC 543.272.75:544.344.015.4. st.140-152.

41. Beycan İbrahimoglu, Beycan İbrahimoglu Jr., Eda Bolayır. Phase Transitions and the Phase Diagrams. SCIREA Journal of Chemistry http://www.scirea.org/journal/Chemistry. November 1, 2021 Volume 6, Issue 2, April 2021.

42. Beycan IBRAHIMOGLU, Yüksel SARIKAYA and Beycan IBRAHIMOGLUJR.Utilization of Graphical Method to Determinethe Characteristics of Desublimation

Equilibrium Curve of Benzonitrile. International OPEN ACCESS Journal Of Modern Engineering Research (IJMER).| IJMER | ISSN: 2249–6645 | www.ijmer.com | Vol. 12 | Iss. 8 | August 2022 | 1 |.

43. Beycan İbrahimoglu, Yuksel Sarikaya, Beycan Jr. Ibrahimoglu. Critical Parameters of Pure Substances. DOI: https://doi.org/10.21203/rs.3.rs-1861011/v1. August 3rd, 2022. This work is licensed under a Creative Commons Attribution 4.0 International License.

44. Beycan İbrahimoğlu, Çiğdem Kanbeş Dindar, Hazal Erol, Salih Karasarı, DETERMINATION OF 1/V-T (P, CONSTANT) DIAGRAMS OF HYDROGEN GASES BY GRAPH-ANALYTICAL METHODS, Journal of Thermal Engineering, Vol. 3, No. 1, pp. 1071-1077, January, 2017, Manuscript Received 29 December.

45. Beycan İbrahimoglu, Beycan İbrahimojlu(jn) Critical States at Phase Transitions of Pure Substances. ISBN 978-3-031-09965-6 Springer Nature Tiergartenstr. 15-17, 69121 Heidelberg, Germany.

46. B. A. Grigoryev, Beycan Ibrahimoglu, Faruk Comert Beycan Ibrahimoglu jun. Determination of the real critical density of substances. Научно-технический сборник · ВЕСТИ ГАЗОВОЙ НАУКИ. № 1 (46) / 2021. 46-51.Moskova.

47. B. Ibrahimoglua;, T. Nejat Veziroglub, Aydin Huseynov. Study of thermodynamic parameters of hydrogen gas by grapho-analytic metho. International Journal of Hydrogen Energy 30 (2005) 515 – 519. doi:10.1016/j.ijhydene.2004.04.013

48. T. Veziroglu, B. Ibrahimoglu, A. Huseynov and D. Schur, et al., “Study of Thermodynamic Parameters of Hydrogen Gas by Grapho-Analytic Method,” Editor of a Chapter in Hydrogen Materials Science and Chemistry of Carbon Nanomaterials,225-232. ©2004 Kluwer Academic Publishers, Netherlands.

49. B. İbrahimoglu, N. Veziroglu ve A. Hüseynov, Schur, D., (2004), Study of thermodynamic parameters of hydrogen gas by grapho- analytic method. Hydrogen Materials Science and Chemistry of Carbon Nanomaterials, S. 225–232.

50. B. Ibrahimoglu, T. Veziroglu, A. Huseynov and D. Schur, “Study of Thermodynamic Parameters of Hydrogen Gas by Grapho-Analytic Method,” Hydrogen Materials Science and Chemistry of Carbon Nanomaterials, NATO Science Series II: Mathematics, Physics and Chemistry, 2005, Volume 172, 225–232.

51. Beycan Ibrahimoglu, Gozde Tekeli. Application of graphic and graphic-analytic geometry systems on the liquid and gas phases of matter. Научно-технический сборник · ВЕСТИ ГАЗОВОЙ НАУКИ. № 1 (38) / 2019. 163-170. Moskova.

52. B. Ibrahimoglu, Y. Sarikaya, A. Veziroglu, B. Ibrahimoglu Jr., M. Onal, B. Gokbel. Supercritical phases of hydrogen, International Journal of Hydrogen Energy, https://doi.org/10.1016/j.ijhydene.2021.07.032.

53. Igor Alexandrov, Boris Grigor'ev, A.A. Gerasimov, B.V. Nemzer. Thermophysical Properties of Individual Hydrocarbons of Petroleum and Natural Gases. Properties, Methods, and Low-Carbon Technologies. ISBN: 9780323952170. DOI:10.1016/C2021-0-02883-2 .

54. N. B. Vargaftik, Y. K. Vinogradov, V. S. Yargin. Handbook of Physical Properties of Liquids and Gases. ISBN Imprimir:978-1-56700-063-4. ISBN Online:978-1-56700-375-8

55. Bruce E. Poling, John M. Prausnitz, John P. O’Connell. Properties of Gases and Liquids, 5th Edition. ISBN: 9780070116825

Deutsche internationale Zeitschrift für zeitgenössische Wissenschaft

• • •

№53 2023

German International Journal of Modern Science

• • •

№53 2023

Deutsche internationale Zeitschrift für zeitgenössische Wissenschaft ist eine internationale Fachzeitschrift in deutscher, englischer und russischer Sprache.

Periodizität: 24 Ausgaben pro Jahr
Format - A4
Alle Artikel werden überprüft.
Freier Zugang zur elektronischen Version des Journals

German International Journal of Modern Science is an international, German/English/Russian/Ukrainian language, peer-reviewed journal.

Periodicity: 24 issues per year
Format - A4
All articles are reviewed.
Free access to the electronic version of journal.

- Edmund Holst (Salzburg) AT
- Michaela Meissner (Köln) DE
- Klara Amsel (Liège) BE
- Briana French (Cambridge) GB
- Joleen Parsons (Manchester) GB
- Dragomir Koev (Sofia) BG
- Stanislav Štěpánek (Praha) CZ
- Valeriya Kornilova (Kyiv) UA
- Dmitriy Aksenov (Lviv) UA
- Valentin Bragin (Moscow) RU
- Mirosław Bednarski (Warsaw) PL
- Daniela Villa (Florence) IT
- Mattia Molteni (Rome) IT
- Sylwia Krzemińska (Ljubljana) SI
- Käte Kraus (Vienna) AT
- Eleonora Lehmann (Berlin) DE
- Alexander Dressler (Marseille) FR
- Zdzisław Małecki (Warsaw) PL
- Adrián Borbély (Budapest) HU

Artmedia24

Anschrift: Industriestraße 8,74589 Satteldorf Deutschland.

E-mail: info@dizzw.com
WWW: www.dizzw.com

Chefredakeur: Reinhardt Roth

Druck: Einzelfirma Artmedia24, Industriestraße 8,74589 Satteldorf Deutschland

Artmedia24

Address: Industriestrasse 8,74589 Satteldorf Germany.

E-mail: info@dizzw.com
WWW: www.dizzw.com

Editor in chief: Reinhardt Roth

Printing: Artmedia24, Industriestrasse 8,74589 Satteldorf Germany.

ISSN (Print) 2701-8369

ISSN (Online) 2701-8377

Edition: № 53/2022 (March) – 53th

Passed in press in March 2023

Printed in March, 2023

Printing: Artmedia 24, Industriestrasse 8,

74589 Satteldorf, Germany.